applied sciences

MDPI

Review

Fewer Dimensions for Higher Thermal Performance: A Review on 2D Nanofluids

José Pereira [1,*], Ana Moita [1,2] and António Moreira [1]

[1] IN+ Center for Innovation, Technology and Policy Research, Instituto Superior Técnico, Universidade de Lisboa, Av. Rovisco Pais, 1049-001 Lisboa, Portugal; anamoita@tecnico.ulisboa.pt (A.M.); aluismoreira@tecnico.ulisboa.pt (A.M.)

[2] CINAMIL—Centro de Investigação Desenvolvimento e Inovação da Academia Militar, Academia Militar, Instituto Universitário Militar, Rua Gomes Freire, 1169-203 Lisboa, Portugal

* Correspondence: sochapereira@tecnico.ulisboa.pt

Abstract: The current work aims to offer a specific overview of the homogeneous dispersions of 2D nanomaterials in heat transfer base fluids—so-called 2D nanofluids. This data compilation emerged from the critical overview of the findings of the published scientific articles regarding 2D nanofluids. The applicability of such fluids as promising alternatives to the conventional heat transfer and thermal energy storage fluids is comprehensively investigated. These are fluids that simultaneously possess superior thermophysical properties and can be processed according to innovative environmentally friendly methods and techniques. Furthermore, their very reduced dimensions are suitable for the decrease in the size of thermal management systems, and the devices have attracted a lot of attention from researchers in different fields. Some examples of 2D nanofluids are those which incorporate graphene, graphene oxide, hexagonal boron nitride, molybdenum disulfide nanoparticles, and hybrid formulations. Although the published results are not always consistent, it was found that this type of nanofluid can improve the thermal conductivity of traditional base fluids by more than 150%, achieving values of approximately 6500 $W \cdot m^{-1} \cdot K^{-1}$ and interface thermal conductance above 50 $MW \cdot m^{-2} \cdot K^{-1}$. Such beneficial features permit the attainment of increments above 60% in the overall efficiency of photovoltaic/thermal solar systems, a 70% reduction in the entropy generation in parabolic trough collectors and increases of approximately 200% in the convective heat transfer coefficient in heat exchangers and heat pipes. These findings identify those fluids as suitable heat transfer and thermal storage media. The current work intends to partially suppress the literature gap by gathering detailed information on 2D nanofluids in a single study. The thermophysical properties of 2D nanofluids and not of their traditional counterparts, as it is usually encountered in the literature, and the extended detailed sections dedicated to the potential applications of 2D nanofluids are features that may set this research apart from previously published works. Additionally, a major part of the included literature references consider exclusively 2D nanomaterials and the corresponding nanofluids, which also constitutes a major gathering of specific data regarding these types of materials. Upon its conclusion, this work will provide a general overview of 2D nanofluids.

Keywords: 2D nanomaterials; heat transfer; thermal management; thermal fluids

Citation: Pereira, J.; Moita, A.; Moreira, A. Fewer Dimensions for Higher Thermal Performance: A Review on 2D Nanofluids. *Appl. Sci.* **2023**, *13*, 4070. https://doi.org/10.3390/app13064070

Academic Editor: Matt Oehlschlaeger

Received: 20 February 2023
Revised: 14 March 2023
Accepted: 20 March 2023
Published: 22 March 2023

1. Introduction

Introductory studies on 1D nanostructures received immediate attention from researchers soon after their introduction by Iijima [1] on carbon nanotubes (CNTs). Following this, various types of 0D and 1D nanostructures were investigated. The recent advances in layered nanomaterials allow the industrial production of different 2D nanomaterials, where their atoms are combined in flat layers that can be stacked on top of each other. Current 2D nanomaterials are of great relevance in the nanotechnologies field of work and research [2], given that their properties, especially in heat transfer practical situations, hold greater

potential compared with traditional nanoparticles [3]. Recently, 2D nanomaterials and nanofluids have become the focus of the scientific community because of their improved thermophysical properties [4]. These innovative nanomaterials and nanofluids include graphene (Gr), graphene oxide (GO), reduced graphene oxide (rGO), CNTs, fullerenes, transition metal dichalcogenides, graphitic carbon nitride, hexagonal boron nitride (h-BN), tungsten disulfide (WS_2), and molybdenum disulfide (MoS_2), MXene, among others, dispersed in adequate base fluids. In this kind of nanomaterial, the heat transfer, photons, and charge carriers will be limited in the 2D plane, leading to intense modifications in the electrical and optical features of such nanomaterials [5]. These materials will perform better than the traditional nanoparticles and corresponding nanofluids due to their large surface area to volume ratio [6]. Apart from three-dimensional nanomaterials, there are two-dimensional (2D), one-dimensional (1D), and zero-dimensional (0D) nanomaterials. The latter are those materials in which all three dimensions are beyond the micro/nanoscale under the form of core–shell nanoparticles, composite nanoparticles, and carbon and graphene quantum dots. One-dimensional nanomaterials are those in which two dimensions are at nanoscale and the remaining dimension is expressed (in most cases) in millimeters. Examples of such nanomaterials are CNTs, carbon nanowires, and graphene fibers. Finally, 2D nanomaterials possess one of their dimensions at nanoscale and the other two dimensions at a different scale. Examples of 2D nanomaterials are graphene nanomesh, nanosheets, and nanowires. In terms of thermal characteristics, such as thermal conductivity (TC) and heat transfer coefficient and rate, these are generally improved during the transfer from the OD nanomaterials to the 2D nanomaterials. However, other factors also influence predominantly the heat transfer capability of these materials, such as the chemical composition, surface-to-mass and volume ratios, and charge carrier mobility, among other factors. For instance, and considering only the heat transfer performance, carbon or graphene quantum dots (0D) are widely used in solar cells and solar light harvesting systems. Those nanomaterials have an improved absorption ability in the ultra-violet region, complementing the solar light harvesting in the visible region of the systems and enhancing their overall efficiencies. There are not used in search of very high TC values, for instance. On the other hand, 1D nanomaterials, such as carbon nanotubes, can achieve a TC of approximately 6000 $W \cdot m^{-1} \cdot K^{-1}$. Furthermore, 2D nanomaterials, such as graphene nanoplatelets, can reach 6500 $W \cdot m^{-1} \cdot K^{-1}$ [7] of TC, and graphene oxide nanosheets can achieve TC values of nearly 6800 $W \cdot m^{-1} \cdot K^{-1}$ [8], enhancing the heat transfer capability to its fullest. Figure 1 shows the materials and their possible forms in 0D, 1D, and 2D nanomaterials.

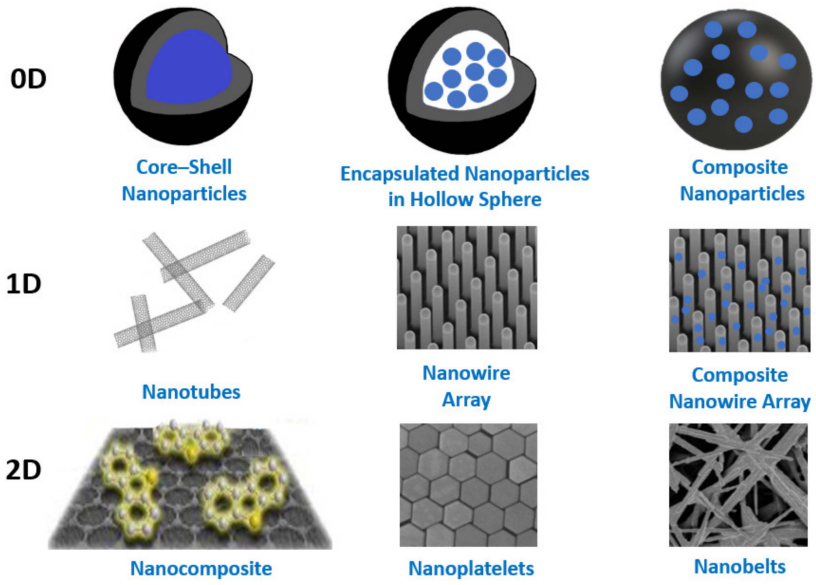

Figure 1. Types of 0D, 1D, and 2D nanomaterials.

One of the most common types of layered nanomaterial is Gr, and it has been widely studied for its superior characteristics and uses in different fields [9]. Two-dimensional nanomaterials can be a suitable option as nanofillers in traditional heat transfer fluids as they present a very high heat transfer area [10]. A common synthesis technique for these layered nanomaterials is exfoliation, where the single layers of the material are separated from each other by chemical or mechanical procedures [11]. It is worth mentioning that even though the exfoliation process can be performed mechanically on a small scale, liquid phase procedures are required for various ends, such as nanoelectronics, micro-electromechanical systems, nanoelectromechanical systems, and sensors, among others. These 2D materials can also be manufactured by chemical growth of the individual layers, which is the most common technique to produce Gr nanosheets [12], using chemical vapor deposition (CVD) onto the surface of catalysts, such as copper or silica, through heating at temperature values up to 1200 °C and passing a carbon-containing gas (e.g., methane) over the catalyst. Coleman et al. [2] demonstrated that it is possible to synthesize 2D materials, such as MoS_2, WS_2, and h-BN, using wet exfoliation procedures. The exfoliation process of 2D insulators, such as h-BN, would decrease its residual bulk conductance [13] and promote the surface-driven effects. This novel class of materials and fluids represent a broadened, unexploited part of 2D systems with superior thermophysical characteristics, high specific surface areas of relevance for thermal management, and thermal energy storage purposes. Furthermore, Gr nanofluids can be potentially investigated and utilized as a promising thermal fluid in many applications, including concentrated solar power (CSP) and PV/T (photovoltaic/thermal) systems due the following advantages:

- Facile preparation methods [14].
- Lower induced erosion, clumping, and corrosivity [15].
- Larger surface area to volume ratios [16].
- Very high TC values.
- Superior heat transfer coefficient (HTC) and rate.
- Enhanced stability in reference to conventional nanoparticles.

These benefits offer the 2D nanomaterials and corresponding nanofluids the possibility to perform better in comparison with conventional nanomaterials and nanofluids. Figure 2 presents a schematic qualitative comparison of the main thermophysical characteristics and cost effectiveness to be considered in heat transfer enhancement applications of the main 2D nanofluids.

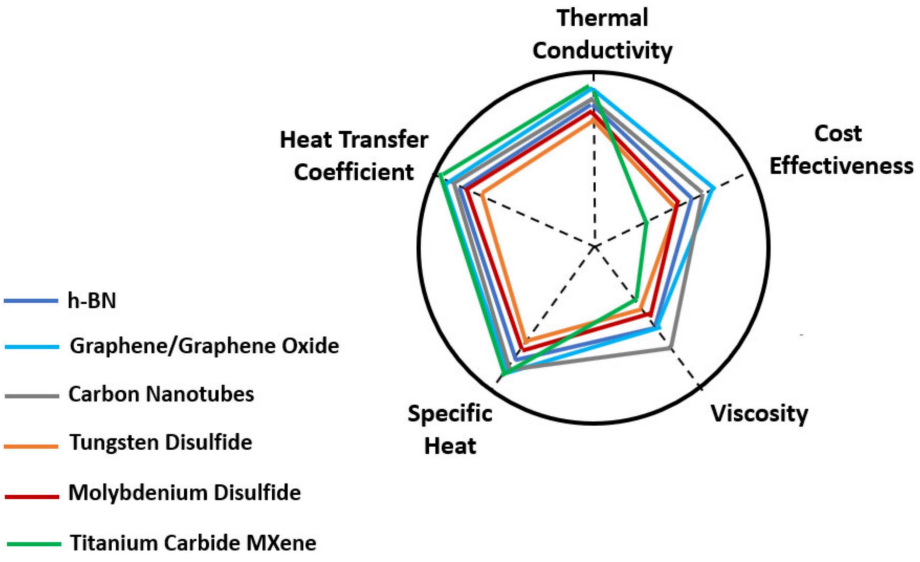

Figure 2. Schematic diagram of the qualitative comparison of the thermophysical properties of the main 2D nanofluids.

Moreover, hybrid nanofluids can be characterized by the incorporation of binary, ternary, and tetra [17] hybrid nanoparticles in base fluids and are very high TC heat transfer fluids when compared, for instance, with some mono-dispersed nanofluids. They exist as metal hybrid nanofluids, metal oxide hybrid nanofluids, and carbon-based hybrid nanofluids, among others. The hybrid nanofluids have composite nanoparticles and nanoparticle-decorated 2D nanostructures and can be synthesized according to various physical and chemical methodologies. The physical methodologies include atom beam splintering, laser induced heating, and ion implantation. Among the chemical synthesis routes, which are facile and inexpensive, there is the sol-gel process, sonochemical synthesis, hydrothermal synthesis, co-precipitation, and seed growth. The hybrid nanofluids are commonly employed to enhance the operating fluid thermophysical characteristics in solar thermal energy conversion and harvesting systems and equipment, such as flat plate collectors. Recent experimental works on innovative hybrid nanofluids [18,19] focused on the extremely high thermal transport capability of hybrid nanofluids and modified hybrid nanofluids flowing in rigid channels or in dilating/squeezing channels. Figure 3 presents the main potential applications of 2D nanofluids.

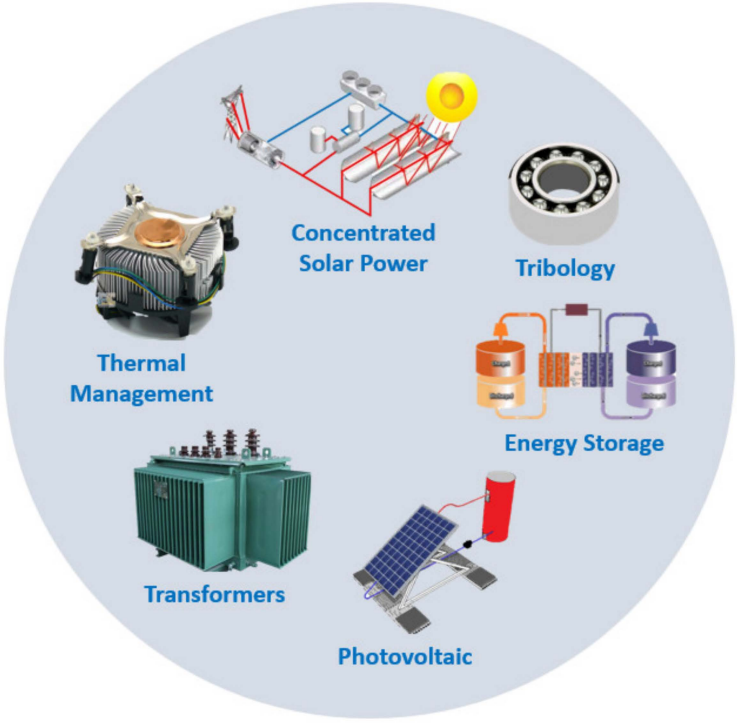

Figure 3. Main practical applications of 2D nanofluids.

2. Types of 2D Nanofluids

2.1. Hexagonal Boron Nitride

Other 2D ordered nanocrystals, different from those in the carbon nanomaterials family, are of great research and practical interest. These include h-BN nanosheets with a very high TC. This thermophysical property of h-BN is approximately 3400 $W \cdot m^{-1} \cdot k^{-1}$. The performant thermal characteristics and the low synthesis cost of the h-BN nanofluids compared to the Gr ones means that they can potentially be used in heat transfer and thermal energy storage. The h-BN innovative 2D material also has other noticeable characteristics, including mechanical stability and electrical resistivity. Furthermore, it is a solid lubricant with high efficiency in different areas, such as metal-working processes and wear-sealing of aerospace engines under high-temperature conditions. There exist many forms of BN, including carbon nanostructures possessing a variety of characteristics and functionalities. For instance, the honeycomb layered BN, also known as white graphite because of its

structural similarity to that of graphite, is a common form of boron nitride that has a configuration similar to graphite with hexagonal ring layers separated by 3.33 Å, in which every boron atom is covalently bonded to three nitrogen atoms and vice versa. Between the layers, every boron interacts by van der Waals forces with a nitrogen atom. Thus, the strong B–N bond gives strength to the h-BN atomic layer and the individual BN layers could be isolated from the bulk h-BN crystals. Since it possesses an improved TC, the BN can overcome other fillers and is suitable for thermal performant hybrids. When synthesized through wet exfoliation, h-BN can offer a maximum exposure to the (002) lattice planes. It should be noted that h-BN is especially useful in thermal management situations where it can play the role of the thermal conductor and the electrical insulator. The application of h-BN in mineral oils, natural esters, and other fluids has already been examined. For instance, Taha-Tijerina et al. [20] demonstrated that h-BN changed the TC of mineral oil and acted as an electric insulator rather than a conductor. This is caused by the ability of the h-BN nanoparticles to trap moving electrons. Additionally, Salehirad and Nikje [21] incorporated h-BN nanostructures in a mineral oil and observed an enhanced TC, decreased viscosity, and improved insulation capability compared with those characteristics of the mineral oil alone. Moreover, Li et al. [22] synthesized ethylene glycol/BN nanofluids with different sized nanoparticles. The investigation team demonstrated that the nanofluids with larger nanoparticles exhibited greater TC enhancements when compared with those with smaller nanoparticles. Bhunia et al. [23] developed a 2D nanofluid with h-BN nanosheets and conventional transformer oil as the base fluid. The prepared nanofluids had stable dispersions with an enhanced dielectric breakdown strength and TC at 35 °C, 45 °C, and 55 °C. The synthesis method of the nanofluids is schematically described in Figure 4.

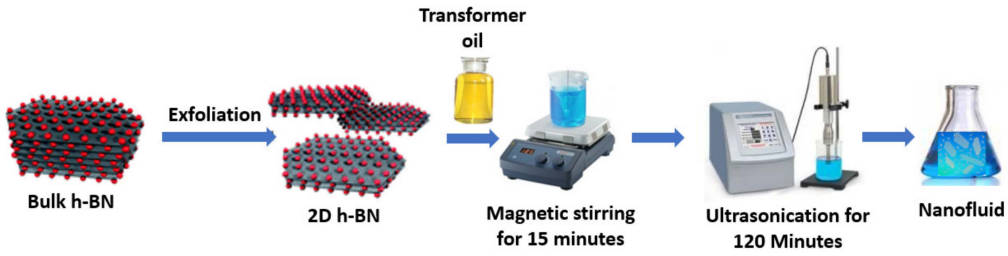

Figure 4. Schematic diagram of the preparation method of the 2D h-BN/transformer oil nanofluids.

The dispersed layered 2D h-BN has high specific area, enabling it to create a larger interfacial region. Due to its (002) plane dominance of the hexagonal phase, the BN possesses an improved TC above 600 $W \cdot m^{-1} \cdot K^{-1}$. The very thin and high specific surface h-BN nanosheets are lipophilic, allowing the existence of a perfect contact with the transformer oil base fluid. The intra-sheet propagation of heat introduces a free path to the phonon, which faces lower Kapitsa resistance and smaller thermal loss. Additionally, the clustering caused by a shorter inter-particle distance leads to the formation of a percolation network that acts as a conductive path for heat propagation. In cases where the clustering of sheets exists, an overlap of the interfacial regions occurs between the nanosheets leading to a continuous Kapitsa region with decreased vibrational density of states in phonons. The thermal imaging analysis of the nanofluids showed that the region of high temperature spreads with an increasing load of h-BN nanosheets, forming a percolation network that promotes the conduction of heat. With increasing temperature and fraction of the nanosheets, the quantity and velocity of the heat conduction phonons increased, and the overall thermal performance was improved. Nevertheless, above 0.05% wt. the rising concentration would promote the agglomeration of the nanostructures caused by the strong van der Waals forces in the vicinity of the nanostructures, provoking saturation. Such saturation is more prominent at higher temperature values and concentrations because of the intensified phonon scattering and eminent agglomeration. Furthermore, the authors found an appreciable increase in the AC breakdown voltage with the use of the nanofluids, which is large when compared with the BN nanoparticles. The referred

increase can be interpreted by the extended nanosheets/oil interfacial regions, also known as Maxwell Garnet regions, of the 2D fillers in terms of charge trapping behavior. The faster heating/cooling rate and the enhanced TC is consistent with the Maxwell prediction model. The improved thermal performance can be explained through the augmented phonon transfer by the large interface between the nanosheets and the transformer oil. Furthermore, the natural electrostatic repulsion between the nanosheets at diluted concentrations promoted enhanced long-term and thermal stabilities compared with their nanoparticle counterpart. Han et al. [24] synthesized h-BN nanoparticles in water nanofluids and evaluated their TC. The authors reported an improved long-term stability of the aqueous nanofluids, and their TC increased by 55% at 0.10% vol. compared with that of the water itself. Table 1 shows some of the recent studies on h-BN nanofluids.

Table 1. Recent studies on h-BN and hybrid nanofluids.

Reference	Authors/Year	Concentration	Base Fluid	Main Findings	Remarks
[25]	Zhi et al., 2011	6% vol.	Water	2.6-fold enhancement of the TC.	Relatively low viscosity increase.
[26]	Fang et al., 2014	1, 2, 5, and 10% wt.	Paraffin phase change materials	60% increase in the TC.	Minor decrease in the latent heat capacity.
[27]	Ilhan et al., 2016	From 0.03 to 3% vol.	Water, water ethylene glycol mixture, and ethylene glycol	TC increases of 26%, 22%, and 16% at 3% vol. for the different base fluids, respectively.	Use of SDS and PVP surfactants. Viscosity increases of 22%, 66%, and 33% for the different base fluids, respectively.
[28]	Ilhan and Erturk, 2017	0.1, 0.5 and 1.0% vol.	Water	Heat transfer enhancements of 7, 10, and 15%, respectively.	Formation of percolating structures and branching network.
[29]	Hou et al., 2018	5, 10, 15, 20, and 25% vol.	Water	298% increase in the TC at 25% vol.	Considerable increase in the viscosity.
[30]	Hussein et al., 2020	Hybrid Gr-h-BN at 0.05, 0.08 and 1% wt.	Water	85% increase in the solar collector efficiency.	Use of Tween 80 surfactant.
[31]	Zhang et al., 2021	0.8% wt.	Solar Salt	16% increase in the specific heat capacity.	Excellent thermal and long-term stabilities after 7200 min. The viscosity of the solar salt increased by 2 to 3 times with the addition of the h-BN.
[32]	Farbod and Rafati, 2022	1% vol.	Ethylene glycol	24% increase in the TC and 30% increase in the heat transfer rate.	No increase in the friction factor in turbulent regime.

There is a research gap regarding the quantity and quality of investigation works concerned with the laminar heat transfer convective performance of h-BN nanofluids in heat exchangers, heat pipes, thermosyphons, and other devices. There is also a lack of sufficient studies on h-BN nanomaterials dispersed in base fluids, such as glycerin, paraffin, silicone oil, and green base liquids, rather than water, ethylene glycol, or mineral oil, for all potential applications. Additionally, there are only a few modest attempts in the literature to use h-BN nanosheets to synthesize hybrid phase change materials to be dispersed in ionic liquids and other types of base fluids and to be used in the thermal energy storage technological area.

2.2. Graphene/Graphene Oxide

Gr, GO, and rGO nanofluids possess very high heat transfer properties and they can be used in almost all heat transfer practical cases, including those related to solar thermal energy conversion and storage, PV/T systems, cooling of electronics, and thermal management solutions such as heat sinks and thermosyphons. Nevertheless, the synthesis of these nanofluids is not inexpensive and the use of Gr family nanofluids entails some important limitations that should be tackled in the future. These and other processing influencing factors, together with the improved thermophysical properties and field of application for Gr nanofluids, will be addressed in this extensive sub-section of this review. Gr is a carbon material originating from graphite in bulk state. It possesses the morphology of a two-dimensional, one-atom thick nanosheet (monolayer) and lattice of hexagonally arranged sp^2 bonded carbon atoms. Its transverse sizes range from several nanometers to the macroscale. Gr was initially synthesized through the pioneering work of Novoselov et al. [33] using mechanical exfoliation by Scotch tape of the bulk graphite. Gr was categorized according to its structural arrangement, ranging from the 0D quantum dots, 1D nanofibers and nanoribbons, and 2D nanosheets, nanoplatelets, and rippled/wrinkled nanomesh. Regarding the 2D Gr nanosheets, a few proper production methods are commonly employed, including the laser-induced graphene production technique, exfoliation by mechanical means, silicon carbide sublimation, graphite fluid exfoliation, and CVD. These fabrication procedures synthesize solid Gr, excepting fluid exfoliation that produces Gr under the form of a colloidal suspension. The mechanical exfoliation method was the first approach to obtain Gr using Scotch tape to peel off a bulk pyrolytic graphite substrate, producing thin films of monolayer Gr attached to the tape. There are other, less common types of mechanical exfoliation, such as ball milling of graphite nanoparticles [34]. The laser-inducement route is usually conducted in ambient conditions through the application of a CO_2 pulsed laser onto a carbon substrate. Such methodology combines bulk Gr fabrication and patterning in a single operating step without using any wet chemicals. Liquid exfoliation involves the application of a peeling force created by a horn ultrasonicator to separate the Gr nanosheets from the bulk graphite immersed in a, for instance, N-methyl-2-pyrrolidone solvent, but aqueous solutions can also be employed if a surfactant is included. The yield from the liquid exfoliation procedure is comparatively low and, consequently, it should be conducted at the centrifugation stage to obtain a significant monolayer and enough to create several layers of Gr flakes in the final dispersion. Moreover, the CVD technique uses hydrocarbon gases to induce the growth of Gr on high carbon solubility metallic substrates (e.g., nickel) by carbon diffusion and segregation. The improved features of Gr are derived mainly from the 2p orbitals that form the π-bonds, which are hybridized together to generate the π–π bands. Those bands are delocalized over the carbon platelet and produce Gr. Accordingly, Gr has excellent stiffness, enhanced TC, and great mobility of the charge carriers. Gr can be arranged according to the following possible configurations and nanomaterials:

- Multi-layer Gr, which is a two-dimensional carbon nanomaterial composed of a small number of well-defined, stacked Gr layers.
- Gr quantum dots, which contain one or few layers of Gr nanosheets mainly used in photoluminescence situations. In general, Gr quantum dots usually have transverse sizes of less than 10 nm.
- Gr nanoplatelets, containing a two-dimensional honeycomb Gr lattice.
- GO, which is a Gr modified chemically and produced by exfoliation and oxidation together with the general modification of the basal plane by oxidation. The GO reveals a monolayer material with an elevated content of oxygen.
- rGO, which is a GO prepared through chemical, thermal, microwave, photo-thermal, and bacterial green methods for reducing the content of oxygen.

The use of Gr nanoparticles is an attractive option, given that they are less costly, and their production is simpler when compared with that of Gr nanosheets or CNTs. Furthermore, a homogeneous dispersion of Gr nanoplatelets is easier to obtain than those of Gr

and CNTs since during dispersion, the single-layered Gr may be curled and the CNTs may be entangled. Moreover, Gr nanoparticles exhibit a much lower surface area compared with Gr nanosheets, but their surface area is still much greater than that of CNTs. It should be noted that the TC of Gr nanoparticles decreases as the number of layers increases [35]. Sadri et al. [36] synthesized covalently functionalized Gr nanoparticle colloidal suspensions that had enhanced stability and environmental benevolence. Gr nanoparticles were functionalized using clove buds through the one-pot method. Then, the clove-treated Gr nanoparticles were incorporated into the base fluid to synthesize the nanofluid using a two-step method. The hydrophilic functionalized groups were confirmed by UV–VIS spectroscopy and their presence resulted in good stability even two months after the as-prepared condition of the nanofluids. Dhar et al. [37] produced Gr nanofluids with the addition of Gr nanosheets, which were synthesized using a two-step preparation method. The oxidation process of the graphite nanopowder into GO nanosheets was performed using the modified Hummers method, which was followed by GO reduction into rGO. Ghozatloo et al. [38] and Park et al. [39] synthesized Gr nanoflakes. They used the CVD technique to create Gr nanosheets on copper foil by catalytic decomposition in a quartz tube furnace. Additionally, Safaei et al. [40] evaluated the heat transfer characteristics, pressure drop, and required pumping power for using an aqueous nanofluid with Gr/silver nanoparticles flowing in a conduit with a rectangular section. It was verified that the heat transfer features were enhanced with an increasing Reynolds number and concentration of the nanoparticles. However, when using the developed nanofluids, an increase in the required initial pumping power was also observed. Yarmand et al. [41] investigated the attributes of Gr nanoparticles and platinum dispersed in water. The prepared nanofluids had improved stability and any noticeable sedimentation was not observed after 22 days. The TC of the nanofluids showed a near 18% enhancement when compared with the TC of the water alone at 40 °C and at 0.1% wt. Since the synthesis of Gr is complex and costly, efforts have been made to develop cheaper procedures to synthesize and use Gr derivatives, such as GO. GO can be synthesized by exfoliating the GO into layered plates through ultrasonication or vigorous stirring and can be incorporated into base fluids, forming GO nanofluids. Vincely and Natarajan [42] conducted experiments using a solar flat plate collector and a GO nanofluid as the heat transfer fluid. The nanofluid was prepared via ultrasonication of GO in water. The enhancement of the collector efficiency was 7.3% at a flow rate of 0.0167 kg/s and a weight fraction of 0.02% wt. compared with that of the water alone. In addition, Yu et al. [43] determined the TC of the nanofluids composed by GO nanosheets and different base fluids. At a weight fraction of 5% wt., the enhancements of the TC were 30.2%, 62.3%, and 76.8% for water, propyl glycol, and liquid paraffin as base fluids, respectively. Owing to the enhanced thermal stability, charge transportation, TC, mechanical strength, and optical properties, rGO and its nanofluids can be used in the development of different types of innovative nanomaterials and thermal fluids in various applications, including solar energy conversion and harvesting systems, filtration, chemical batteries, and nanoscale electrodes. In this sense, Lin et al. [44] synthesized an innovative surfactant composed of two-dimensional charged zirconium phosphate nanoplatelets and applied it in the dispersion of rGO in a base fluid. The obtained results show that rGO nanofluids were altered from non-homogeneous, non-Newtonian nanofluids into homogeneous Newtonian nanofluids after exfoliation with the charged zirconium nanoplatelets. Zubir et al. [45] utilized an rGO nanofluid for improving the thermal performance of a closed duct structure. The authors produced the rGO using the reduction process with tannic acid from the chemically exfoliated GO. The heat transfer enhancement of the nanofluid was higher than the TC enhancement because of the considerable effects of the nanoparticles and turbulent induced flow features. Schlierf et al. [46] employed pyrene derivatives for stabilizing rGO dispersions due to the forces of repulsion and the π–π interaction between functionalized pyrene derivatives and the π systems of rGO. The chemical reduction of GO possesses the beneficial features of being a simple and inexpensive method, resulting in a greater yield of Gr with proper scalability for large-scale applications. The Gr family of

nanofluids can be synthesized using the one-step route or two-step route. In the one-step route, the nanofluids are directly synthesized and are produced directly through chemical processes. In the two-step route, the Gr nanosheets are initially manufactured in nanopowder form by physical or chemical methods such as grinding, laser ablation, or the sol-gel method, and then are dispersed in a base fluid. Fan et al. [47] oxidized graphite nanoflakes using an ameliorated Hummer method. A mixture of phosphoric acid and sulfuric acid was incorporated into a mixture of Gr flakes and potassium permanganate. After vigorous stirring, the mixture was air cooled. When the mixture exhibited a yellow coloration after the addition of hydrogen peroxide, the deposit was centrifuged, and the remaining material was washed. The GO sheets were manufactured after air drying. Lee et al. [48] synthesized nanofluids with GO nanosheets dispersed in water. The investigation team prepared the GO nanosheets through CVD. The pH and zeta potential of the developed nanofluids were 3.58 and −31.5 mV, respectively, indicating a reasonable stability. Yu et al. [49] proposed an easy method for preparing ethylene glycol-based nanofluids, including Gr and GO nanosheets. The TC of the ethylene glycol increased up to 86% with the incorporation of the nanosheets. The TC of the GO nanofluid and Gr nanofluid were 4.9 W/mK and 6.8 W/mK, respectively. Lee and Rhee [50] produced ethylene glycol nanofluids incorporating Gr nanoplatelets, which exhibited similar TC enhancement at a weight fraction of 2% wt. and at temperature values between 10 °C and 90 °C. The TC of the nanofluids was much greater than that provided by the Hamilton–Crosser model [51], which may be due of the greater surface area and two-dimensional nanostructure of the Gr nanoplatelets. Akhavan-Zanjani et al. [52] measured the TC and viscosity of a nanofluid composed of Gr nanosheets dispersed in water. The experimental results revealed a considerable increase in the TC and a moderate increase in the viscosity with the incorporation of the Gr nanosheets. The maximum increases were of 4.95% and 10.30% for the viscosity and TC, respectively. Moreover, the authors Liu et al. [53] investigated the TC, specific heat capacity, viscosity, and density of the nanofluids based on Gr nanosheets suspended in an ionic base fluid. The TC of the nanofluid at 0.06 wt.% showed an enhancement within 15.2–22.9% in the base fluid itself in cases where the temperature values were raised from 25 °C to 200 °C. The viscosity of the prepared nanofluid was considerably decreased with increasing temperature. The specific heat capacity and density of the nanofluids suffered a minor reduction compared with those properties of the base fluid alone. Park and Kim [54] examined the evolution of the TC and viscosity of different types of Gr nanosheets dispersed in water, including those containing GO nanosheets and Gr nanosheets with diverse sizes. The enhancement of the TC in the GO nanofluid was the highest among all tested nanofluids, whereas the maximum increase in the viscosity was found for the Gr nanofluid with the largest nanosheets. Tesfai et al. [55] studied the rheological characteristics of aqueous suspensions in GO nanosheets. The suspensions exhibited a shear thinning behavior under small shear rates, which was followed by a shear-independent behavior. The shear thinning behavior became more intense with an increasing incorporated fraction of the nanosheets. Furthermore, the nanofluids possessed a considerable viscosity due to the high aspect ratio of the GO nanosheets. Ijam et al. [56] evaluated the viscosity of GO nanosheets dispersed in water and ethylene glycol. The nanofluids exhibited a shear thinning behavior under low shear rates and a Newtonian behavior under high shear rates. The viscosity of the nanofluid increased by up to 35% compared with that of the base fluid at 0.1% wt. and a temperature of 20 °C. The majority of experimental works on Gr and GO nanofluids have stated that the TC is temperature dependent; however, Sun et al. [57] reported inconsistent results, which was expected since a more in-depth understanding is required to establish precise correlations between the thermophysical characteristics of this type of nanofluid and many factors, including the size and incorporated fraction of the nanoparticles, rheological features, stability over time, the aspect ratio of the Gr nanosheets, pH regulation, zeta potential, and operating temperature. Naghash et al. [58] studied the HTC of nanofluids prepared from porous Gr nanosheets. The TC of the 0.1% wt. nanofluid remained almost unchanged with only a minor increase of 3.8%, while the HTC suffered a considerable enhancement of 34%. This

confirmed that aside from TC enhancement, more factors may influence the heat transfer of Gr nanofluids, including the local order of the molecules of the base fluid present in the surroundings of the Gr nanosheets, parallel structure, and π–π stacking. Bahiraei et al. [59] examined the hydrothermal features of an eco-friendly Gr nanofluid flowing in a spiral heat exchanger. The results demonstrated that with an increasing Reynolds number or concentration, the overall HTC and heat transfer rate were increased. Furthermore, the pressure loss was enhanced with an increasing Reynolds number, and the nanofluid exhibited higher pressure losses compared with those using water, especially at high Reynolds numbers. The nanofluids with Gr nanosheets usually have a better convective heat transfer performance than GO nanosheet nanofluids. Indeed, GO nanosheets have sp2-hybridized and sp3-hybridized carbon atoms with epoxide and hydroxyl groups. The presence of the atoms of oxygen and saturated sp3 bonds in the GO nanosheets decreases the TC, promotes phonon scattering, and decreases the heat transfer of nanofluids in reference to the Gr nanosheets. Hu et al. [60] evaluated the pool boiling of Gr nanosheets dispersed in ethylene glycol and water. The authors observed that at lower concentrations, the heat transfer behavior was improved with the increasing concentration of the nanosheets, which was mainly due to the surface wettability enhancement induced by the deposition over time of the nanoparticles. Nonetheless, further enhancements in the concentration decreased the HTC caused by the sedimentation over time in the Gr nanosheets and the resulting blockage of the available nucleation sites. Moreover, at concentrations of Gr inferior to 0.02%, the critical heat flux was increased as the concentration increased. Zhang et al. [61] employed GO/water nanofluids to conduct flow boiling experiments in microchannels. The heat transfer capability was reduced as the concentration increased. The authors argued that the deposition process of GO nanoparticles was intensified with the increasing flow rate, operating temperature, and concentration of the nanoparticles. Table 2 summarizes some recent experimental works on 2D Gr family nanofluids.

Table 2. Recent works on Gr, GO, and hybrid 2D nanofluids.

Reference	Authors/Year	Concentration	Base Fluid	Main Findings	Remarks
[62]	Ahammed et al., 2016	Gr at 0.05%, 0.10%, and 0.15% vol.	Water	Viscosity increased by approximately 47% at 0.15% vol.	Surface tension decrease of approximately 19% at 0.15% vol.
[16]	Das et al., 2019	Gr at 0.1% wt.	Water	17% increase in the TC.	Considerable increase in the viscosity.
[63]	Dong et al., 2021	Gr at 0.2% wt.	Propylene glycol–water Mixture	The TC increased with increasing concentrations until 0.2% wt.	The HTC almost remained unchanged for concentrations above 9.2% wt.
[64]	Borode et al., 2021	Gr at 0.25% wt. and different surfactants	Water	TC increased from 5.5% to approximately 9%, depending on the added surfactant.	Viscosity increased from approximately 6% to 23%, depending on the added surfactant.
[65]	Kanti et al., 2022	GO from 0.05% to 1.0% vol.	Water	14.4% increase in the TC at 1.0% vol.	Good stability over time with the PVP surfactant.

Table 2. *Cont.*

Reference	Authors/Year	Concentration	Base Fluid	Main Findings	Remarks
[66]	Kanti et al., 2022	Gr from 0.05% to 1.0% vol.	Ionic Liquid	27.6% increase in the TC at 0.5% vol. and at 60 °C.	The viscosity of the ionic nanofluids was lower than that of the ionic liquid alone.
[67]	Huminic et al., 2022	Go-Si at 0.25% wt.	Water	A new correlation was proposed for the viscosity.	Improved efficiency in laminar and turbulent flows.
[68]	Ali, 2022	Gr at from 0.01 to 0.1% vol.	Water	125.7% increase in the TC.	5% decrease in the viscosity. Stable after 45 days with the addition of SDS.
[69]	Rahman et al., 2022	Gr functionalized with apple cider vinegar at 0.1% wt.	Clove	24.4% increase in the TC in reference to water.	The TC of the nanofluids was slightly lower than that of the conventional Gr nanofluids.

Further studies on the decrease in the elevated cost of Gr nanomaterials and their derivatives and corresponding nanofluids are highly recommended since the current processing methodologies are very complex and demand the intensive use of chemicals and are otherwise energy consuming. A profound benefit–cost analysis should be performed to evaluate the use of Gr family nanofluids considering the balance between the obtained improvements in the thermophysical properties versus the high initial investment associated with such heat transfer solutions. More experimental works on the high temperature stability of Gr and GO nanofluids are required. In addition, there is a lack of studies on Gr and GO hybrid nanofluids in certain types of nanomaterials, such as metallic and metallic oxides. Innovative techniques based on the surface modification of Gr nanomaterials with hydrophilic groups should be further developed to ameliorate the stability over time of the Gr nanofluids. Additionally, further experimental investigation should be carried out to evaluate conclusively the trade-off between the extremely high values of TC inherent to Gr and derivative nanofluids and the increased density and viscosity leading to higher pressure drops, which are typical in this type of fluid. In this regard, there is a need to pursue the optimal concentration of Gr nanostructures that maximizes the TC of the thermal fluids and, simultaneously, minimizes the density and viscosity enhancements which, considering the published background on the subject, represents a significant challenge. Finally, more life cycle assessments of Gr nanomaterials are required to mitigate the negative impacts on the environment and human health derived from the production, use, and disposal of such materials.

2.3. Carbon Nanotubes

Nanofluids containing CNTs are very promising heat transfer operating fluids in several technological fields. For instance, the use of such nanofluids can improve the efficiency of different types of solar thermal energy collectors due to their enhanced light absorption ability and extremely high TC. The CNTs dispersed in base fluids can ameliorate the thermal performance of several types of thermal management equipment, such as heat exchangers, heat pipes, and thermosyphons to be used in a wide spectrum of applications, including, for instance, the cooling of electronics. CNTs are Gr nanosheets rolled into cylindrical tubes with a diameter of less than 1 nm with a half fullerene-capped end.

Considering the number of consistent tubes, CNTs can be divided into single-walled carbon nanotubes (SWCNTs), double-walled carbon nanotubes (DWCNTs), and multi-walled carbon nanotubes (MWCNTs). SWCNTs are composed of only one tube, whereas DWCNTs and MWCNTs comprise of two and three or more tubes, respectively. The fundamental synthesis techniques of CNTs are laser ablation, arc discharge, and CVD. The preparation method based on laser ablation also uses the evaporation of a rod of graphite with a metallic-based catalyst to produce CNTs. The laser ablation synthesis procedure applies high-energy laser irradiation to heat a carbon substrate, leading to the transition from the solid to the gaseous phase, as the nanomaterial is deposited in a cold trap placed within the synthesis chamber. Using arc discharge methodology, doped graphite rods and catalysts are vaporized at temperature values of up to 5000 K in a closed chamber by an electric arc, resulting in a sediment of CNTs. On the other hand, the CVD decomposes carbonaceous gases on catalytic nanoparticles to fabricate CNTs. The employed catalytic nanoparticles are grown during the synthesis or, alternatively, are produced by a separate procedure. Moreover, the major benefit of the CVD is the improved controllability over the operating parameters, such as the carbon supply rate, temperature of growth, size of the catalytic nanoparticles, and nature of the CNTs growing substrate. The nanofluids with CNTs are used in different solar energy systems, such as PV/T collectors and water heating technology (it has been previously demonstrated that nanofluids with CNTs ameliorate the efficiency of the CSP systems in terms of energy and exergy standpoints). Their performance in solar energy harvesting may be affected by various parameters, such as the type of CNTs, operating conditions, concentration, and involved systems. CNTs have various beneficial features, such as their very high aspect ratio and improved thermal, mechanical, and optical characteristics. The TC of CNTs reaches 6000 W/m·K, which is a much higher value than that of the metals in bulk form. Liu et al. [70] observed that the suspension of CNTs at 1% vol. in ethylene glycol resulted in an enhancement of 12.4% in the TC. This increase was one of approximately 30% in the case of suspending CNTs in engine oil at 2% vol. Furthermore, Sadri et al. [71] evaluated the influence of the type of the surfactant on the TC of MWCNTs dispersed in water at 0.5% wt. The investigation team observed a maximum enhancement in the TC in the case of the nanofluids with MWCNTs of 22.3% compared with water itself. Kumar et al. [72] numerically investigated MWCNTs dispersed in water flowing in a double helically coiled tube heat exchanger, which resulted in an increase of 30% in the Nusselt number when compared with that of water. Apart from their extremely high TC, CNTs also possess favorable optical properties. This makes them suitable for application in solar systems, as the use of colloidal suspensions in CNTs in will result in a spectral absorptivity alteration over the entire solar range. It has been previously demonstrated that incorporating CNTs and their hybrid structures into thermal base fluids can reduce transmittance, which will improve their competence in solar energy systems [73]. For instance, Hjerrild et al. [74] stated that using a nanofluid with CNTs instead of using only water led to a reduction in transmittance between 5% and 10% in the long wavelength and visible spectra. The transmittance reduction was found to depend on the concentration of CNTs in the base fluid. In the experimental work conducted by Gorji et al. [75], absorption spectroscopy was used to determine and compare the radiation absorption of water and functionalized CNTs dispersed in water. The results revealed a higher absorption of radiation when the functionalized CNTs were incorporated into the water. Moreover, the authors confirmed that the increase in the working temperature of the nanofluid promoted a decrease in radiation absorption. The higher absorption characteristics of nanofluids in CNTs makes them favorable for application in solar thermal energy. These nanofluids are suitable in solar energy systems such as collectors, solar ponds, and PV/T devices and systems. Applying nanofluids to these technologies has resulted in their efficiency enhancement and size reduction. Furthermore, the dynamic viscosity of CNT nanofluids deserves special attention from researchers. The rheological properties of water-based carbon nanofluids have been comprehensively studied for heat transfer enhancement and lubricant applications [76].

Studies on rheology included measurements with diverse types of SWCNTs [77] and MWCNTs [78]. Additionally, viscosity measurements on covalently functionalized CNTs have been also reported [79]. CNT suspensions in water are non-Newtonian fluids at comparatively high concentrations. Nonetheless, such nanofluids present a behavior close to the Newtonian one in the region dominated by low concentrations [80]. The CNTs possess extreme aspect ratios, considerably exceeding those of metal rods, cylinders, and discs. The viscosity of dilute CNT dispersions has been correlated with the length of the CNTs [81]. Ansón-Casaos et al. [82] evaluated the viscosity of 1D diluted CNTs dispersed in water, performing viscosity measurements on the nanofluids of CNTs and functionalized CNTs. One type of functionalized CNT was directly suspended in water, and the other CNTs and functionalized CNTs were dispersed with the aid of surfactants. The authors evaluated the viscosity of the nanofluids based on the aspect ratio of the CNTs using prediction models. The CNT aspect ratio can be defined as the ratio between the size of the nanotube along a symmetry rotation axis and its perpendicular diameter. For CNTs, the aspect ratio parameter is the ratio between the nanotube length and its diameter and was found to be much larger than one. The authors concluded that the experimentally measured viscosity of the dilute CNTs could be fitted into the Maron–Pierce model [83] as a function of the concentration of the nanotubes and working temperature. The experimental data obtained for the CNTs agree well with the theoretical predictions through first principles that determine the intrinsic viscosity as a function of the aspect ratio. It was argued that the aspect ratio is the main factor in the evaluated range. The surface functionality implied only a minor correction, as it does not provoke considerable aspect ratio modifications. Table 3 summarizes some studies on CNT 2D nanofluids.

Table 3. Some studies on 2D CNT nanofluids and hybrids.

Reference	Authors/Year	Concentration	Base Fluid	Main Findings	Remarks
[84]	Kumaresan and Verlaj, 2012	MWCNTs at 0.15%, 0.30%, and 0.45% vol.	Water and ethylene glycol mixtures	Approximate 19.8% increase in the TC.	Maximum specific heat capacity increase at 0.15% vol.
[85]	Glory et al., 2013	MWCNTs from 0.01% to 3% wt.	Water	64% increase in the TC at 3% wt.	The TC increase was temperature independent up to 2% wt. of MWCNTs.
[86]	Fadhillahanafi et al., 2013	MWCNTs at 0.5% wt.	Water	22.2% increase in the TC.	Addition of 0.01% wt. of PVP surfactant.
[87]	Tong et al., 2015	MWCNTs at 0.25% wt.	Water	4% increase in the efficiency of an enclosed-type U-tube solar collector.	Considerable decrease in CO_2 emissions.
[88]	Delfani et al., 2016	MWCNTs at 25, 50, and 100 p.p.m.	Water and ethylene glycol mixtures	From 10% to 29% increase in a direct absorption solar collector.	The efficiency of the collector increased with an increasing concentration and flow rate.
[89]	Esfe et al., 2017	MWCNTs-SiO_2 at 0.05% to 1.95% wt.	Ethylene glycol	Increase of 22.2% in the TC at 1.94% wt. and at 50 °C.	A correlation was proposed based on the temperature and concentration for the TC of the hybrid nanofluids.
[90]	Mahbubul et al., 2018	SWCNTs at 0.05%, 0.1%, and 0.2% vol.	Water	10% increase in the efficiency of a tube solar collector in reference to the water alone.	Critical solar irradiance of 900 W/m^2, after that no considerable enhancement was verified.

Table 3. *Cont.*

Reference	Authors/Year	Concentration	Base Fluid	Main Findings	Remarks
[91]	Hammed et al., 2019	MWCNTs at 0.1% wt.	Kapok seed oil	Approximate 6.2% increase in the TC.	TC accurately predicted by the Khanafer and Vafai model.

Further and conclusive experimental works on the inclusion of hybrid CNT formulations in solar thermal energy conversion and harvesting systems and in the nanofiltration of PV/T systems are welcome. There is a lack of studies on the use of CNT nanofluids in some specific heat transfer technologies, such as solar saline water desalination. Furthermore, research must prioritize the search for innovative synthesis procedures using new surfactants to mitigate the absence of the stability over time in the CNT nanofluids. Further studies regarding the impact of the size of CNTs on the thermophysical characteristics of the corresponding nanofluids are required. This factor should be comprehensively analyzed within the scope of the energy and exergy efficiencies of solar thermal energy systems, and not only with regard to its influence on heat transfer enhancement features. Moreover, further studies on the potential miniaturization and entropy generation of heat transfer systems should be experimentally and numerically undertaken to encourage some conclusive research on this matter.

2.4. Tungsten Disulfide

Tungsten disulfide nanostructures can be synthesized using different methods. These methods are presented in Figure 5.

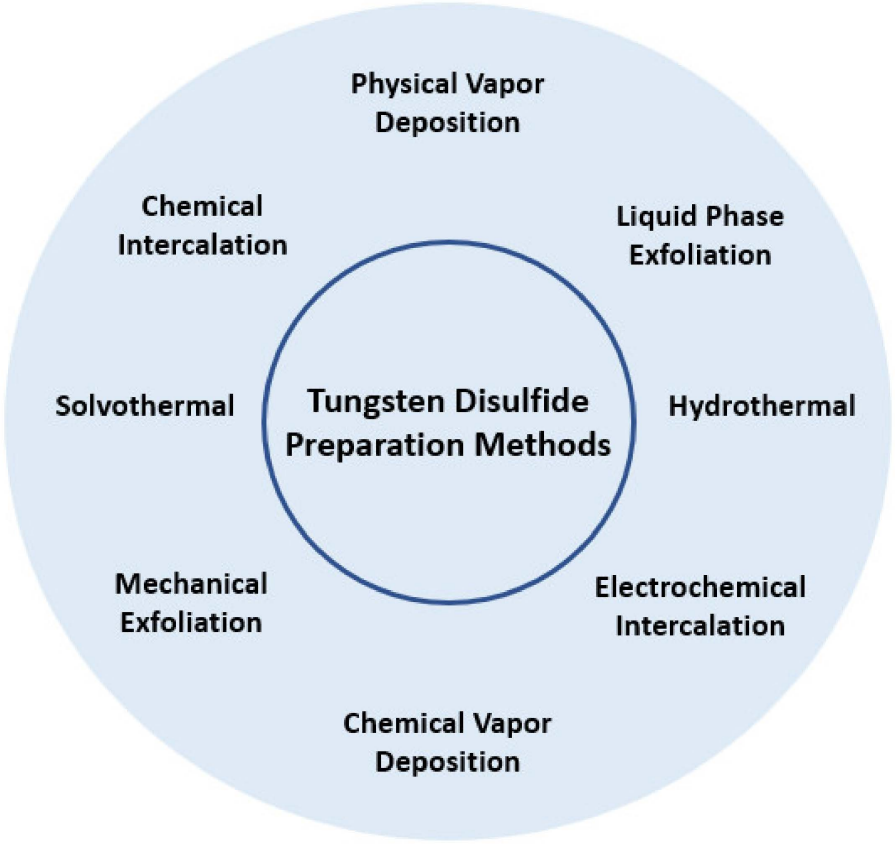

Figure 5. Main tungsten disulfide preparation methods.

WS_2 nanofluids are promising in heat transfer applications within the CSP technological field. WS_2 nanosheets are well-defined and highly stable, and do not significantly alter certain characteristics such as the surface tension, friction coefficient, viscosity, and Reynolds number of heat transfer systems. The incorporation of WS_2 may improve the TC of synthetic oil base fluids by approximately 30%. Additionally, the authors Martínez-Merino et al. [92] prepared 2D WS_2 nanosheet-based nanofluids with the oil commonly used as heat transfer fluid in CSP stations. The surfactants cetyl-trimethylammonium CTAB and polyethylene glycol PEG-200 were added to the nanofluids to improve the exfoliation procedure and the stability over time of the colloidal suspensions. The experimental results showed that an increase in the ultrasonication duration and the amount of the surfactant enhanced the stability over time of the nanofluids prepared with the surfactant CTAB. Furthermore, in the nanofluids synthesized with the surfactant PEG-200, the increase in the surfactant amount was the main factor contributing to the high concentration of stable nanomaterial suspended in the thermal oil. The size of the agglomerates in the stable nanofluids prepared with the addition of CTAB was between 200 nm and 250 nm, whereas in the PEG-200 nanofluids, the same measurement was approximately 180 nm. Furthermore, the viscosity of the oil base fluid increased to a maximum of only 1.5% with the nanosheets of WS_2 and the surfactant. This minor increase would not result in considerable pressure-drop concerns in the circuits of the CSP plants. Moreover, the nanofluid with a concentration of 0.75% wt. of surfactant PEG-200 with four hours of ultrasonication (Case A) and the 0.01% wt. CTAB with eight hours of sonication (Case B) showed enhancements of 33% and 29% TC, respectively, compared with that of the thermal oil itself. Furthermore, the nanofluid in Case A was found to have a specific heat value 6.5% higher than that of the heat transfer fluid alone. The improvement in the specific heat and TC resulted in an enhancement in the HTC of 21% in the Case A nanofluid and of 17% in the Case B nanofluid when compared with that of the oil itself. On the other hand, a numerical analysis demonstrated that the efficiency of the CSP facilities was enhanced by up to 31% or 18% if the Case B or Case A nanofluids, respectively, are used compared with the commonly employed thermal oil. The predicted efficiency for a volumetric collector working with 2D WS_2 nanofluids is a slightly lower than the efficiency of a surface collector operating with nanofluids; however, such efficiency is higher than that achieved using the surface collector with the thermal oil commonly used at the present time. All in all, the authors believe that the WS_2-developed nanofluids are a promising alternative to the thermal oil commonly used in solar energy plants and would enable the adoption of volumetric collectors, which are less costly than traditional surface collectors. In the work conducted by Shah et al. [93], 2D nanofluids with WS_2 volume fractions of 0.005% vol., 0.01% vol., and 0.02% vol., together with the surfactants sodium dodecyl sulfate (SDS), sodium dodecylbenzene sulfonate (SDBS), and CTAB surfactants at 0.05, 0.5%, 1%, and 2% were synthesized and characterized. The authors arrived at the following main conclusions:

- The maximum enhancement in the agglomerate sizes were of 172%, 245%, and 261% with 0.005% WS_2 and 2% SDS, 0.01% WS_2 and 2% SDS, and 0.02% WS_2 and 0.05% SDS, respectively. Collectively, the zeta potential saw an improvement of 554%, whereas the mean particle size presented an enhancement of up to 411% mainly caused by the adsorption of the surfactant molecules. This would entail a long-term agglomeration risk, resulting in the clustering and sedimentation of nanoparticles.
- The maximum TC increases were approximately 2.8%, 1.9%, and 4.5% for combinations of 0.05% SDS and 0.005% WS_2 at temperature values of 25 °C, 50 °C, and 70 °C, respectively. The authors argued that the TC reduced with increasing concentrations of the SDS. Alongside the 0.005% of WS_2 filler concentration, the higher fractions of 0.01% and 0.02% of WS_2 also exhibited higher TC enhancements with lower concentrations of surfactant.
- The high-temperature condition revealed a pendular behavior concerning the TC. The reason behind this response may be the eventual detachment of the surfactant molecules and further interaction with the WS_2 nanosheets.

- The rheological analysis confirmed the formation of a nanostructured network inside the nanofluids with WS_2 nanosheets and depicted the transition of the nanofluids from viscous to elastic behavior with the inclusion of surfactants. Such transition suggests that a higher pumping power was required to initiate the flow of the working fluid. The maximum decrease in viscosity of 8.2% was found at the minimum concentration of 0.005% vol. of WS_2, confirming the superior fluidity of the developed nanofluids. This reduction was amplified at a concentration of 0.05% vol. of SDS, enlarging the referred value by approximately 10.5%.
- The developed nanofluids evolved from non-Newtonian to Newtonian behavior under a 10 s^{-1} shear rate.

The most prominent conclusion is that surfactants, such as SDS, provide their steric hindrance effect to produce a more uniform dispersion of the WS_2 nanosheets in the ethylene glycol base fluid and contribute to the interfacial tension reduction in the nanofluids, which may also promote a decrease in the viscosity of the system. On the other hand, the WS_2 nanoparticles have already demonstrated [94] great potential as fillers in lubricating and engine oils. WS_2 has shown improved lubricity due to the weak intermolecular interactions among the nanosheets, causing easy shearing with a fullerene-like structure. In lubrication, one of the main factors of the 2D nanofluids that contributes the most towards their lubricating ability is the amount of nanosheets present in the base fluid, as illustrated in Figure 6.

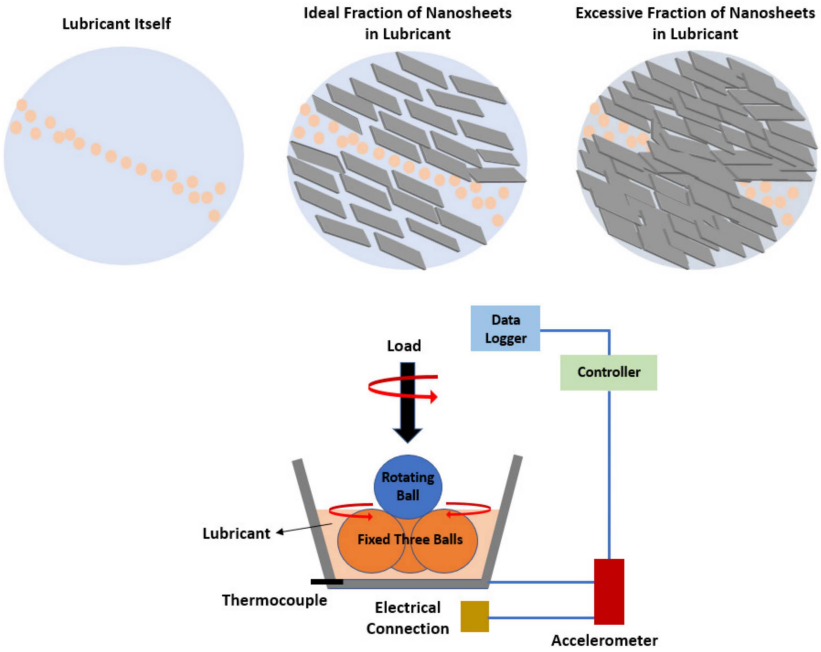

Figure 6. Schematic diagram of a four-ball tribometer and effect of the concentration of nanosheets.

However, more molecular dynamics are required for the WS_2 nanostructures dispersed in the synthetic oils most commonly used in CSP plants, which are a mixture of biphenyl and diphenyl oxide, to provide useful insights into the heat transfer capability of WS_2 nanofluids. The decoration of WS_2 requires further theoretical and experimental confirmation, given that the decoration of the WS_2 edge may induce considerable beneficial effects on the rheological and heat transfer characteristics of WS_2 nanofluids. Furthermore, there is a lack of published studies considering the interactions between the surfactants, incorporated nanostructures, and liquid medium used in the liquid phase exfoliation of WS_2 nanosheets. For instance, numeric analyses based on density functional theory determinations and electron localized functions are welcome to better understand the WS_2 liquid phase exfoliation process.

2.5. Molybdenum Disulfide

MoS2 nanofluids have already proven to be an attractive option for application in, for instance, volumetric parabolic trough collectors. These nanofluids can improve by 5% or more the thermal efficiency of such collectors and, at the same time, reduce the initial required pumping power by around one-fifth. Furthermore, the use of MoS2 nanofluids diminishes the thermal stress on volumetric receivers and the overall required investment. Molybdenum disulfide is a 2D transition metal dichalcogenide with MX_2 as chemical formula, where X denotes a chalcogen, such as sulfur, selenium, and tellurium, and M denotes the transition metal. MoS_2 possesses improved thermal and chemical stabilities. It can be applied as a catalyst and lubricant because of its superior characteristics, including inertness, anisotropy, and photocorrosion resistance. MoS_2 nanostructures have good thermophysical properties and great anti-friction properties, making it a promising material as reinforcement in the cooling process of nanofluids. Moreover, parameters including the type and concentration of nanoparticles, the nature of the base fluid, the synthesis procedure, and the stability/surfactant addition balance affect the thermophysical characteristics of the nanofluids, including the viscosity and thermal transport. Su et al. [95] investigated the thermal stability of MoS_2 in water and oil nanofluids at weight fractions from 0.01% wt. to 0.5% wt. The authors found that with the enhancement in the amount of MoS_2, the TC of the nanofluids was increased. The investigation team also reported that the TC improvement was higher in water-based nanofluids than in oil-based nanofluids. This fact was explained as the consequence of the improved dispersion and stability over time of the water nanofluids. Nagarajan et al. [96] prepared MoS_2 nanosheets to be suspended in SAE 20W50 diesel engine oil to produce an effective lubricant. MoS_2 nanoparticles were synthesized using a microwave hydrothermal reactor. The schematic diagram of the synthesis procedure is presented in Figure 7.

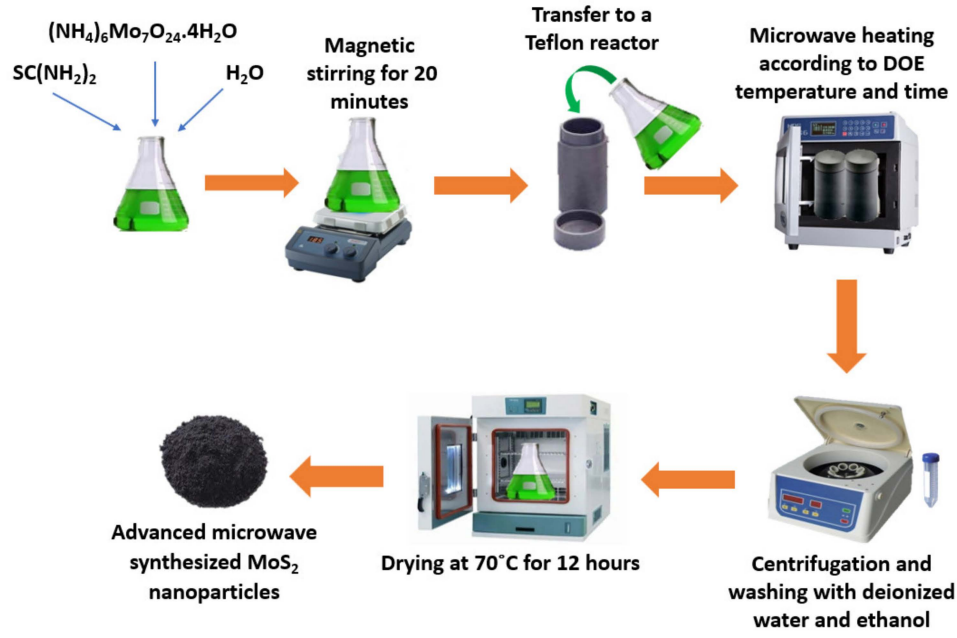

Figure 7. Schematic diagram of microwave-synthesized molybdenum disulfide nanoparticles. Adapted from [96].

The tribological and oxidation analysis showed that the lubricant with a weight fraction of 0.01% wt. of MoS_2 nanoparticles provided better results than those of other concentrations and, hence, the nanofluid with this fraction was further evaluated for its TC. The authors reported an improvement in the TC of the 0.01% wt. nanofluid of approximately 10% compared with that of the base engine oil alone. Due to the lower amount of the MoS_2 nanoparticles, the enhancement in the TC was due to the molecular collisions between the

oil and the nanoparticles. The researchers argued that the TC behavior indicated that this enhancement was due to the Brownian motion of the nanosheets. The TC and heat transfer capability of a nanofluid depend on the Brownian motion of the incorporated nanoparticles. Indeed, the Brownian motion-driven convection and effective thermal conduction by the percolating paths mechanism of the nanoparticles are the most likely factors that promote the improved heat conduction in nanofluids. The percolation mechanism involves the formation of thermal conductive paths based on the enhanced thermal conductance that improves the overall TC. A schematic diagram of the percolation mechanism is presented in Figure 8. The Brownian motion allows the direct solid–solid transport of heat from one particle to the adjacent one, resulting in an increase in the thermal conductivity. The Brownian motion and resulting micro mixing of the nanoparticles and clusters, as well as aggregation kinetics of nanoparticles and clusters, are the main issues in the evaluation of the thermal conductivity of nanofluids. Any effort to understand the behavior of nanofluids is not complete without considering at the same time all these effects. Accordingly, the thermal transfer of the colliding nanoparticles increased the TC of the lubricant. This is why the TC of the lubricant increased more than that of the engine oil for temperature values higher than 60 °C, given that a more intense Brownian motion of the nanoparticles takes place.

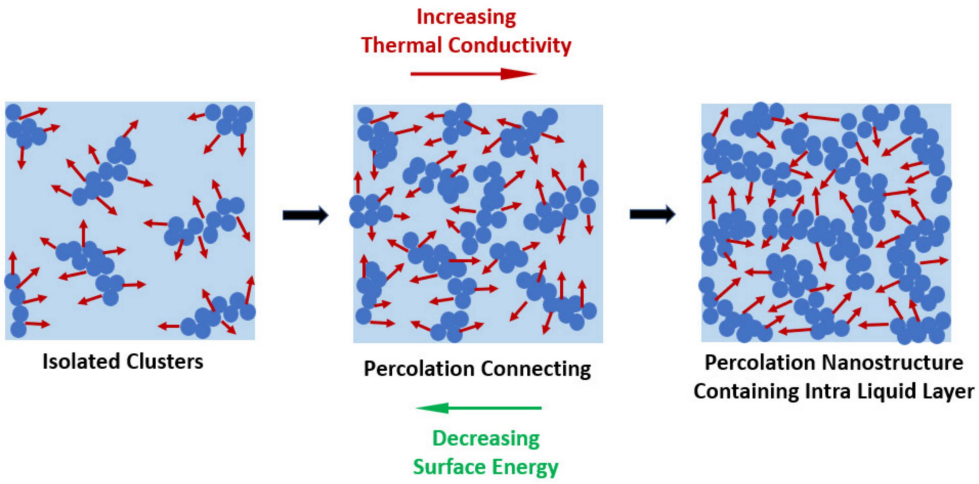

Figure 8. Schematic diagram of the percolation mechanism of nanofluids.

Zeng et al. [97] synthesized lipophilic MoS_2 nanoparticles through surface modification using stearic acid and prepared molybdenum disulfide/heat transfer oil *B350* 2D nanofluids with weight fractions of the nanoparticles from 0.25% wt. to 1.0% wt. The researchers found that the TC of the nanofluids changed by increasing the concentration of the nanoparticles and by increasing the temperature from 40 °C to 180 °C. The obtained results from the laser flash method show that TC enhancement achieved a maximum of 38.7% at 1.0% wt. and at 180 °C. Furthermore, TC enhancement was reduced in cases where the temperature was near the flash point of the base oil. The investigation team argued that the long-term stability and improved TC make the lipophilic MoS_2 nanoparticles a very promising filler to be used in thermal performant situations. Table 4 presents some recent studies regarding 2D MoS_2 nanofluids.

There is a lack of experimental works concerning MoS_2 nanofluids and their ability to optimize CSP stations with the generalized use of volumetric collectors, which are more thermally efficient and cost effective than surface collectors. Further studies are recommended to achieve a better understanding of the mechanisms associated with the formation of percolation paths and their contribution towards the enhanced TC of MoS_2 nanofluids.

Table 4. Recent studies on 2D MoS_2 nanofluids.

Reference	Authors/Year	Concentration	Base Fluid	Main Findings	Remarks
[98]	Shah et al., 2022	MoS_2 at 0.005%, 0.0075%, and 0.01% vol.	Ethylene Glycol	11% increase in the TC.	Approximately 14.7% maximum decrease in the viscosity at 50 °C and at 0.005% wt.
[99]	Arani and Sadripour, 2021	MoS_2 at up to 4% wt.	Water	The performance evaluation criterion of a solar collector at 3% wt. and brick-shaped nanoparticles was of 1.269.	Higher pressure losses for the nanoplatelets than for the brick-shaped nanoparticles.
[100]	Martínez-Merino et al., 2019	MoS_2	Byphenil and diphenyl oxide mixture	46% increase in the TC. 4.7% increase in the specific heat capacity. 3.2% increase in the viscosity.	21.3% increase in the efficiency of solar collectors.

2.6. Titanium Carbide MXene

MXene nanofluids possess great potential in solar thermal energy conversion and harvesting. Alongside enhanced heat transfer properties, MXene nanofluids present a high extinction coefficient, giving them an enhanced solar light absorption capability. Single-layer and thin-layer MXene nanofluids have a higher specific surface area and surface chemistry richness than their multilayer counterparts, which provides nanofluids of the MXene family with the highest stability and TC. Furthermore, a novel type of two-dimensional nanocrystalline carbide transition metal materials designated by MXene (Ti_3C_2) has already been synthesized [101]. Two-dimensional MXene is hydrophilic and can be etched selectively from its MAX-phase structure, where M represents an early transition metal such as titanium, A represents one of the A-group elements (e.g., aluminum), and X represents carbon or nitrogen. The employment of the environmentally benevolent MXene is common for different purposes in diverse research areas. Figure 9 schematically presents the acid etching and ultrasonication synthesis method for obtaining 2D MXene nanosheets dispersed in a base fluid.

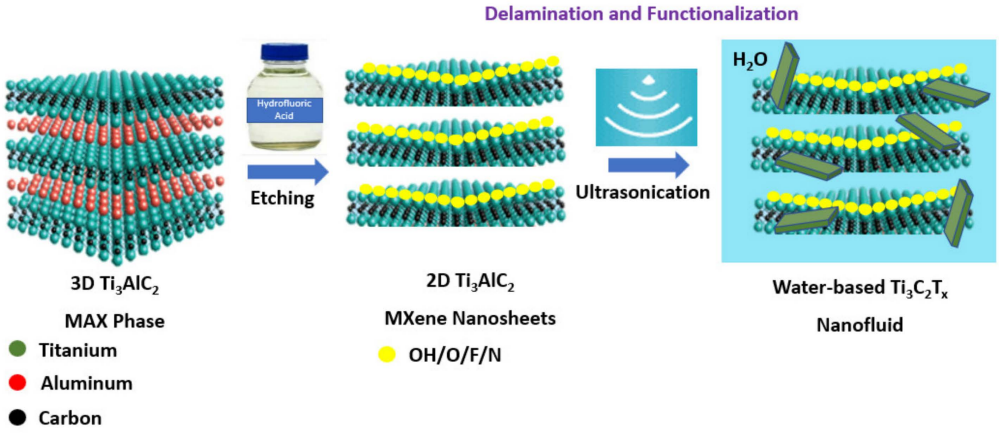

Figure 9. Schematic diagram of the synthesis procedure of MXene nanosheets in a water-based nanofluid.

Evaluations of the thermophysical characteristics of the MXene nanostructure have focused mainly on its solid phase, and only a few studies have investigated its corresponding nanofluid capability. Nevertheless, the study carried out by Rafieerad et al. [102] assessed the thermophysical properties of Ti_3C_2Tx MXene with non-covalent Gr nanoparticles and covalently functionalized COOH- and NH2-Gr nanoparticle nanofluids. The authors synthesized and studied the microstructure and thermophysical properties of different water-based nanofluids with 2D metal-carbide MXene and nanosheets of Gr. The obtained results confirmed the superior TC of MXene nanofluids compared with that of the Gr nanofluids. There were also observed increases in the TC and density at a concentration of nanosheets of 0.2 mg mL^{-1}, which were provided by the high surface area of these nanostructures. In addition, the authors used lamellar MXene membranes with an improved photothermal ability to demonstrate the heat-driven and light-induced ion transport in nanofluidic systems and their capabilities in osmotic energy system amelioration. Considering they were working under a salinity gradient, performant directional ion transport was employed to obtain an enhanced osmotic energy conversion output exhibiting appreciable results, such as the output power density increase of 1.68 $mW \cdot m^{-2}$, which is a pathway towards better harvesting of the salinity gradient energy and towards promote the physical stimuli-facilitated, ion-related mass transport and energy conversion. Moreover, the stability over time, the TC, and electrical conductivity of MXene nanofluid would enable its wide application in advanced heat transfer systems. In the experimental work conducted by Rubbi et al. [103], a 2D nanofluid composed of MXene nanoparticles at weight fractions from 0.025 to 0.125% was developed, using soybean oil as the base fluid. The main steps of the preparation method used are presented in the schematic diagram of Figure 10.

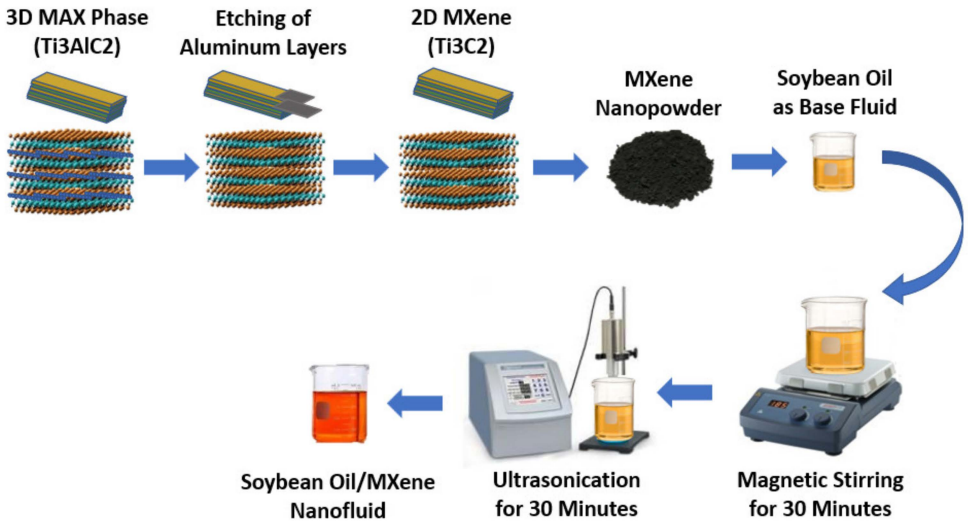

Figure 10. Main steps of the preparation of the MXene/soybean oil 2D nanofluid. Adapted from [103].

Considering the potential application of the developed nanofluid in a hybrid PV/T solar collector system, the investigation team reported that the nanofluid was thermally stable up to 320 °C and it possessed a TC value of 0.125% wt. that was 60.8% higher than that of the soybean oil base fluid. The maximum augmentation of the specific heat of the nanofluids was reported to be 24.5% at a 0.125 weight fraction. Furthermore, the density and viscosity of the nanofluid both changed with the inclusion of nanoparticles by 1% and 13.3%, respectively. Nevertheless, these properties decreased significantly at high temperatures and exhibited Newtonian behavior up to 100 s^{-1} shear rates. Furthermore, the implementation of the prepared nanofluid on a PV/T system was tested using a numerical approach using COMSOL Multiphysics v. 5.5 software. The obtained results demonstrated that the use of the developed nanofluid resulted in a considerably improved performance

compared with the operating fluids of water, alumina/water, and MXene/palm oil. One of the optimized outcomes was that the overall thermal efficiency achieved 84.3% using the developed nanofluid with a 0.07 Kg.s^{-1} mass flow rate. Furthermore, the electrical output of the PV/T system was increased by 15.4% compared with the alumina in water nanofluids under an irradiance of 1000 W.m^{-2} and a mass flow rate of 0.07 kg/s. The HTC was enhanced with rising mass flow rate and the maximum enhancement of 14.3% was found at 0.06 kg.s^{-1} for the nanofluid compared with that of the alumina/water nanofluid. Additionally, Aslfattahi et al. [104] manufactured a nanofluid composed of MXene nanoparticles dispersed in silicone oil to be used in a concentrated solar photovoltaic thermal (CSPT) collector. The researchers found a considerable maximum TC enhancement of 64% at a 0.1% weight fraction of nanoparticles compared to that of the silicone oil itself. The authors also stated that the viscosity of the nanofluids was independent of the incorporation of MXene into the silicone oil and decreased with increasing temperature. Indeed, the viscosity was reduced by 37% in the case where the temperature was increased from 25 °C to 50 °C at different weight fractions of MXene, which was a promising result since the viscosity decrease will reduce the required pumping power in the system. Moreover, the research team also found that the synthesized nanofluid at a 0.1% weight concentration had thermal stability up to 380 °C. The most improved electrical efficiency of the CSPT collector was obtained when using the nanofluid with 0.1% wt. Adding more MXene nanoparticles into the silicone base oil will enhance the electrical efficiency of the PV cells because of the improved cooling of MXene nanofluids. Higher solar concentration resulted in a PV module with a higher average temperature, which in turn will raise the thermal energy gain. Table 5 presents some recently published works on 2D MXene nanofluids and hybrid forms.

Table 5. Recent studies on 2D MXene nanofluids and hybrids.

Reference	Authors/Year	Concentration	Base Fluid	Main Findings	Remarks
[105]	Wang et al., 2021	MXene at 5, 10, 20, 40, and 60 p.p.m.	Water	Maximum of 63.4% in the photothermal conversion efficiency at 20 p.p.m.	Near-zero spectral transmittance at 60 p.p.m.
[106]	Bakthavatchalam et al., 2021	Mxene at 0.1%, 0.2%, 0.3%, and 0.4% wt.	Diethylene Glycol and Ionic Liquid Mixtures	Increase of 78.5% in the PV/T thermal efficiency.	Increase of 6% in the PV/T heat transfer coefficient.
[107]	Das et al., 2022	MXene-Al_2O_3 at 0.05%, 0.1%, and 0.2% wt.	Therminol 55	61.8% increase in the TC.	Approximate 17.1% increase in the viscosity.
[108]	Said et al., 2022	MXene at 0.05%, 0.08%, and 0.1% wt.	Silicone Oil	Approximate 70% increase in the TC at 25 °C and near 89% at 150 °C and at 0.1% wt.	Approximate 0.50% increase in the viscosity at 25 °C and near 2.4% at 150 °C and at 0.1% wt.
[109]	Arifutzzaman et al., 2023	MXene-functionalized Gr at 0.02% wt.	Silicone Oil	Approximate 68% increase in the TC.	Thermal stability up to near 393 °C. The viscosity decreased by approximately 31 with the increase of 25 °C in the temperature.

Table 5. *Cont.*

Reference	Authors/Year	Concentration	Base Fluid	Main Findings	Remarks
[110]	Sundar et al., 2023	MXene at from 0.1% wt. to 1.0% wt.	Water and Ionic Liquid Mixture	56.6% increase in the TC at 1.0% wt.	Approximate 18% increase in the viscosity at 1.0% wt.
[111]	Qu et al., 2023	MXene at from 10 to 300 p.p.m.	Water	63.5% increase in the photothermal conversion efficiency at 220 p.p.m.	Approximate 12% increase in the temperature rise at 220 p.p.m.

MXene formulations, rather than Ti3C2Tx, should be considered in future studies on MXene nanofluids. More practical measures are required to understand and improve the oxidation resistance of the MXene family, which is a relevant issue when studying the long-term stability of nanofluids containing MXene. Apart from solar thermal energy conversion and storage, new applications of MXene nanofluids should be explored. Moreover, there is a lack of studies regarding economic analyses, operating uncertainties, and the impacts on the environment and human health through a life cycle assessment. Finally, more bio-friendly solutions should be explored, such as dispersions of MXene nanostructures in palm oil.

2.7. Hybrid

The use of hybrid nanofluids as nanocomposite fillers are a promising but not completely studied route. Indeed, hybrid nanofluids may utilize the synergistic overall effect of the combined usage of two or more types of nanomaterials and related nanostructures, and they are capable of surpassing the beneficial thermophysical features of the traditional mono suspended nanofluids. This results in the improved heat transfer and thermal storage capacities of hybrid nanofluids, which also enables the miniaturization of thermal management devices and systems. Examples include the hybrid formulations of graphene or graphene oxide nanofluids with a very wide spectrum of possible coupling arrangements with different nanomaterials from the hematite to the cotton seed green nanocomposite. Askari et al. [112] prepared hybrid nanofluids with Fe_3O_4/Gr nanoparticles dispersed in water and studied their TC. As a result, the researchers reported an increase of 32% in the TC at 40 °C for the nanofluid with a weight fraction of 1% wt. The investigation team also evaluated the heat transfer behavior of the nanofluids in a tube heat exchanger, reporting an increase of 14.5% in the HTC for the nanofluid with 0.1% wt. under a regime defined by a Reynolds number of 4248 compared to that of the water alone. The viscosity of the 0.5% wt. nanofluid was 1.15 mPa·s at 20 °C, which is not significant when considering its potential applications. In the experimental work performed by Barai et al. [113], a rGO/Fe_3O_4 nanocomposite was synthesized using ultrasonication. The nanocomposite had a nearly spherical morphology with 10 to 20 nm-sized Fe_3O_4 nanoparticles finely dispersed on the rGO nanosheets. This fine dispersion was due to the collapse of the cavities provoked by the sonication process, which in turn led to the formation of shock waves, intense mixing, shearing action, and turbulence, which causes the total exfoliation of the rGO nanosheets. The synthesis procedure of the rGO-Fe_2O_3 nanocomposite is schematically illustrated in Figure 11.

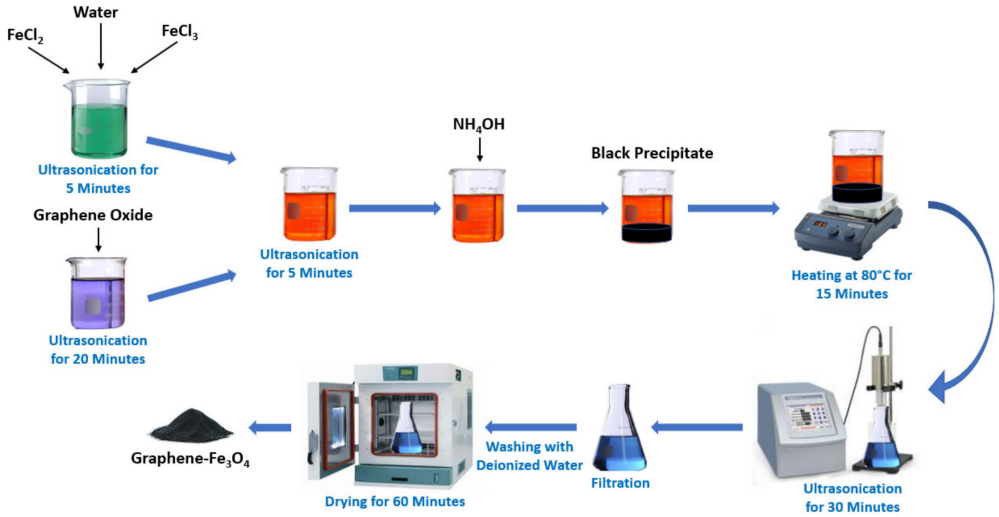

Figure 11. Schematic diagram of the rGO-Fe_2O_3 nanocomposite. Adapted from [113].

The authors prepared nanofluids with diverse volume fractions between 0.01% vol. and 0.2% vol. of the referred composite nanoparticles suspended in water and studied the TC and viscosity of the nanofluids at temperature values ranging from 25 °C to 40 °C. In addition, a study of convective heat transfer was also performed considering the 0.01% vol. and 0.02% vol. of the rGO-Fe_3O_4 nanofluid and a pressure-drop analysis comparing the water and the 0.01% vol. nanofluid. The authors found that the developed nanofluids exhibited a significant enhancement in the TC of 83.4% for the 0.2% vol. nanofluid at 40 °C. It was also confirmed that for a given volume fraction of the nanoparticles in the base fluid, the TC increased with the rising temperature values. This evidence was interpreted based on the intensification of the Brownian motion associated with the nanoparticles with increasing temperature, resulting in greater heat dissipation induced by the nanoparticles. With increasing temperature, the surface energy of the nanoparticles decreased, hence diminishing their agglomeration and the viscosity of the nanofluid, leading to a greater Brownian motion of the nanoparticles. Thus, the TC changed from 9.21% at 25 °C to 83.44% at 40 °C for the 0.2% vol. nanofluid. Furthermore, it was also observed that an increase in the concentration of the rGO-Fe_3O_4 nanoparticles led to a greater TC. The nanoparticles as solids suspended in fluids are continuously in motion and can be considered as heat carriages transporting the energy in the form of heat and as natural involuntary stirrers that induce the convection process to enhance the TC of the nanofluids by increasing the motion of the particles and, consequently, the collisions between them. On the other hand, the specific heat of the 0.2% vol. nanofluids decreased by 0.25% compared with that of the water itself. It has already been argued that the existing interactions at the interface between the nanoparticles and the base liquid are paramount for the reduction in the specific heat of the nanofluids. An increase in the number of nanoparticles alters these collisional effects and, in turn, the heat transfer by conduction. Furthermore, the rheological analysis of the nanofluids revealed a shear thinning non-Newtonian behavior. In addition, the HTC increased from 3444.1 $W/m^2 \cdot K$ at 0.01% vol. to 4289.5 $W/m^2 \cdot K$ at 0.02% vol. at the outlet and at a Reynolds number of 7510 ± 5. The HTC also increased from 1043.3 to 4289.5 $W/m^2 \cdot K$ with the enhancement of the Reynolds number from 940 to 7510 ± 5 at a volume fraction of 0.02% vol. Finally, it was revealed that the nanofluids had a negligible impact on the pressure drop and friction factor, which suppresses any need for additional pumping power requirements. Mbambo et al. [114] synthesized nanofluids with gold nanoparticle-decorated Gr nanosheets dispersed in ethylene glycol. The Gr/gold nanohybrids were prepared using a pulsed Nd:YAG laser to ablate a bulk graphite substrate followed by the gold in the ethylene glycol. The synthesis method is depicted in the schematic diagram of Figure 12.

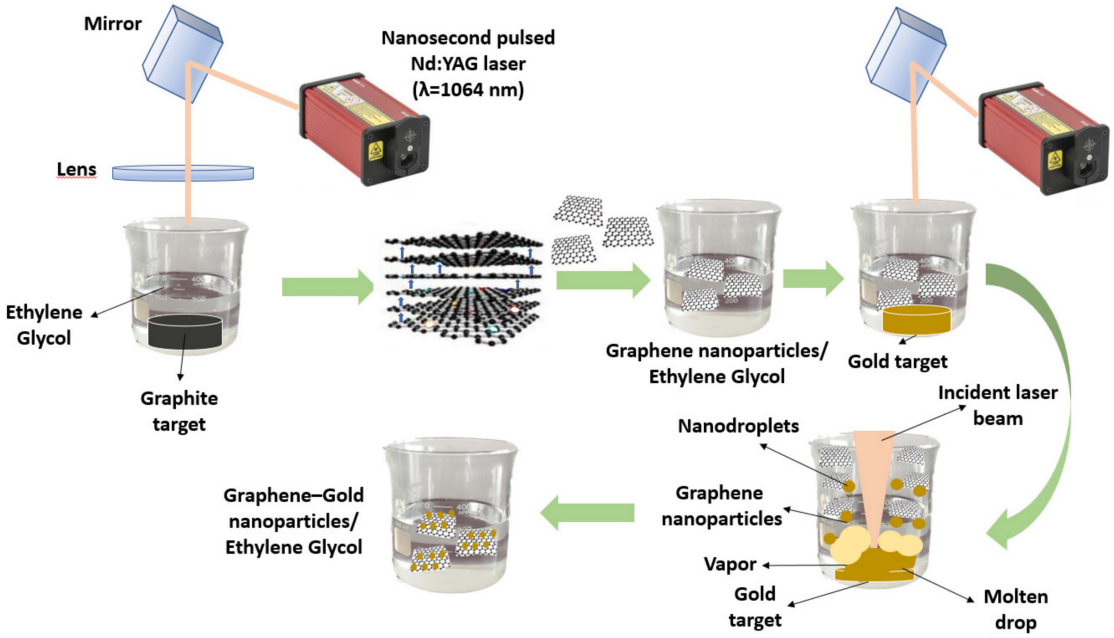

Figure 12. Preparation method of the Gr-gold nanoparticles in ethylene glycol 2D nanofluid. Adapted from [114].

Furthermore, TC measurements in the temperature range of 25–45 °C revealed that the Gr-gold/ethylene glycol 2D nanofluid possessed an enhanced TC of 0.41 $W \cdot m^{-1} \cdot K^{-1}$ compared with that of the Gr/ethylene glycol nanofluid at 0.35 $W \cdot m^{-1} \cdot K^{-1}$, gold/ethylene glycol nanofluid at 0.39 $W \cdot m^{-1} \cdot K^{-1}$, and ethylene glycol alone at 0.33 $W \cdot m^{-1} \cdot K^{-1}$. The TC of the ethylene glycol and Gr/ethylene glycol nanofluids showed enhancements of 1.8% and 3%, respectively, with rising temperature values between 25 °C and 45 °C. The ethylene glycol base fluid possesses poor heat transfer features [115], and the increase found in the Gr/ethylene glycol TC with temperature may be caused by a decrease in the interfacial thermal resistance between the ethylene glycol and the nanoparticles at higher temperatures, and to the high TC of Gr. Additionally, alterations in the TC as a function of the temperature are expected to be caused by the Brownian motion of the nanoparticles [116]. The Gr–gold/ethylene glycol nanofluid exhibited a TC increase of up to 26% in the temperature values between 25 °C and 45 °C compared with the base fluid itself. This increase is higher than those numbers previously reported for Gr composite-based ethylene glycol nanofluids. The authors explained the TC of the developed nanofluid based on the synergistic effect between the gold nanoparticles and the Gr, which both possess intrinsic high thermal conductivities. The obtained results show this hybrid nanofluid to be suitable for improved heat transfer purposes. Furthermore, in the work carried out by Taha-Tijerina et al. [117], 2D nanofluids with synthetic and natural esters were prepared as base fluids with h-BN nanosheets, MoS_2 nanosheets, and hybrid h-BN/MoS_2 filers. The nanofluids were synthesized with weight fractions of 0.01, 0.05, 0.10, 0.15, and 0.25% wt. The incorporation of the MoS_2 into natural esters showed an ameliorated evolution of the TC similar to that of h-BN. Moreover, the addition of the h-BN/MoS_2 nanohybrid to natural esters resulted in considerable enhancements in the TC with maximums of 0.25% wt. of 30% for the FR3 base fluid and 32% for the VG-100 base fluid. The authors argued that the h-BN contributed towards the improvement of the TC and the MOS_2 contributed towards the reinforcement of the fluid, which helped to obtain a homogeneous dispersion of the fillers because of its superior lubricant properties. It was proposed that the verified TC increase was caused by the percolation mechanism and by the Brownian motion of the included nanosheets. In cases where the fraction of the 2D nanostructures was augmented in the synthetic or natural esters, the probability of the phonons being scattered into the adjacent nanostructures increased proportionally, leading to increased

contact conductance. In addition, thermal conduction channels were formed that may enhance the TC because of the percolation mechanism. The heat transfer capability between colliding structures may enhance the TC of the nanofluids. Indeed, a higher temperature value corresponds to a stronger Brownian motion. Consequently, at a temperature of 323 K, the TC of the developed nanofluids was more evident than at other temperature values. The liquid layering at the interface between the 2D nanostructures and the base fluid can also contribute towards TC enhancement. Furthermore, at room temperature it was observed that the impact of the combined usage of h-BN and MoS_2 was similar to that of the single component reinforcements. Nevertheless, the TC became higher than that of the single component nanofluids with increasing temperature. Yarmand et al. [118] prepared a 2D nanofluid with ethylene glycol as the base fluid and a nanocomposite of an empty fruit bunch and GO. The TC determination results showed an enhancement of 6.47% for the 0.06% wt. activated carbon–Gr/ethylene glycol nanofluid. Furthermore, the viscosity of the nanofluids showed a nonlinear increase with the increase in activated carbon–Gr fractions because of the reinforcement of the internal shear stress. The compound nanostructure of activated carbon–Gr enhanced surface interactions in the ethylene glycol. An extremely low concentration of nanoparticles was incorporated to avert sedimentation and an excessive enhancement of the viscosity. The highest increase in the viscosity was by 4.16% at 0.06% wt. The viscosity decreased gradually with increasing temperature, particularly at 45 °C. The viscosity increase was low for all tested nanofluids, which makes them adequate for heating applications with only small penalties affecting the required initial pumping power. Additionally, the density of the activated carbon–Gr/ethylene glycol nanofluids increased with the increasing fraction of nanoparticles and decreased with increasing temperature. The highest verified density enhancement was by 0.09% at 0.06 wt.% and 20 °C, and such a negligible enhancement can be caused by the interface effects on the liquid bulk induced by the surface of nanoparticles and by the interactions among the added nanoparticles themselves. When the temperature was increased from 20 °C to 50 °C, the specific heat capacity of the nanofluids also increased. The specific heat of the nanofluids at 0.06% wt. was 2.25%, superior to the specific heat of the pure ethylene glycol at 50 °C. A minor increase was observed in the specific heat of the hybrid nanofluids with the increasing concentration of activated carbon–Gr nanoparticles. Nonetheless, the majority of the published studies state that the specific heat decreased with the inclusion of nanoparticles, but a few unexpected results were also reported. It appears that the specific heat of the base fluid and the nanoparticles affects the final specific heat of the nanofluids, and the interfacial solid/liquid free energy is altered with the modification of the included nanoparticles. Due to the greater surface area of the nanoparticles, their surface free energy has a greater impact on the capacity of the system, affecting the specific heat of the composite nanomaterials. In the study conducted by Sundar et al. [119] GO nanosheets with a homogeneous dispersion of spherical Co_3O_4 nanoparticles were prepared using in situ growth and co-precipitation. The reduction of aqueous cobalt chloride in the presence of GO with sodium borohydrate led to the production of hybrid GO/Co_3O_4 nanoparticles. The hybrid nanofluids were synthesized by scattering the GO/Co_3O_4 nanoparticles in water, ethylene glycol, and ethylene glycol/water base fluids. The results revealed that the TC increase in the aqueous nanofluid was 19.1% and the ethylene glycol-based nanofluid was 11.9% at 0.2% vol. at 60 °C compared with the corresponding base fluids. The viscosity enhancement of the aqueous nanofluid was 1.7-times higher and that of the ethylene glycol-based nanofluid was 1.42-times higher at 0.2% vol. at 60 °C. In the ethylene glycol-based nanofluids, the TC increase associated with the GO/Co_3O_4 nanoparticles was more pronounced compared with those of other GO nanofluids. This is due to the synergistic thermal properties of the hybrid nanoparticles. The increase in the viscosity of the GO/Co_3O_4 nanofluid was similar to that of the GO nanofluids. Table 6 summarizes the experimental works on 2D hybrid nanofluids.

Table 6. Recent experimental works on 2D hybrid nanofluids.

Reference	Authors/Year	Concentration	Base Fluid	Main Findings	Remarks
[120]	Ahammed et al., 2016	Gr–Al_2O_3 at 0.1% vol.	Water	Increase of approximately 63.1% in the HTC. Increase in the pressure drop of approximately 20.3%.	Increase in the cooling capacity and coefficient of performance of a thermoelectric cooler by nearly 31.8%. Decrease in the total entropy generation in a heat exchanger of 19.6%.
[121]	Verma et al., 2018	MWCNTs-CuO and MWCNTs-MgO at 0.25% to 2% vol.	Water	Increases in the thermal efficiency of a flat plate solar collector for the MWCNTs-CuO was approximately 18% at 0.75% vol. and at mass rate of nearly 0.025 kg/s compared with the water alone, and nearly 20.5% for the MWCNTs-MgO.	Increase in the exergetic performance of the MWCNTs-CuO of 30.09% compared with the water alone. The homologous value for the MWCNTs-MgO was nearly 33.8% compared with the water itself.
[122]	Omri et al., 2022	Gr–copper oxide at concentrations until 1% wt.	Water	HTC increases of approximately 23.7% and of nearly 79.7% at 0.2% wt. and 1% wt., respectively.	Use of a vertical helical coil heat exchanger.
[123]	Mahamude et al., 2022	Gr–crystal nano cellulose at 0.1%, 0.2%, and 0.5% vol.	Water and ethylene glycol mixture	194% increase in the TC.	Maximum efficiency of a flat plate solar collector of approximately 16.9% at 0.5% wt.
[124]	Jin et al., 2022	Gr–MXene at 1.8% wt. Gr + 0.2% wt. MXene, 1.5% wt. Gr + 0.5% wt. MXene, and 1.0% wt. Gr + 1.0% wt. MXene	Water	Approximate 60% increase in the TC with the 1.8% wt. Gr + 0.2% wt. MXene.	The viscosity and viscosity increase in the Gr–MXene nanofluids decreased as MXene concentration increased.

In sum, the already published research on nanofluids are mostly devoted to the employment of mono nanofluids in certain heat transfer purposes, such as the heat exchangers field of actuation. There appears to be a shortage of works on the heat transfer capability provided by the hybrid nanofluids in affordable and sustainable solutions. Further studies are required to fully understand and explore the performant thermal characteristics of the hybrid nanofluids in areas including the cooling of electronics, borehole heat exchangers, and PV/T systems.

3. Application of 2D Nanofluids

3.1. Heat Exchangers

Two-dimensional nanofluids are a good alternative to the traditional heat transfer fluids used in heat exchangers. This thermal management equipment has widespread application in diverse technologies including the cooling of electronics, heating/cooling of buildings, fabrication large-scale processes, energy recovery systems, energy conversion and production means, and the cooling of combustion engines. The most studied and used types of heat exchangers are the pinned-tube, shell and tube, plate, and double heat exchangers. Considering the application of 2D nanofluids in heat exchangers, the authors Arzani et al. [125] synthesized MWCNTs covalently functionalized with aspartic acid and suspended in water. The developed nanofluids had a good colloidal stability characterized by less than 20% sedimentation occurring for the highest nanotube weight fraction of 0.1%. The heat transfer rates of the nanofluids with different concentrations were studied in a horizontal annular heat exchanger under three different heat fluxes. In view of the experimental results, the investigation team concluded that the TC, HTC, viscosity, density, and Nusselt numbers of the nanofluids with MWCNTs fillers were enhanced compared with those of the water alone. However, the specific heat capacity was significantly reduced in comparison with that of the water alone. Additionally, the developed fluids entailed only a modest pressure drop increase, requiring little extra pumping power. Considering the findings of this experimental work, it was concluded that nanofluids possessed advantageous thermophysical properties to be employed in a wide range of large-scale applications using annular heat exchangers. Ghozatloo et al. [126] evaluated the heat transfer performance of Gr nanosheets dispersed in water flowing in a shell and a tube heat exchanger under a laminar regime. The results revealed that with an incorporation of 0.075% of Gr nanosheets, the TC of the water was enhanced by 31.8%. An increase was also observed in the HTC which depended on the conditions of the fluid flow, e.g., temperature of the fluid. The HTC of the prepared nanofluids was improved by a maximum of 35.6% compared to that of the water itself at 0.1% wt. of Gr nanosheets at 38 °C. The HTC was increased by 13.1% when the temperature was raised from 25 °C to 38 °C at a concentration of 0.1% wt. as a result of the impact of the Gr nanosheet concentration being more intense at higher temperatures. In this sense, the authors noticed that by augmenting the weight fractions of the Gr filler from 0.025% wt. to 0.1% wt., the HTC was enhanced by 15.3% at 25 °C and by 23.9% at 38 °C. On the other hand, Baby and Ramaprabhu [127] synthesized hydrogen-exfoliated Gr dispersed in ethylene glycol and deionized water. The Gr was synthesized through hydrogen-induced exfoliation of graphite oxide under a hydrogen atmosphere at 200 °C. It was found that a volume fraction of 0.05% vol. of hydrogen-exfoliated Gr in deionized water exhibited enhancements in the TC of 16% at 25 °C and of 75% at 50 °C compared with the base fluid alone. Moreover, the authors stated that the TC of the prepared nanofluids increased with increasing volume fraction and temperature. Additionally, the Nusselt number changed with the increasing concentration of hydrogen-exfoliated Gr and an increasing Reynolds number. Table 7 presents some of the recent experimental works on the application of 2D nanofluids in different types of heat exchangers.

Table 7. Recent experimental works on the use of 2D nanofluids in heat exchangers.

Reference	Authors/Year	Nanomaterial/Concentration	Base Fluid	Heat Exchanger Type	Main Findings	Remarks
[128]	Esfahani and Languri 2017	GO at 0.01% and 0.1% wt.	Water	Shell and tube	Increases of 8.7% and 18.9% in the TC at 0.01 wt.% and 0.1 wt.% and at 25 °C and 40 °C, respectively.	Decreases of 22% and 109% in the exergy loss at 0.01 and 0.1 wt.% under laminar regime.
[129]	Poongavanam et al., 2019	MWCNTs at 0.2%, 0.4%, and 0.6% vol.	Solar glycol	Shot Peened Double Pipe	Increase of approximately 115% in the HTC at 0.6% vol. and at a mass flow rate of 0.04 kg/s. Increase of approximately 30.6% in the TC at 0.6% vol. and temperature values between 30 °C and 50 °C.	Increase of 1.56 times in the pressure drop at 0.6% vol. and at mass flow rate of 0.08 kg/s.
[130]	Fares et al., 2020	Gr at 0.2% wt.	Water	Shell and tube	Increase in the HTC of 29% at 0.2% wt.	Increase in the thermal efficiency of 13.7% at 0.2% wt.
[131]	Sen and Variyenli, 2021	Gr–CuO at 0.5% vol.	Water	Concentric tube	Increase of 9.6% in the HTC.	Decrease of 55% in the total exergy loss.
[132]	Abdalahh et al., 2021	Gr at 0.02%, 0.055%, and 0.06% wt.	Water	Double	Increase of 51.1% at a Reynolds number of 425 and at 0.06% wt. and 0.055% wt.	The pressure drop and pumping power were higher at 0.06% wt. than at the other concentrations.

In essence, additional studies should be conducted on the corrosive and erosive consequences and fouling formation associated with the flow of 2D nanofluids in the exchanger channels and surfaces. There is also a research gap concerning the high-temperature usage of two-dimensional nanofluids in different types of heat exchangers. These studies are pivotal, given that it has already been reported in the literature that the pressure drop in the piping and the initial pumping power are decreased at high fluid inlet temperature values. Efforts should be made to undertake in-depth studies concerning other thermophysical characteristics of 2D nanofluids flowing in heat exchangers aside from the usually scrutinized TC and viscosity, such as the specific heat capacity and latent heat capacity. Additionally, more experimental and numerical works on the applicability of 2D nanofluids are required, such as Gr family dispersions in the role of thermal fluids operating in heat exchangers and similar equipment, investment analysis, and potential heat transfer working gains. Finally, more studies on 2D nanofillers based on h-BN nanostructures to be applied in all types of heat exchangers are lacking in the literature.

3.2. Thermal Management of Electronics

Two-dimensional nanofluids are promising alternatives that can be employed in liquid blocks with channels (e.g., heat sinks), thermosyphons, heat pipes, and channels with special configurations for electronic thermal management. The published literature focus fundamentally on the use of Gr and CNT nanofluids and some hybrid forms in the thermal management of the electronic components, where the miniaturization of the cooling and operating systems is of paramount importance. Balaji et al. [133] investigated the thermal performance of 2D functionalized Gr nanoplatelets in distilled water. They discussed the impact of the mass flow rate and the concentration of Gr nanoparticles on the HTC, Nusselt number, temperature, and pressure drop. The obtained results demonstrated that the functionalized Gr platelets exhibited an improved heat transfer capability compared with the distilled water alone. The nanofluids at 0.2% vol. of Gr platelets remained stable for an extended period without any settlement occurring, which was confirmed by the zeta potential measurements. Furthermore, the TC and viscosity of the nanofluids were enhanced by 11% and 13.3% in comparison with those of the water alone. The HTC and Nusselt number increased 71% and 60% at 50 °C, respectively, compared with the pure water. By applying this nanofluid in the cooling system of electronic ships, the temperature drops in the heat sink increased by up to 10 °C, improving the performance of the ships. There was a slight increase in the pressure implying the need for extra pumping power, but it can be noted that the enhanced thermal properties of the synthesized nanofluids compensated for this negative feature. In essence, the findings of this experimental work confirmed that the functionalized Gr nanoplatelet nanofluids were capable of removing the heat generated by the chips under different heat loads. It was demonstrated that the developed nanofluids were more stable and had a better heat transfer performance than the conventional coolants; therefore, they have potential in liquid-cooled electronic cooling systems. Nevertheless, more studies should be conducted on the heat transfer enhancement of the liquid blocks and double-layer liquid blocks of the heat sinks employing 2D nanofluids in the thermal management of electronic components. In addition, there is a lack of studies on the use of 2D nanofluids along with the investigation of the inclination angle or gravity on the thermal performance of heat pipes in the cooling of CPU. Studies on the thermosyphon boiling process of 2D nanofluids as operating fluids are rather scarce and new insights should be pursued. More investigation works are highly recommended to better understand the heat transfer capability when using two-dimensional nanofluids in specially designed novel structures, such as wavy channels. Moreover, due to the very narrow size of the channels used in the thermal management of electronics, the minimal dimensions of the 2D nanostructures dispersed in base fluids are of great interest and are suitable for use in such systems. Nevertheless, the agglomeration effect of the suspended nanostructures gains intensified impact in the cooling of electronics. There is a research gap closely linked with the use of 2D nanofluids together with the use of phase change

materials, as they promote temperature uniformity in commonly used liquid blocks of heat sinks used in electronic thermal management. This uniformity will ensure higher thermal performance. Finally, more options based on the green and bio-friendly functionalization of Gr 2D nanostructure dispersions should be studied. These nanofluids are suitable candidates for use in the cooling of electronics.

3.3. PV/T Systems

Two-dimensional nanofluids can be included in the novel class of heat transfer fluids in the most recent PV/T systems, owing to their extremely high TC and heat transfer rates. It has also been reported that PV/T systems using 2D nanofluids, such as Gr, CNTs, or hybrid formulations, in conjunction with the use of phase change materials, can improve the overall efficiency of existing PV/T systems by 20% or more compared with the same systems operating with traditional heat transfer fluids. The uniform dispersion of the 2D nanostructures in the base fluids is vital for achieving an enhanced solar radiation absorption and to achieve a very high TC. In addition, the hybrid 2D nanofluids employing, for instance, Gr and its derivatives and CNTs, are great contributors to the high thermal and electrical energy output by effectively controlling the solar radiation that is transmitted to the PV module. Of all the two-dimensional nanomaterials, the Gr is very suited to play the role of transparent conducting electrode and Schottky barrier junction layer for PV cells because it is lightweight, ultrathin, and flexible. Two-dimensional nanomaterials are progressing and emerging as PV cells and on-chip integrated configurations of energy storage systems and equipment with energy harvesting purposes. Moreover, 2D nanomaterials can respond to the needs of novel PV systems, entailing less expenditure and high efficiency rates. These nanomaterials are welcome in synthesis procedures of nanofluids to dissipate enhanced heat charges from the solar panel and in evoking more attention from the scientific community than other types of nanoparticles. For this reason, some researchers are studying different Gr hybrid nanofluids, prepared using different methods dispersed into different fluids such as oil, ethylene glycol, and water. Figure 13 schematically illustrates the typical PV/T configurations of PV/T systems operating with nanofluids as coolants.

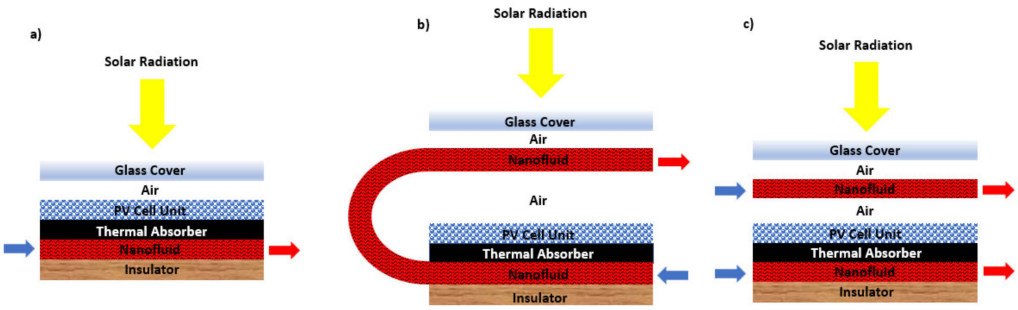

Figure 13. Configurations of typical PV/T systems with nanofluids: (**a**) as a coolant; (**b**) as a coolant and spectral filter with double-pass channel; (**c**) as a coolant and spectral filter with separate channels.

Aravind and Ramaprabhu [134] manufactured Gr-wrapped MWCNTs dispersed in water nanofluids using a solution-free, eco-friendly method. The obtained results revealed an enhancement of 10.5% in the TC for the Gr-MWCNT, which was higher than the TC increase of only 9.2% when using the 0.04% vol. Gr nanofluid. The TC increase was explained based on the production of strongly bonded clusters that determine the interfacial thermal resistance because of the ameliorated heat transfer capability between them. Yarmand et al. [135] prepared Gr nanoplatelet–silver hybrid nanofluids using a facile chemical procedure. The GO was synthesized from graphite flakes using the Hummer method and was then chemically reduced. The fundamental steps of the GO preparation method are presented in the diagram of Figure 14. The results indicated a 32.7% increase in the Nusselt number and a 1.08-fold friction factor enhancement with a pumping penalty

compared with the water itself for a concentration of 0.1% wt. and a Reynolds number of 17,500.

Figure 14. Schematic diagram of the Hummer method for the synthesis of GO.

Zubir et al. [136] prepared rGO and produced hybrid complexes with other carbon sources, including MWCNTs, carbon nanofibers, and Gr nanoplatelet aqueous nanofluids to achieve an improved heat transfer capability. The obtained results exposed a heat transfer increase when employing the hybrid nanomaterials in comparison to the rGO alone. The results also showed an increase of 63% in the HTC and a 144% increase in the Nusselt number. In the study performed by Wahab et al. [137], an effective approach to use active and passive cooling mediums to decrease the temperature of the PV surface was followed. This reduction is relevant given that the rise in the ambient temperature has a negative impact on the heat transfer behavior of the PV cells. The operating thermal fluids used were water alone and Gr at 0.05% and 0.15% volume fractions in water nanofluids. The experiments were conducted at flow rates between 20 L and 40 L per minute. An exergy analysis of the performance of the various PV modules, together with the changes in the concentration of the nanofluids and flow rates, was performed. Figure 15 schematically represents the configuration of the experiments for the four studied cases.

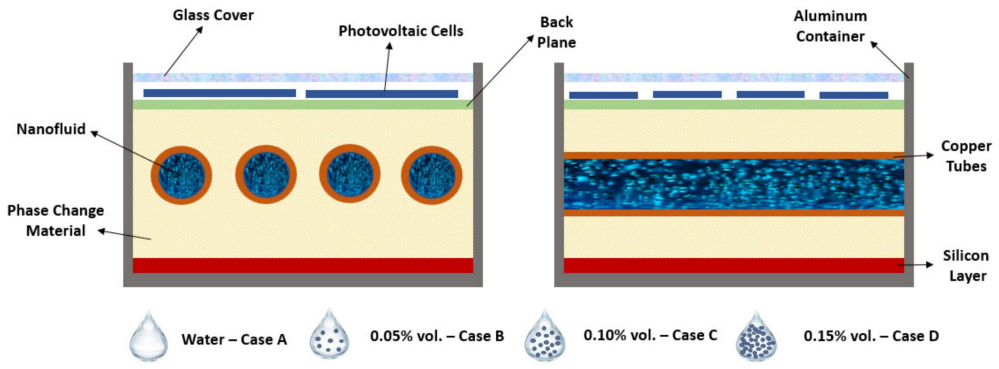

Figure 15. Schematic diagram of the configuration of the PV/T system for four different conditions. Adapted from [137].

Considering the experimental results, the authors concluded the following points:

- The enhancement in the volume fraction of the Gr nanoparticles from 0.1% vol. to 0.15% vol. resulted in a poorer performance of the system because of the agglomeration and settling of the nanoparticles in the distilled water. The agglomeration lowered the heat transfer capability since the Brownian motion of the nanoparticles was restricted.
- The exergy losses and entropy generation were decreased by the increasing flow rates in the PV/PCM (phase change material) system. Consequently, the increase in the flow rates of the operating fluid promoted the extraction of energy.

- The sustainability index increased with increasing flow rate and a maximum of 1.17 was reported for the system with PCM and 0.10% vol. concentration of Gr nanoparticles. The same system presented a minimum improvement potential by demonstrating that this configuration was most efficient.
- The electrical exergy contributed more to the overall exergy efficiency than the thermal exergy. This fact can be interpreted based on the inferior thermal energy produced by the PVT/PCM system.

Many efforts were undertaken to develop different solar cell technologies, but researchers are still trying to find the best way to enhance the large-scale performance of PV cells. Attention should be paid to the research topics concerning the geometry of the channels, flow pattern configuration and distribution, and maintenance requirements of the PV cells to improve the heat transfer between the solar module and the hybrid nanofluids. The channels with a hexagonal honeycomb geometry demonstrated an 87% thermal efficiency compared with other channel geometries. In addition, the carbon hybrid nanofluids showed a maximum of 63% enhancement in the HTC and a 144% enhancement in the Nusselt number, higher than the other types of hybrid nanofluids. Furthermore, the f-MWCNT/HEG)/water hybrid nanofluids exhibited a 289% increase in heat transfer capability for 0.01 vol% of hybrid nanofluids at a Reynolds number of 15,500 in comparison to the base fluid. It is highly recommended that a detailed review is undertaken to assess the main causes behind the modifications to the heat transfer characteristics induced by hybrid nanofluids. The economic analysis of PV/T systems should incorporate the time value of money for their design and implementation. The cost of factors including maintenance needs, parts warranty, and reduction in electrical performance of the system should be an important feature of the economic analysis. The main point is the payback period, which is expected to be shorter than the PV panel lifetime and less than 14.5 years. The solar energy field and hybrid nanofluids will take advantage of the low carbon content, low initial investment, green methodologies, and the production of non-fossil fuel electricity, which shows a remarkable impact on the environment by limiting the emission of toxic gases and non-renewable resources depletion. In the long run, the use of hybrid nanofluids may enhance the performance of PV/T systems by reducing their overall operating cost. The science and technology associated with hybrid nanofluids will entail economic and environmental profit by enhancing the efficiency of the systems and by reducing the emission of greenhouse gases. Table 8 presents some recent experimental and numerical works on the application of 2D nanofluids in PV/T systems in the field of technology.

Further experimental works on the use of PV/T systems with phase change materials dispersed in water or other base fluids flowing in different piping arrangements inside the hybrid phase change materials are required. The combined usage of 2D nanofluids and phase change materials has proved that systems with this solution presented higher efficiencies than those operating with only phase change materials. Innovative configurations of PV/T systems should be developed and implemented, such as PV/T systems with loop pipes and 2D nanofluids. Moreover, geometrical and structural factors, such as the radius, thickness, and roughness of the involved channels and tubes should be optimized in the near future. In addition, there is a literature gap linked with the dynamic performance of PV/T systems using 2D nanofluids and its main results and influencing factors, including the reflective coating and TC of the base fluids. Furthermore, there is a lack of studies on two-dimensional nanomaterials dispersed in bio-friendly base fluids to work in PV/T systems. Finally, the viability of PV/T systems operating with 2D nanofluids should be further addressed considering technological, economic, and environmental features.

Table 8. Recent works on the use of 2D nanofluids in PV/T systems.

Reference	Authors/Year	Nanomaterial/Concentration	Base Fluid	Main Findings	Remarks
[138]	Hassan et al., 2020	Gr at 0.05%, 0.1%, and 0.15% vol. and RT-35HC phase change material	Water	Decreases of 23.9 °C, 16.1 °C, and 11.9 °C in the PV temperature for nanofluid-based PVT/PCM system, water-based PVT/PCM system and PV/PCM system, respectively. Increase of 17.5% in the thermal efficiency of the hybrid PVT/PCM system in comparison to that of the water-based hybrid PVT/PCM system, and overall efficiency increase of 12%.	Increases of 23.9%, 22.7%, and 9.1% in the electrical efficiency, respectively, in reference to the conventional PV system.
[139]	Abdelrazik et al., 2020	rGO–Ag from 0.0005% to 0.05% wt.	Water	The hybrid solar PV/T system with rGO–Ag/water nanofluids obtained thermal efficiencies between 24% and 30%.	Improved performance at concentrations inferior to 0.0235% wt. compared to the PV system without the integration of optical filtration.
[140]	Venkatesh et al., 2022	Gr at 0.3% vol.	Water	Increases of 23% and 13% in the energy efficiencies of the PV and PV/T systems, respectively.	Decrease of approximately 20 °C in the temperature of the panel at 0.3% vol. and at 0.085 kg/s.
[141]	Sreekumar et al., 2022	MXene at 0.2% wt.	Water	Increase of approximately 21.4% in the HTC at 0.2% wt. and at a flow rate of 40 kgh^{-1}	Decrease of 10% in the PV surface temperature compared with the water alone.

3.4. Concentrated Solar Power

Two-dimensional nanofluids containing Gr, CNTs, and metal chalcogenides possess thermophysical properties of great interest in the CSP field of technology, such as improved long-term and thermal stabilities, enhanced heat transfer rates, and TC in reference to the traditional heat transfer synthetic oils currently employed in the CSP stations. The present subsection will briefly describe the potential applicability of two-dimensional nanofluids in the CSP area of actuation, its drawbacks, and the associated future challenges. In recent decades, CSP technology has become one of the most attractive options for energy harvesting and conversion. The increasing interest in this route has resulted in several studies on the more effective configuration of CSP systems. For instance, in systems with parabolic trough collectors, a heat transfer fluid flows through an absorber tube positioned along the central axis of the mounted mirrors in which the solar radiation is concentrated. The absorber tube is coated with a selective absorber, enabling the maximization the absorbed radiation amount by the collector in CSP plants. One of the most interesting solutions for improving the efficiency of CSP plants is to improve the thermophysical characteristics of the employed thermal fluid. Several works have stated that incorporating low concentrations of nanoparticles to a base liquid may enhance its thermophysical characteristics, including the TC and HTC. Moreover, nanoparticles usually minimize the thermal resistance between the existing sublayers of the heat transfer fluid, reducing the drop in temperature from the wall to the liquid bulk. The changing of the heat transfer properties contributes to the efficiency improvements in the base fluid and, consequently, in the overall efficiency of CSP plants. Metallic and metallic oxide nanoparticles are appealing to several researchers due to their superior TC. The transition metal dichalcogenides are also an important part of the recent advances in the sector because of their two-dimensional laminar nanostructure with promising characteristics, such as those in graphite. Two-dimensional nanomaterials present covalent intra-laminar distributions with interlaminar van der Waals forces interactions, resulting in enhanced high in-plane TC and much reduced out-of-plane losses. Due to these facts, the investigation of nanofluids incorporating transition metal dichalcogenide fillers is of great interest in the heat transfer field of research. Research has also been performed which considers how nanofluids improve the overall efficiency of solar thermal collectors, including the utilization of the two-dimensional nanofluids of interest in solar thermal energy applications. Furthermore, the use of 2D nanomaterials is expected to enhance the long-term stability of nanofluids due to their large surface area. In this direction, the liquid phase exfoliation technique is one of the easiest and most promising preparation methods for 2D nanomaterials [2]. The stability of nanofluids without the formation of aggregates can be enhanced by the inclusion of surfactants or dispersants in synthesis formulations and by adjusting their pH. Regarding CSP systems, the added nanoparticles have a remarkable impact on improving the heat transfer capability of the heat transfer base fluid and in increasing the absorption of incident solar radiation, resulting in noticeable improvements in the efficiency of solar plants. Additionally, due to the verified enhancement in the solar irradiation absorption induced by the nanoparticles, some authors have recommended the use of nanofluids in direct solar collectors. For instance, Kasaeian [142] investigated MWCNTs suspended in ethylene glycol nanofluids as working heat transfer fluids in a direct absorption parabolic trough collector. The best results were achieved using nanofluids at 0.3% wt. of MWCNTs, with an optical efficiency of approximately 71% and a thermal efficiency increase of 17%. In the study performed by Martinez-Merino et al. [92], 2D nanofluids were synthesized based on the inclusion of WS_2 nanosheets in a eutectic mixture of biphenyl and diphenyl oxide, which consisted of a typical heat transfer solution for CSP facilities to evaluate their viability to be employed in this technological field. The nanosheets of WS_2 were produced in situ in the heat transfer oil through liquid phase exfoliation where the inter-layer van der Waals forces of the bulk WS_2 were broken through ultrasonication in a fluid with the auxiliary action of the polyethylene glycol as the surfactant. The hydrogen bond interaction between the hydroxyl groups of the polyethylene glycol and the sulfur atoms of the WS_2 stabilizes the

nanosheets within the fluid. The experimental results on stability revealed no appreciable alterations in the size of the nanosheets and zeta potential, which was confirmed by the low sedimentation levels observed. The enhancement of the polyethylene glycol fraction improved the stability of the 2D nanofluids and their viscosity was reported to be similar to that of the eutectic mixture base fluid, with only a slight increase reported at higher concentrations. The nanofluids provided a specific heat increase of 10%, whereas the TC showed an increase of 37.3% in compared with the base fluid itself. It was also confirmed that the HTC increased in all nanofluids by up to 22.1%, despite being synthesized with different amounts of polyethylene glycol and different ultrasonication times. The improved long-term stability of the nanofluids and heat transfer ameliorations were linked with the high surface area of the WS_2 nanosheets. The determined dynamic viscosity revealed that the developed nanofluids carry relevant features to be used in CSP plants, given that they would not entail the limitations associated with the piping obstruction and pressure drop in the involved systems. All findings suggested that these nanofluids would be a promising heat transfer medium in the CSP technological field. Aguilar et al. [143] considered GO 2D nanofluids as very promising for solar thermal applications given their high TC, simple exfoliation process of the filler, and intense black coloration. The researchers prepared a nanofluid composed of GO dispersed in the eutectic mixture of diphenyl oxide and biphenyl through liquid phase exfoliation. The nanofluids were synthesized by liquid phase exfoliation from the bulk GO with the aid of a Triton X-100, PEG-200, and other surfactants. It was observed that the most effective exfoliation was achieved with the Triton X-100 with the highest number of suspended nanostructures which were stable over time. The authors reported that 6.6%, 45.5%, and 29.7% enhancements for the specific heat, TC, and HTC, respectively, were observed in the Triton X-100-synthesized nanofluid. The determination of sunlight extinction and spatial distribution in the thermal fluid enabled the estimation of the dimensions of the direct solar absorbers using the Triton X-100 nanofluid. This nanofluid exhibited an almost complete sunlight attenuation between 3.5 mm and 20 mm depending on the weight fraction of the incorporated GO. The sunlight special distribution was revealed to be increasingly more intense near the input surface at greater amounts of GO. These findings allowed the researchers to arrive at the conclusion that the incorporating Triton-X surfactant nanofluids constitute a promising option to be used as customized sunlight absorbers to be employed in thermal solar collectors. In addition, these nanofluids were found to be strong-colored meaning they are suitable for the conceptualization and implementation of direct absorption solar collectors. Yan et al. [144] synthesized atomic-layer thick h-BN nanosheets and dispersed them into molten salt base fluid solar salt ($NaNO_3$-KNO_3 with 60:40 of molar ratio). It was stated that the prepared nanofluids enabled a superior thermal performance in CSP technology, mainly due to the improved TC and enlarged specific surface area of the BN nanosheets, which reduced the thermal resistance and facilitated the formation of additional semi-solid boundary layers and active nucleation sites. The authors reported that the TC and specific heat of the nanofluids were superior by 76.8% and 12.8%, respectively, compared with those of the solar salt itself. Simultaneously, the supercooling degree was reduced considerably from 12.2 °C to 4.7 °C. The obtained results were of relevance in the CSP field since the ameliorated TC and specific heat provide an enhanced heat transfer capability, an appreciable reduced cost, and dimensions of the necessary equipment. The decreased supercooling degree averts the phase separation and the blockage of the piping. Hence, the researchers concluded that this type of 2D molten salt nanofluid can be employed as improved heat transfer and thermal energy storage fluids in CSP plants. Table 9 summarizes some of the recently published works on the use of 2D nanofluids and their hybrids in the CSP field of actuation.

Table 9. Recent works on the use of 2D nanofluids and hybrids in the CSP field of technology.

Reference	Authors/Year	Nanomaterial/Concentration	Base Fluid	Main Findings	Remarks
[145]	Hordy et al., 2014	MWCNTs from 5.6 mg/L to 53 mg/L	Water, ethylene glycol, propylene glycol, and Therminol™ VP-1	Long-term stability even after eight months in the ethylene glycol and propylene glycol-based nanofluids. The MWCNTs were highly absorbent over most of the solar spectrum, allowing for nearly 100% solar energy absorption, even at low concentrations.	Glycol-based nanofluids presented the best overall thermal performance.
[30]	Hussein et al., 2020	Gr-h-BN at 0.10% wt.	Water	Increases of 12% and 64% in the TC at 20 °C and 60 °C, respectively, and at 0.10% wt.	Thermal efficiency of the system up to 85% at 0.10% wt. and 20% higher than that of the water alone.
[146]	Hosseinghorbany et al., 2020	GO at 0.5%, 1%, and 2% wt.	Ionic liquid	Increase of 6.5% in the TC. Increase of 27% in the specific heat capacity.	Increase of 7.2% in the HTC at 0.5% wt.
[144]	Yan et al., 2022	h-BN at 0.5%, 1.0%, 1.5%, and 2.0% wt.	Solar Salt	Increase of nearly 76.8% in the TC. Increase of 29.8% in the specific heat capacity.	Decrease from 12.2 °C to 4.7 °C in the supercooling degree.
[147]	Kumar and Tiwari, 2022	h-BN at 0.25%, 0.50%, 0.75%, 1.0%, 1.25%, 1.5%, 1.75%, and 2.0% wt.	Water	Maximum energy efficiency of nearly 72.1% at 1.5% vol. and at 0.051 kg/s mass flow rate. The maximum increase in the energy efficiency of approximately 84% was obtained at 1.50 vol% and at 0.051 kg/s mass flow rate. The maximum exergy efficiency of 13.1% was obtained at 1.25% vol. and at 0.017 kg/s of mass flow.	The lowest value of entropy generation of 42.9 W/K was obtained at 1.25% vol. The entropy generation increased with increasing mass flow rate and decreasing concentration.
[148]	Zhu et al., 2022	h-BN-titanium nitrate at 20, 40, 60, 80, and 100 p.p.m.	Water	Exergy efficiency of 83% at 80 p.p.m.	Maximum of 78% in the photothermal conversion efficiency at 80 p.p.m.

There is a lack of studies on metal chalcogenide 2D nanofluids using base fluids of eutectic mixtures of biphenyl and diphenyl oxide, which are typical in CSP plants. More experimental works employing WS_2 and MoS_2 in the form of nanowires and nanosheets should be conducted, since these nanostructures are already known to possess higher stability over time. Further numeric simulations at the molecular level can offer useful insights into the structure and performance of the metal chalcogenide 2D nanofluids on their reactivity with the molecules of the base fluids most used in solar thermal energy collectors. Additionally, the feasibility of 2D nanofluid application in enhancing the overall thermal efficiency of several possible CSP configurations should be further addressed. There is a research gap regarding the use of 2D nanofluids in the design and large-scale implementation of volumetric solar energy collectors, which, among other benefits, are cheaper than surface collectors. More experimental and numerical works on the dispersion of 2D nanomaterials in molten salt base fluids should be conducted, as they are a very promising option for CSP plant operation. Furthermore, future studies on operating configuration factors together with the use of 2D nanofluids will bring useful insights for the CSP technological field. Some factors worth mentioning are the optimization of solar absorber or solar thermal energy tubes, amelioration of the nanofluid using modes, steam in the direct steam generation system, and the thermal energy storage behavior enhancement of direct steam generation CSP systems.

3.5. Transformers

The high TC and superior dielectric performance of 2D nanofluids, together with their general low-cost synthesis processes, makes them a strong solicitant for application in thermal management devices and systems, such as electrical transformers. The present section elucidates upon the improved thermophysical properties, and the possible applications and research gaps related to the employment of two-dimensional nanofluids in electrical transformers. To ameliorate the transformer oil thermoelectric characteristics, diverse experimental works based on the replacement of the traditional transformer mineral oil with vegetable oils have been performed, since these possess improved insulation and thermal performance. However, vegetable oils become easily contaminated which can result in the degradation of the oil properties, which in turn alters the chemical reactivity with the transformer operating parts. The degradation of the inner parts of the transformer may result in serious faults, economic losses, and extended shutdown. To solve these problems and to enhance the heat transfer and insulation features of the transformer, nanoparticles suspended in a base fluid are becoming of great interest to researchers in this field. Particularly, 2D layered nanomaterials are gaining importance in the transformers field of research and 2D nanofluids may be a promising alternative to two-dimensional fillers in the transformer liquid insulation circuit due to their very high surface area, surface-to-volume ratio, and improved stability. The facile and low-cost synthesis of 2D nanofillers makes them useful in the thermal management systems of transformers and in the breakdown voltage of the insulating fluid. Beheshti et al. [149] incorporated MWCNTs into a transformer mineral oil and found a marked enhancement in the TC, a reduction in the viscosity, and a rising temperature in comparison to those properties of the transformer oil. Moreover, the authors Maharana et al. [150] prepared a nanofluid with mineral oil as the base fluid and with the incorporation of h-BN and titanium oxide nanoparticles to be used as a transformer coolant. They exfoliated 1 μm-sized bulk h-BN nanoparticles into 2D nanosheets with dimensions of 150 nm to 200 nm, increasing the surface area of the exfoliated h-BN. After the zeta-potential analysis, the weight fractions of 0.01% wt. and 0.1% wt. of the nanoparticles were selected to evaluate the heat transfer and insulation characteristics of these fractions dispersed in mineral oil, which are the main functionalities of a transformer oil. The TC and charging dynamics analysis were performed by the authors to infer the potential of the developed nanofluids to be used as dielectric fluid for transformers in comparison to the traditional mineral oil. Particularly, the charging dynamics investigation confirmed the increase in

the AC breakdown voltage of the exfoliated h-BN nanofluids. Considering the results, the authors arrived at the following conclusions:

- The inclusion of 0.01 wt.% of exfoliated h-BN nanoparticles resulted in a more stable solution and possessed the most improved cooling and insulation properties.
- The high aspect ratio and enhanced surface charges in h-BN were the main factors contributing to the higher TC of the mineral oil-based h-BN nanofluid. The higher moisture content in the mineral oil and nanofluids reduced the AC breakdown voltage. Nonetheless, the exfoliated h-BN nanoparticles possess low affinity towards moisture and increase the AC breakdown voltage in reference to mineral oil and other nanofluid fillers.

In the study developed by Almeida et al. [151], the thermophysical and electric characteristics of a traditional transformer oil were determined with the incorporation of 0.01% wt., 0.03% wt., and 0.05% wt. Gr nanoparticles within a temperature range of 20–90 °C. Based on the experimental results, the authors stated the following conclusions:

- The 0.05% wt. Gr nanofluid exhibited a viscosity and density superior by 2.5% and 16.6% to that of the conventional transformer oil base fluid.
- The 0.05% wt. Gr nanofluid showed a maximum surface tension decrease of 10.1%. The increasing temperature and enhanced weight fraction of the Gr nanoparticles improved the Brownian motion, contributing to a more uniform temperature distribution in the working fluid caused by the decrease in the forces of cohesion (because of the high temperature and increased vibration) between the nanoparticles. This resulted in surface tension reduction and to the improvement of the heat transfer rate compared with that of the transformer oil.
- The specific resistance for all weight fractions of the nanofluids was reduced and a 79% decrease compared with the transformer oil was found for the maximum concentration of 0.05% at a temperature of 90 °C. The use of 2D nanofluids also decreased the specific resistance and enhanced the electrical conductivity and, consequently, the breakdown voltage.

Table 10 exhibits some recent experimental works on 2D nanofluids applied in the electrical transformer field of technology.

In sum there is a research gap on the incorporation of nanoparticles dispersed in transformer oil rather than in synthetic oils, as described in the majority of the literature. Further studies should be performed on the potential application of the quasi-2D amorphous Gr nanofluids in the electrical transformer technological area. More innovative preparation methods and novel ways to incorporate the Gr quantum dots into the electrical transformer heat transfer fluids are welcome. Moreover, there is a need for further studies on the potential inclusion of small amounts of CNTs in mineral oil, with the purpose of altering the breakdown voltage and lifetime of electrical transformers. Additionally, there is a need to prevent the eventual damage of the internal structure of electrical transformers by altering their electrical stress distribution. This drawback may be provoked by using nanofluids that may negatively affect the permittivity and loss factor of the transformers. Hence, nanofluids to be used in the thermal management of electrical transformers should be carefully selected considering these issues. Further works on the incorporation of Gr and its derivatives in non-edible and bio-friendly oils (e.g., cottonseed oil) should be undertaken in the near future.

Table 10. Recent studies on the use of 2D nanofluids in electrical transformers.

Reference	Authors/Year	Nanomaterial/Concentration	Base Fluid	Main Findings	Remarks
[152]	Amiri et al., 2015	CNTs functionalized with hexylamine at 0.001% and 0.005% wt.	Transformer oil	Increase of 10% in the TC compared with that of the transformer oil alone at 0.005% wt.	Increases in the natural convection and forced convection HTC of 23% and 28%, respectively, at 0.005% wt.
[153]	Amiri et al., 2017	Gr quantum dots at 0.001% wt.	Transformer oil	Increase in the HTC of 23.9%.	Negligible increase of 1.3% in the viscosity.
[154]	Suhaimi et al., 2020	MWCNTs at up to 0.02 g/L	Disposed Transformer oil	Increases of approximately 212.6% and 40% in the AC breakdown strength and lightning impulse pattern indicated at 0.005 g/L concentration compared with the transformer oil alone.	The presence of the MWCNTs resulted in a decrease in the dissipation factor, and an increase in the permittivity and resistivity of the transformer oil alone.
[155]	Alizadeh et al., 2022	MWCNTs functionalized with OH at 0.001% and 0.01% wt.	Transformer oil	Increases of approximately 26.2% and 30.1% in the HTC at 0.01% wt. and 0.001% wt., respectively.	Decrease of nearly 28.4% in the breakdown voltage at 0.01% wt.
[156]	Suhaimi et al., 2022	CNTs from 0.01 g/L to 0.2 g/L	Mineral oil	Increases of nearly 118.3% in the breakdown voltage at 1% probability and at 0.01 g/L.	At 0.01 g/L, the nanofluid strongly impacted on the storage modulus, viscosity, and thermal behavior, which contributes to the breakdown performance.

3.6. Cold Thermal Energy Storage

Cold thermal energy processes are pivotal in certain applications, such as the thermal energy management of air-conditioning systems in large buildings. Two-dimensional nanofluids with high thermal storage capabilities provided mainly by their enhanced latent heat capacity, which is the case in Gr 2D nanofluids, are suitable for such heat storage purposes. The hybrid formulations composed by 2D nanofluids and phase change materials have already been demonstrated as strong candidates to successfully store cold thermal energy. In subzero cold thermal energy storage systems, it is current practice to explore ethylene glycol nanofluids as phase change materials. These nanofluids normally exhibit a large supercooling degree, an extended freezing time, a poor storage capacity, and poor colloidal stability. To overcome these limitations, Zhang et al. [157] prepared stable nanofluids composed of 2D GO nanosheets suspended in ethylene glycol to evaluate their suitability to operate as performant subzero cold thermal energy storage phase-change media. The authors stated that the uniformly dispersed monolayer nanosheets of GO reduced the supercooling degree, accelerated the charging and discharging processes, and retained the enhanced specific heat of the phase change nanofluids. Furthermore, the incorporated nanosheets provided heterogeneous nucleation points, enabling the formation of crystals and reducing the freezing time and supercooling degree. Particularly, the supercooling degree was found to be reduced by 87.2%, the freezing period was reduced by 78.2% (in reference to those of the pure base fluid), and the latent heat was maintained at 98.5%. The synthesized nanofluids increased the TC up to 12.1% compared with that of the ethylene glycol itself. Moreover, the nanofluids maintained their thermal stability after being subjected to 50 cycles of freezing/melting, which guarantees a consistent performance as a cold thermal energy storage fluid during extended working periods. In sum, the improved thermophysical characteristics, together with the facile method of preparation and low loading needs, makes GO nanosheet ethylene glycol nanofluids suitable for use in high-performance subzero phase change cold thermal energy storage systems. Nonetheless, there is a lack of research on the development of effective thermal energy management with rapid charging modes using 2D nanofluids. The energy saving potential of the combined use of 2D nanofluids and phase change materials during the freezing process should be addressed in further research. Additionally, there is a literature gap on the impact of 2D nanofluids on the rate of supercooling and freezing. Moreover, there are few experimental or numerical works on the 2D nanofluid-based storage unit potential in efficient chiller-based air-conditioning systems for the cooling of large buildings.

3.7. Geothermal Heat Recovery

Two-dimensional nanofluids are suitable for use in heat exchangers in geothermal systems. They possess great potential for use in geothermal borehole heat exchangers or ground heat exchangers as circuit heat transfer fluids. In recent decades, the need for energy consumption is increasing continuously. A major part of the energy requirement is satisfied through the use of traditional resources of energy, such as gas and coal, resulting in elevated resource spending rates. Nearly one quarter of the total energy is applied in responding to worldwide heating/cooling needs of the large-scale industrial and commercial sectors by conventional equipment, which requires a large amount of improved energy, mainly originating from power plants working with fossil fuels, releasing large number of discharges into the environment. The ever-increasing concern of pollution has persuaded researchers to shift their focus to the design and implementation of eco-friendly energy systems with minimized greenhouse gasses emissions to satisfy heating/cooling global demands by employing a smaller electrical energy input quantity. Consequently, there is an urgent need to substitute the polluting energy resources with renewable energy resources, and the sustainable energy ground source heat pump system (GSHPS) is an alternative solution. The GSHPS is an environmentally benevolent system capable of (partially) meeting universal heating/cooling requirements. The system has gained popularity in house heating and cooling, since these applications directly contact the ground energy resource that remains

almost constant in the in-depth temperature profile beyond 15 meters of depth. The performance of the GSHPS depends on a heat interaction within the ground by a ground heat exchanger (GHE), also known as a geothermal heat exchanger. The heat transfer efficiency of the GSHPS is higher because of the heat rejection and the extraction is carried out under an almost constant ground temperature. Traditional energy systems are conceived to work under continuously changing ambient temperatures to fulfill space conditioning loads. The vertical borehole GHE is commonly employed in GSHPS. The elevated installation cost of the GSHPS compared with conventional air conditioning systems hinders their global implementation. A decrease in the depth of the borehole with negligible alterations in the output of the GHE is required for the economic viability of the system. As a result, many researchers have searched for the most adequate mode to improve the efficiency of the GHE. Faizal et al. [84] found that an enhanced thermal conductive filler and material can also be mixed with concrete for the heat transfer to reach considerable amelioration. Only small improvements were observed in the efficiency of the GHE with different methods. This may be justified as the operation of the GHE was within a small temperature difference between the working thermal fluid and the underground soil temperature values. Nanofluids may be considered as suitable working fluids to enhance the heat transfer performance of a GHE for a better use of the ground available energy. The mathematical modeling developed by Tarodiya et al. [158] was applied to different nanoparticles, including MWCNTs and Gr, with varying concentrations dispersed in water to study the influence of the nanofluids in the ground source heat pump system. The most relevant findings of the modeling and numeric simulation were the increase in the outlet temperature difference of the heat transfer fluid, and the decreases in the length of the ground heat exchanger, pressure drop of the system, and vertical temperature profile in a single U-tube vertical closed-loop ground heat exchanger. The impact of the concentration of the nanoparticles, imposed flow rate, and temperature gradient between the soil and the inlet operating fluid, pipe and borehole radius, and overall depth on the ground heat exchanger efficiency was also determined. Although the best overall performance was given by graphite nanofluids, the 2D nanofluids used also exhibited an improved performance. The main conclusions were as follows:

- The temperature of the working fluid at the outlet increased in heating mode, while the required pipe length decreased when using the nanofluids compared with the water alone.
- The outlet temperature difference was reduced with the flow rate enhancement of the operating nanofluids.
- The effect of the increase in the GHE efficiency using the nanofluid decreased with the increasing flow rate of the operating fluid and the decrease in the difference between the soil and inlet fluid temperature values. The efficiency of the system was improved with the increases in the pipe and borehole radii and total depth.
- The reduction in the fluid temperature at the outlet was obtained with MWCNTs and Gr nanoparticles of approximately 65% with an increase in the flow rate of 0.4 L/s.
- The reduction in the pipe length was obtained with MWCNTs of approximately 32.9% with an increase of 0.4 L/s in the flow rate. The homologous value for the Gr nanoparticles was approximately 37.1% with the same enhancement in the flow rate.
- The maximum outlet fluid temperature difference and GHE length reduction were 11.4% and 53.4%, respectively, using MWCNTs and when the pipe diameter was changed from 20 to 50 mm. The homologous values for the Gr nanoparticles were 12.06% and 50.2% with the same pipe diameter enhancement.
- An augmentation of 14% in the outlet temperature and a reduction of approximately 20% in the pipe length were achieved when the borehole size was increased from 70 to 110 mm for the MWCNTs. The homologous values for the Gr nanoparticles were 18.9% and approximately 20% with the same increase in the borehole size.

- The maximum increase in the fluid temperature at the outlet and pipe length reduction were obtained with the MWCNTs and Gr nanoparticles at approximately 68% and 61.7%, respectively, with the increase in the difference between the temperature of the inlet and that of the soil (16 °C) from 7 °C to 15 °C.

More numerical simulations in both laminar and turbulent regimes of 2D nanofluids flowing in geothermal heat exchangers are required in the future. Further studies on the innovative use of 2D nanofluids and hybrid formulations in modern geothermal heat exchangers, such as the finned conical helical type, should be addressed. Additionally, efforts should be made to optimize the use of 2D nanofluids with appropriate flow rates and specifications. Considering the flow rate, some geothermal energy extraction systems working with nanofluids have demonstrated that an increased flow rate provoked a returning flow in a geothermal heat exchanger with a lower temperature and an enhanced ground heat extraction. Special emphasis should be attributed to the sedimentation of the nanoparticles in the borehole heat exchangers, since it can be verified in the published literature works that after many hours of continuous operation, the accumulation of the nanostructures completely blocked the bottom of the borehole in cases where the nanofluids circulated with relatively low velocities. Numerical simulations on the subject are also recommended.

4. Environmental Impact of the 2D Nanofluids

Two-dimensional nanofluids have been demonstrated as a promising alternative to traditional heat transfer fluids; however, it is also of relevance to evaluate the impact of the former on the environment. Published studies have rather scarcely addressed the environmental impact (EI) of 2D nanofluids; however, a few authors have argued that these thermal fluids are a sustainable alternative. The EI of 2D nanofluids is derived fundamentally from parameters including the HTC, TC, analysis of the emissions and pressure drop, and energy efficiency, which is the ratio between the energy output and the overall energy input. Renewable energy is an attractive area of actuation, especially considering the actual environmental conditions and, consequently, harnessing energy from these sources must be effective. Two-dimensional nanomaterial thermal fluids are more performant because of their high surface area and TC. This results in size reduction in the equipment, as shown by Sundar et al. [159]. Less CO_2 emissions and more biofriendly methods consequently occur. Although emissions are low during the production of nanoparticles, they should be considered while evaluating the overall EI. Despite the broadened utilization and benefits of 2D nanomaterials, their environmentally detrimental synthesis processes must be evaluated. Additionally, the inadequate disposal of effluents generated during the manufacture of 2D nanomaterials and toxic emissions pose a negative impact to existing ecosystems and human health. Nanomaterials in general are produced by laser ablation, CVD, chemical reduction, and sol-gel, among other techniques. CVD is the technique that achieves a high yield, with large scale processing of CNTs and other 2D nanomaterials at relatively low cost. It is consequently used as a common production method for 2D nanomaterials. An EI study for CNTs synthesized by CVD using the LCA technique was undertaken by Trompeta et al. [160]. The analysis of the emissions, disposal of the effluents and by-products, and power generation were considered, and the corresponding EI was assessed considering two different pathways of CNT production through CVD. Singh et al. [161] used SimaPro v. 7.0 software to carry out an analysis on the EI of CNT preparation and verified the formation of smog and effluents, such as Fe_2O_3, Co_2O_3, MoO_3, and NaOH. The authors strongly recommended that these by-products should be carefully treated to mitigate their EI. On the other hand, the laser ablation technique produces high-purity 2D nanomaterials without creating harmful emissions or the formation of toxic by-products. Suitable by-product evaluations and disposal procedures are recommended to effectively analyze the overall EI of the process. An efficient recovery of the base liquid and nanoparticles of the nanofluids will have a lesser EI by restricting the pollution of the water. Consequently, the design and implementation of proper recovery procedures, such as centrifugation followed by evaporation of the supernatants,

are vital for the recovery process. In most cases, the innovative materials and chemicals still pose environmental and human health risks, including the polychlorinated biphenyls, dichlorodiphenyltrichloroethane, benzene, and halocarbon emissions. Consequently, they must be carefully assessed to mitigate the health hazards [162]. The respiratory tract is the main pathway by which nanoparticles enter the human body and, hence, the lungs are the most vulnerable organs to the exposure of nanomaterials. The chemical and structural characteristics of nanoparticles considerably impact their adversity. Size, aggregation, and chirality are the most important factors to consider. Additionally, human exposure to nanomaterials can be harmful to the cytoskeleton, DNA repair, cell signaling, and may involve the production of inflammatory cytokines and chemokines [163]. The dimensions and chemical composition of 2D nanomaterials are the main factors of toxicity in humans. As an example, researchers studied the risk to human health of 2D nanomaterials such as Gr and MoS_2 [164]. Furthermore, the researchers proposed that the toxicity will increase with the decreasing size of the nanomaterials, as their dimensions are the main influencing toxicity factor [165]. The use of in situ air purifiers and water filtration equipment reduce the intake via the respiratory and digestive pathways [166]. Additionally, commercially available nanomaterials should be intensively tested to determine their toxicity to the environment. An extensive life cycle assessment (LCA) of various nanomaterials may be helpful for the design and implementation of procedures to decrease their negative features on the environment and human health.

5. Life Cycle Assessment

A LCA analysis is conceived to determine the effect of products on the environment and resources. This method enables the determination of effects across an entire product life cycle, from the raw material extraction to the production stage and usage [167]. LCA studies of 2D nanofluids involved fundamentally a LCA analysis of the included 2D nanomaterials. The already performed nanomaterials LCA analysis revealed that their manufacturing procedures are much more energy consuming than conventional materials. Nonetheless, some specific parameters, including the selection of the precursors and temperature of the preparation stage, may strongly impact energy consumption and environmental issues. The preparation of nanoparticles to be included in the base fluid requires an appreciable energy amount; however, this limitation may be outweighed by the improved performance of 2D nanofluids during their working lifespan. Some examples can be cited, such as self-cleaning nanoparticle coatings, which may drastically reduce maintenance requirements by way of compensating the undesirable EI from the manufacturing procedure. Arvidsson et al. [168] conducted an LCA analysis of ultrasonicated and chemically reduced Gr and found that the diethyl ether recovery may strongly decrease the inherent EI. Additionally, Cossuta et al. [169] applied the LCA to evaluate the scalability of three different Gr production methods: graphite electrochemical exfoliation, thermal reduction or chemical oxidation, and CVD. The researchers reported that the chemical reduction procedures were those with less propensity to be applied in large-scale Gr manufacturing processes. In conclusion, the LCA analysis of 2D nanomaterials evaluated alternative manufacturing procedures to follow and associated environmental effects, aiding in the design and implementation of an alternative synthesis method with minimized EI. The following sub-sections of this review briefly describe the LCA analysis conducted for some of 2D nanomaterials overviewed in this work.

5.1. Graphene

The study performed by Beloin-Saint-Pierre and Hischier [170] compared the previous Gr nanomaterial LCA studies with new results associated with ball milling of few-layer Gr. This study consisted of a reliable overview of the actual knowledge on the environmental sustainability of the Gr nanomaterials through three different life cycle impact assessment (LCIA) analyses. The international life cycle data (ILCD) midpoint method was chosen first since it provides the EI evaluation according to the general recommendations of the

European Commission. This methodology enables the comparative examination of Gr nanomaterials in various EI categories by determining the involved extraction of the resources and emission of pollutants as a function of the equivalent effects of the polluting substances of reference for each category. The LCIA method IMPACT 2002+ was used at the endpoint or damage level. This approach advances one step and regroups the EI at midpoint into their effects on the climate change, human health, the ecosystem, and available natural resources. The ILCD and IMPACT 2002+ methods were chosen mainly because of their enhanced representativeness within the European context. The cumulative energy demand (CED) method returns the global cumulative energy needs. These LCIA methods were taken from the current Ecoinvent package. The results from the IMPACT 2002+ method were translated from points to kg of CO_2 equivalent (eq.) for the categories CC, PDF.m^2·year for EQ, DALY for HH, and MJ primary for Res to facilitate the comparison with the ILCD and CED methods. The initial general finding is the major influence of the chemical products and electricity consumption in a Gr nanomaterial life cycle. Their relevance varies according to the type of Gr nanomaterial and manufacturing procedure. As an example, the EI from the GO synthesis mainly comes from the employment of chemical substances, whilst the impacts of Gr nanomaterial production are largely connected to the electricity consumption required, except for the ultrasonication procedure which is dominated by diethyl ether usage. These points highlight the main overall inputs on which the technology should be focused for EI mitigation in future manufacturing processes of Gr nanomaterials. Two general recommendations should be respected: the use of chemical products should be reduced (mainly in GO synthesis), and energy efficiency in production for all manufacturing processes should be pursued. These general recommendations are compliant with the green chemistry principles that provide the guidelines to decrease EI in the production of Gr nanomaterials. The contribution study confirmed that the usual discrepancy between the published works can be interpreted based on the different aggregation of the different system models rather than by the input dissimilarities for the considered manufacturing processes. This demonstrates the need for a study based on a harmonized framework, given that it clarifies that previous works exhibited a general agreement on the main contributors of the EI from the synthesis of Gr nanomaterials. The analyzed impacts for the solution of dry material offered new insights on the important meaning of the output state for Gr nanomaterials. Keeping Gr nanomaterials under solution may be environmentally benevolent if it can be directly employed as an input to the system. These findings also indicate that the recycling processes for chemical substances may cause a significant increase in the EI from Gr nanomaterial products if they require dialysis of their solutions. The selection of energy sources or country of production could bring a meaningful reduction in the potential impacts. Energy efficient recycling options to diminish the utilization of chemical substances may be pivotal to ensure the environmental benevolence of Gr nanomaterials. The evaluation of the uncertainty associated with Gr nanomaterial manufacturing routes confirms that there is still significative ambiguity on interpreting their potential EI, except for the cases considered in the most recent studies [171]. The uncertainty degree associated with manufacturing methods is considerable for most types of Gr nanomaterial, preventing the identification of cleaner manufacturing alternatives. When the comparative results of the impacts and the contribution analysis were taken together, the electricity requirement surges as the principal source of uncertainty in the current models, even though it is not the main promotor in all procedures. This fact can be interpreted through the observed considerable variability in the inputs of electricity demand in studies where the production of Gr nanomaterials reach industrial scalability. The comparison of Gr with other competing materials indicates that manufacturing methods might result in EI mitigation for certain applications, such as touch screens or back contacts in PV cells. While this study proposes some innovative solutions to reduce the EI of the production of Gr nanomaterials, it is also limited on the analysis of certain concerns that should be tackled in future LCA studies. One of those concerns is the lack of quantified descriptions of functional characteristics of Gr nanomaterials which hinders the ability to

obtain a balanced comparative analysis upon the potential applications of Gr nanomaterials. For instance, this study considers an in-depth analysis in cases where Gr nanomaterials are compared, because it is not probable that all nanomaterials possess the same functional properties that would make them interchangeable. Additionally, the measured demand for electricity in the synthesis stage must deal with considerable uncertainties associated with the values reported in previous studies that have used patents and scientific articles instead of measurements [171,172]. The differences may be interpreted by using different equipment or by the quality of the manufactured Gr nanomaterials, but the identification of the fundamental sources of discrepancy is still very challenging until further studies are performed on all processes. A reduction in the uncertainty associated with the input data should also be prioritized to clarify if the life cycle impacts of the Gr nanomaterial manufacturing processes are still overlapping or if certain alternatives might have improved environmental benevolence. This is a pressing matter in the production of GO and Gr nanomaterials, even if the Gr-associated uncertainties avert the identification, for instance, of any distinction between two types of CVD synthesis methods. The measurement of input flows in the laboratory environment could be a suitable way to reduce uncertainties until the industrial large-scale production level is reached. Moreover, the toxicity of Gr nanomaterials is often inferred within the European Graphene Flagship research initiative [173], and some characterization factors for GO have been proposed for freshwater [174]. For now, the baseline characterization factor of 777.5 CTUh·m^3 ·year/kg of GO indicates that GO emissions in freshwater might bring a significant alteration to the FEcotox impact. The FEcotox impact of the synthesis process would double if 41% of the manufactures GO was released, for instance, at its end of life. In addition, the impact of GO would be less concerning for manufacturing methods with higher impacts in which a total release of GO would increase the corresponding FEcotox impact by approximately 4%. When the functional properties were defined for the family of Gr nanomaterials, the prediction models for the use stage and end-of-life stage should gain more importance. The application of new characterization factors should also be conducted to account completely for the EI of Gr nanomaterials. Additionally, the assessment should include alterations to the lifetime of the equipment when working with Gr nanomaterials, instead of those verified for competing nanomaterials. The study of previous LCA studies and the new data from the production of Gr nanomaterials, within a harmonized modelling framework, will undoubtedly provide more insights on the EI from all aspects of Gr nanomaterial production. Generally, the need to emphasize the decrease in impacts derived from the chemical products and electricity consumption in Gr nanomaterial production is widely accepted to ameliorate their environmental sustainability. Furthermore, the different production processes that depend on the type and physical state of the Gr should be considered. Additionally, the trend of European electricity mixes until the year of 2040 might not show relevant alterations in the current environmental situation of Gr nanomaterials. The comparative analysis with Gr competing materials also indicated that Gr might not be the best environmental alternative for certain applications. The study of the available publications showed that the large-scale fabrication of Gr could reduce the EI of the production stage. Many features affecting the EI of Gr nanomaterials are still not totally understood, raising important questions on their actual analysis. Indeed, there are still unresolved questions that require further investigation, such as quantified evaluations of the functional properties and toxicity level of Gr nanomaterials. Exact energy consumption values during the manufacturing stage of Gr nanomaterials would be helpful to improve the knowledge of the scientific community on the differentiation of current and further production routes.

5.2. Carbon Nanotubes

Climate change provoked by excessive worldwide CO_2 emissions into the atmosphere has recently attracted global concern. The actual large-scale methods generally utilize monoethanolamine for the capture of CO_2. Nonetheless, CO_2 regeneration requires high temperature values, and every adsorption/desorption cycle is an energy-demanding pro-

cess, as it also entails material losses. The amines with enhanced capture capability are currently implemented as adsorbents to overcome existing limitations. Nevertheless, the EI caused by the adsorbents were not often discussed in the past. Wu et al. [175] determined the EI of new CO_2 capture adsorbents by synthesizing CNTs with adsorbed and covalently bonded polyethyleneimine and compared them with those associated with the conventional monoethanolamine capturer using the LCA technique. Carbon payback periods were also studied to achieve an improved knowledge on the scalability of the evaluated new materials. The obtained results suggested that the use of CNTs contributed to most of the EI for CNTs with polyethyleneimine. The corresponding carbon payback periods are over 40 times longer than when applying monoethanolamine during the production stage. Nonetheless, the energy consumption of the adsorbed polyethyleneimine may be reduced by up to 60% in comparison to the monoethanolamine in each adsorption/desorption cycle due to its lower heat transfer capability. Additionally, the rate of CO_2 remission for CNT-polyethyleneimine is two-fold greater than that associated with monoethanolamine, revealing its potential for application in large-scale CO_2 captures. In essence, the study indicated that solid amine is a promising option for CO_2 capture but nevertheless requires several further ameliorations. Future investigation works should be focused on reducing the initial manufacturing of the nanomaterials and increasing the product lifespan based on their environmental tradeoffs. Moreover, the authors highlighted that the emphasis on only the CO_2 capture effectiveness by the innovative materials may not be totally adequate, and more extensive studies should be performed based on the comparison during the nanomaterial LCA. The life cycle environmental and health impacts were modeled using SimaPro software with Ecoinvent and United States Life Cycle Inventory databases. Among others, the midpoint categories that were examined were ozone depletion (kg CFC-11 eq.), global warming (kg CO_2 eq.), carcinogenic (CTUh), respiratory impact (kg PM2.5 eq.), ecotoxicity (CTUe), and fossil fuel depletion (MJ surplus). The researchers argued that the energy penalty, functional units, and scalability among other topics are the main limitations and challenges that are overlooked in the capture and storage of carbon studies [176]. The obtained results suggested that carbon payback depends appreciably on the lifetime of the CNT-polyethyleneimine. Many published works revealed a consistent recovery up to 100 cycles; however, the findings of this work indicated that a total of more than 900 adsorption/desorption cycles are needed to achieve a breakeven CO_2 payback for physically adsorbed CNT-polyethyleneimine. Moreover, to optimize fabrication and improve the CO_2 adsorption capability, further studies should also be carried out to ensure the maximum lifetime capability of the CNT-polyethyleneimine under extreme conditions to receive more payback outcomes. The researchers have simplified the analysis by assuming no extra environmental burden is induced by the degradants of the monoethanolamine. The monoethanolamine degradant dilution may decrease their CO_2 capture capability. Such practical limitations may reduce the effectiveness of the liquid phase capturing solutions and highlight the advantages of the solid amine for CO_2 remission. Despite published studies claiming that the use of solid-state amines for the capture of CO_2 still define the embryonic stage of development and a considerable number of challenges still needed to be successfully resolved, the solid amines have become gradually more appealing in CO_2 capture, given that the process does not employ any kind of solvent, reducing the energy penalty from regeneration in comparison with the conventional capture in liquid state. Nonetheless, the considerable energy requirements for the synthesis of the adsorbent are still a concern that may counteract the energy needs for the regeneration process. In sum, the CNT-polyethyleneimine as an amine absorbent exhibited higher environmental costs than the commonly used monoethanolamine method during the production stage. The production of CNTs was considered as the main contributor to the life cycle EI. Nonetheless, there is still room to improve the technology, such as using more sustainable energy sources, scaling up, and recycling to enhance the production efficiency. In sum, having higher CO_2 remission rates, capture capability, and reusability, the physically adsorbed CNT-polyethyleneimine is a promising alternative to surpass limitations including the off-

set CO_2 cost and sustainability of CO_2 capture. Given that CO_2 emissions are of paramount importance in climate change, the development of methods that diminish CO_2 emissions is recommended. The authors emphasized that the focus on the CO_2 capture by innovative materials alone is not sufficient, and more extensive EI comparisons using material LCAs should be carried out in the future.

5.3. Tungsten Disulfide

Regarding the LCA analysis of WS_2 nanomaterials, a study was conducted by Bobba et al. [177] considering the EU-FP7 project AddNano to evaluate the EI of the gas phase reaction in the production of WS_2 nanoparticles. The authors performed a preliminary review of the published literature and highlighted many data gaps because of the little or no communication between stakeholders and the lack of published LCA studies and results related to nanomaterials in general with regards to the main stages of the LCA of nanoparticles. A from-cradle-to-gate LCA of the industrial processing of WS_2 nanoparticles was carried out. The obtained results confirmed that the production of WS_2 nanoparticles is very energy consuming, and the tungsten trioxide is the raw material with the greatest contribution. It should be clarified that the EI evaluation referred to the synthesis of one gram of nanosized WS_2. The production of WS_2 was found to be a strongly energy-consuming procedure. The LCIA CML1992 study revealed that the contribution of electricity in the preparation stage of WS_2 was, in every mode, higher than 26%, with 26.1% human toxicity and approximately 31% greenhouse gas impact. It was found that the impacts derived from the scrubbing solution and gas mixture were very low. Indeed, regarding the CML1992 and ReCiPe2008 impact categories, the overall impact of these products never surpassed 3.84%, with the highest value related to the human toxicity of 1.97E-05 HC for 1 g of WS_2 and 8.64% with the highest value associated to the human toxicity of 2.57E-04 kg 1,4-DB eq. for 1 gr of WS_2. Considering the electricity consumption, it was found that the contribution of electricity to the entire production stage of WS_2 was very high for all considered impact categories. The authors conducted the LCA analysis based on data gathered from the industrial sector and, hence, the results are in reference to large-scale production processes, averting scale-up simplifications. Due to the scarce number of published LCA studies on nanomaterials, with the available studies often fragmented, it is very complex to gather data to better understand LCA approaches and to apply the corresponding outcomes for developing new and more accurate analyses. Furthermore, the available datasets and environmental assessments of the nanomaterials are usually based on data from laboratory pilot experiments and not on large-scale industrial implementation processes. The conducted review of the published LCA data emphasized an urgent need for the implementation of datasets and the improvement of communication between the various nanotechnology sectors and between producers and customers. In this regard, the LCA analysis concerning the production of WS_2 nanomaterials was consistent with the published LCIA results.

5.4. Molybdenum Disulfide

The industrial production of MoS_2 nanomaterials may raise concerns regarding environmental and health impacts. To mitigate these concerns, Hachhach et al. [178] applied the LCA method to the scaled-up production of MoS_2-engineered nanomaterials using the solvothermal process. The method was undertaken through the combined use of Aspen Plus and from cradle-to-gate LCIA IMPACT 2002+ considering 1 kg of MoS_2. The results demonstrated that most of the impact categories were linked with the production and inherent sub-processes of the lithium hydroxide. The EIs were analyzed to identify the fundamental problems and to propose technological routes to reduce, or even eliminate, the environmental burdens. The impact assessment was carried out with the aid of the 2002+ impact inferring method. The impact 2002+ LCIA approach proposes the implementation of a midpoint/damage route, linking all types of LCI results through 14 midpoint categories [179]. The researchers fundamentally focused on the categories of resources

and energy consumption, given that the production of MoS_2-engineered nanomaterials demands a high amount of energy and resource use. To achieve an improved understanding of the EIs and corresponding solutions to mitigate them, it is necessary to assess the contribution of every process in the impact category. Among the investigated impact categories, it has already been demonstrated that the ecotoxicities and non-carcinogen impacts derived only from the existence of aluminum emissions to the water originated from the production of lithium hydroxide according to the Ecoinvent database. The impact category of land use summarized the EIs closely linked with the tasks of human occupation, reshaping, and exploration of the land, and this can refer to the time of extended occupation on the land or to the change in the type of land that contributes to the emission of CO_2 [180]. In this sense, the authors considered that the land EI originated from the occupation of the forest, implementation of industrial and traffic areas, and dumpsites. The climate change impact fundamentally originated from the release of greenhouse gases, namely CO_2 and methane. The CO_2 emanated mainly from the production of steam with 42.6 kg CO_2 eq. and electricity consumption with 347.7 kg CO_2 eq., which surpassed the CO_2 generated by the land use of 0.03 kg CO_2 eq. Similarly, methane production contributed to the climate change category with 1.03 kg CO_2 eq., which was generated in the steam production from natural gas. The impact of mineral extraction dealt with the extraction of the molybdenum itself as the component for the precursor $(NH_4)_6Mo_7O_{24}$. The extraction of molybdenum may result in wastes containing concentrations of up to 4000 mg/kg of molybdenum, resulting in the contamination of the soil, sediment, and water. The findings were consistent with those reported in [180] which, for the same WS_2 and boundaries of the involved system, confirmed that this was the principal contributor to a major part of the considered impacts, being responsible for more than 64% of the sum of the impact categories. Molybdenum is widely recognized as an essential trace metal for almost all organisms due to its role as a cofactor in diverse enzymes. Nonetheless, when present in high doses, molybdenum can be toxic [181]. In the referred study, the origins of the already mentioned chemical compounds were various. The extraction of the mineral processes impacted the environment through the extraction of pure molybdenum, and the climate change impact was generated mainly through the production of steam and electricity. The terrestrial and aquatic ecotoxicity and non-carcinogenic impact categories could be affected by the acetone production, whereas the remaining impact categories were essentially caused by the production of lithium hydroxide that can be replaced by a similar strong base, given that the lithium hydroxide is not consumed during the synthesis of engineered nanomaterials. It was confirmed that this production is resource- and energy-consuming and can translated to comparatively high impact, such as global warming, non-renewable energy mineral extraction, and intense land occupation, meaning intense deforestation. Nonetheless, it was verified that the process is not toxic for humans, flora, or fauna. To reduce the EI, the origins of the impact categories were determined, and it was found that acetone, molybdenum, and lithium hydroxide were fundamentally responsible, given that the molybdenum and acetone are vital for the production stage and are spent during the process, whereas lithium hydroxide is not consumed but is incorporated as a pH adjuster. Consequently, it can be replaced by cheaper and cleaner sodium hydroxide. Hence, the replacement of lithium hydroxide by sodium hydroxide showed positive results and may drastically reduce the associated environmental burdens. A decrease of 56% in the use of non-renewable energies and land occupation was recently reported.

6. Limitations and Future Prospects

The fundamental limitations and future prospects related to 2D nanofluids are summarized in the following points:

- The measurement of the thermophysical properties of 2D nanofluids should be further improved. For instance, the actual TC data may be erroneous since incoming data from identical thickness samples differ appreciably from each other, which is not surprising given the lateral sides and the operating conditions considerably, hindering an accurate measurement and the comparison of results.
- The results on the TC of 2D nanofluids show that the maximum TC enhancement did not correspond to the maximum zeta potential. Hence, a precise concentration level optimization is the main factor for achieving the optimal heat transfer nanofluid.
- Regarding the tungsten disulfide nanofluids with the addition of surfactants (e.g., SDS), the enhanced amount of SDS reduced the TC of 2D nanofluids. However, under high temperature values the behavior oscillates. The reason behind this fact could be the detachment of the molecules of the surfactant and the consequent interaction between the WS_2 nanosheets. Thus, further studies are required to better understand this high-temperature behavior.
- Further experimental evaluation studies of 2D nanofluids are recommended to stablish a database with the stability over time, specific heat, TC, and rheological characteristics for comparison purposes.
- More experimental and numerical works on the size reduction possibility when using 2D nanofluids in heat transfer equipment and in systems such as PV/T are required such as those analyzed in the work conducted by Sreekumar et al. [142].
- Despite the extremely high intrinsic TC of Gr, the verified increases in the TC of Gr nanofluids were up only by 50%. This fact should be further investigated with the aid of numerical modeling and in-depth theoretical studies to achieve a better TC.
- Since it was already reported that the viscosity of the Gr nanofluids is higher than that of other metals and metallic oxide nanofluids that may result in enhanced flow friction and pumping power needs, an accurate investigation of the friction, pressure drop, and pumping power needs is recommended to fully interpret the tradeoff between the improved TC and the augmented friction and pumping requirements.
- The economic feasibility of Gr nanofluids should be further evaluated to identify the balanced commitment between the technical and economic feasibility of Gr nanofluid solutions. Most of the economic challenges are associated with current Gr synthesis procedures, which are expensive, material intensive, and energy demanding. Consequently, welcome advancements in Gr manufacturing would relieve the technical and economic limitations for the practical application of Gr nanofluids.
- Further hybrid evaluation methods should be implemented through the combined usage of molecular dynamic numerical simulations and fluid dynamic laboratory experiments to achieve a better understanding the behavior of 2D nanofluids.
- Studies on the impact of the hybrid approach of the inclusion of metal (e.g., copper, gold) or metal oxides (e.g., iron oxide) into Gr nanosheets should be undertaken in order to improve the thermal characteristics of Gr nanofluids.
- More research on the stability, TC, and viscosity of WS_2 nanoparticles suspended in ethylene glycol nanofluids with the addition of surfactants should be conducted. Playing the role of stabilizers and rheological modifiers, the careful use of surfactants such as SDBS and CTAB can improve suspension stability over time and reduce the viscosity of 2D nanofluids.
- Further studies are recommended to evaluate as accurately as possible the real electronic contribution of phonon transport to the TC of Gr. Definitive laboratory data supporting the electronic contribution are still missing.
- Further experiments should be conducted on the interfacial thermal conductance of 2D nanofluids and nanomaterials. Apart from the common acceptance that interfacial coupling increases interfacial thermal conductance, precise laboratory measurements of this property are scarce.

- Future research should be conducted in the field of PV/T systems regarding heat transfer media, as it is possible to replace the commonly used phase change materials with stable nano-scaled PCMs to achieve a significant improvement in the heat transfer performance of PV cells. The thermophysical properties of the working fluid can be enhanced with 2D nanofluid usage.
- In certain potential applications, such as enhanced oil recovery, the wettability of 2D nanofluids and nanomaterials is of great importance. Nevertheless, the already published findings regarding the wettability and contact angle measurements of the included nanoparticles are not consistent with each other. Consequently, further in-depth investigations are needed to clarify this matter and to achieve well-accepted values and trends.

7. Conclusions

The fundamental conclusions of this review can be summarized in the following points:

- The employment of 2D nanofluids can improve the thermal performance of heat transfer systems and devices. Hence, the dimensions of heat changers, heat pipes, and thermosyphons, among others, can be noticeably reduced, resulting in greater efficiency, reliability, reproducibility, and less associated EI.
- The results of the TC measurement of 2D nanofluids with the addition of nanosheets revealed that the maximum TC enhancement did not coincide with the zeta potential maximum. Consequently, an accurate concentration of the nanoparticles is one of the most important factors for achieving the optimal heat transfer performance when employing 2D nanofluids.
- The size reduction in heat transfer and storage equipment and systems using 2D nanofluids is an issue of relevance and has been studied previously. For instance, in the study performed by Sreekumar et al. [142] it was demonstrated that, from the same thermal output of a PV/T system, the MXene 2D nanofluids achieved a reduction in the solar collector area between 4.5 and 14.5%, depending on the concentration of the MXene in reference to a water-based operating PV/T system.
- The rheological analysis suggested the formation of a structured network in the nanofluids of the WS_2 nanoparticles and showed that there was a transition from the viscous behavior to the elastic behavior in WS2 nanofluids with the addition of surfactants. This transition usually requires a higher initial pumping power in the system.
- Gr nanofluids revealed a higher TC at much lower concentrations in comparison to those of the metallic and metallic oxides, such as silver, copper, alumina, and silica, exhibiting enhancements between 40% and 50% at only 0.1% wt. weight fraction. However, Gr nanofluids possess a higher density and viscosity, with the latter reported to be higher than that of the other mentioned nanofluids even at lower concentrations.
- The improved thermophysical characteristics of the rGO are related to its monolayer or multi-layered nanostructures. Nonetheless, the adjacent rGO nanosheets cause them to aggregate into macro-scaled carbon allotropism. Consequently, the assurance of a homogeneous dispersion of the nanosheets is pivotal for the synthesis of rGO 2D nanofluids.
- Two-dimensional nanofluids with the incorporation of Gr nanosheets are commonly found to exhibit higher convective heat transfer parameters than GO nanosheets. The difference may be related to the diverse order of the molecules in the base fluid in the proximity of the Gr nanosheets, parallel structure, and π–π plan stacking.
- It is important to prevent the agglomeration and sedimentation of 2D nanoparticles in base fluids by modifying the charge distribution of their surface. The scientific community have used different technological solutions to tackle this limitation, including covalent functionalization by the modification of the chemical structure, non-covalent functionalization with the incorporation of surfactants, and plasma functionalization. Plasma functionalization usually involves very complex processes and overall costs.

- The possibility of studying the thermal characteristics and mechanisms rarely detected in the bulk nanomaterials is one of the most remarkable characteristics of 2D nanomaterials and corresponding nanofluids. One example is the electronic contribution of the TC of the ballistic and hydrodynamic phonon transport in Gr. This contribution is as high as 10% and is important in thermoelectric applications.
- Regarding 2D hybrid nanoparticles, the thermal contact resistance between the different components may limit the heat transfer capability in thermal management applications. This is the case in CNT/Gr nanofluids, where the thermal contact resistance between the individual Gr nanoflakes and the CNTs remains a problem that should be solved.
- The incorporation of surfactants to improve the colloidal stability of 2D nanofluids should be carefully performed, given that it may be, in some cases, a counterproductive measure due to the absorption of the surfactant molecules on the surface of the 2D nanostructures, which can induce phonon scattering, impacting negatively on the heat transfer capability of 2D nanofluids.

Author Contributions: Conceptualization, J.P.; methodology, J.P. and A.M. (Ana Moita); software, A.M. (Ana Moita); validation, A.M. (Ana Moita) and A.M. (António Moreira); formal analysis, A.M. (Ana Moita); investigation, J.P.; resources, A.M. (António Moreira); data curation, J.P.; writing—original draft preparation, J.P.; writing—review and editing, J.P.; supervision, A.M. (Ana Moita) and A.M. (António Moreira); project administration, A.M. (António Moreira); funding acquisition, A.M. (António Moreira). All authors have read and agreed to the published version of the manuscript.

Funding: The authors are grateful to the Fundação para a Ciência e a Tecnologia (FCT), Avenida D. Carlos I, 126, 1249-074 Lisboa, Portugal, for partially financing the Project "Estratégias interfaciais de arrefecimento para tecnologias de conversão com elevadas potências de dissipação", Ref. PTDC/EME-TED/7801/2020, António Luís Nobre Moreira, Associação do Instituto Superior Técnico para a Investigação e o Desenvolvimento (IST-ID). José Pereira also acknowledges FCT for his PhD Fellowship Ref. 2021.05830.BD.

Institutional Review Board Statement: Not applicable.

Informed Consent Statement: Not applicable.

Data Availability Statement: Data sharing not applicable.

Conflicts of Interest: The authors declare no conflict of interest.

References

1. Iijima, S. Helical microtubules of graphitic carbon. *Nature* **1991**, *354*, 56–58. [CrossRef]
2. Yang, P.-K.; Lee, C.-P. 2D Layered Nanomaterials for Energy Harvesting and Sensing Applications. In *Applied Electrochemical Devices and Machines for Electric Mobility Solutions*; Intechopen: London, UK, 2019.
3. Khan, A.H.; Ghosh, S.; Pradhan, D.A.; Shreshta, L.K.; Acharya, S.; Ariga, K. Two-Dimensional (2D) Nanomaterials towards Electrochemical Nanoarchitectonics in Energy-Related Applications. *Bull. Chem. Soc. Jpn.* **2017**, *90*, 627–648. [CrossRef]
4. Zhang, H.; Chhowalla, M.; Liu, Z. 2D Nanomaterials: Graphene and transition metal dichalcogenides. *Chem. Soc. Rev.* **2018**, *47*, 3015–3017. [CrossRef] [PubMed]
5. Zhao, H.; Chen, X.; Wang, G.; Qiu, Y.; Guo, L. Two-dimensional amorphous nanomaterials: Synthesis and applications. *2D Mater.* **2019**, *6*, 032002. [CrossRef]
6. Tan, C.; Cao, X.; Wu, X.-J.; He, Q.; Yang, J.; Zhang, X.; Chen, J.; Zhao, W.; Han, S.; Nam, G.-H.; et al. Recent Advances in Ultrathin Two-Dimensional Nanomaterials. *Chem. Rev.* **2017**, *117*, 6225–6331. [CrossRef] [PubMed]
7. Shahil, K.M.F.; Balandin, A.A. Graphene-Multilayer Graphene Nanocomposites as Highly Efficient Thermal Interface Materials. *Nano Lett.* **2012**, *12*, 861–867. [CrossRef]
8. Yu, A.; Ramesh, P.; Itkis, M.E.; Bekyarova, E.; Haddon, R.C. Graphite Nanoplatelet-Epoxy Composite Thermal Interface Materials. *J. Phys. Chem. C* **2007**, *111*, 7565–7569. [CrossRef]
9. Singh, S.; Hasan, M.R.; Sharma, P.; Narang, J. Graphene nanomaterials: The wondering material from synthesis to applications. *Sens. Int.* **2022**, *3*, 100190. [CrossRef]
10. Ali, B.; Qayoum, A.; Saleem, S.; Mir, F.Q. Effect of graphene/hydrofluoroether (HFE-7100) nanofluids on start-up and thermal characteristics of pulsating heat pipe. *J. Therm. Anal. Calorim.* **2023**. [CrossRef]

11. Le, T.-H.; Oh, Y.; Kim, H.; Yoon, H. Exfoliation of 2D Materials for Energy and Environmental Applications. *Chem. Eur. J.* **2020**, *26*, 6360–6401. [CrossRef]
12. Guo, S.; Dong, S. Graphene nanosheet: Synthesis, molecular engineering, thin film, hybrids, and energy and analytical applications. *Chem. Soc. Rev.* **2011**, *40*, 2644–2672. [CrossRef]
13. Knobloch, T.; Illarionov, Y.Y.; Ducry, F.; Schleich, C.; Wachter, S.; Watanabe, K.; Taniguchi, T.; Mueller, T.; Waltl, M.; Lanza, M.; et al. The performance limits of hexagonal boron nitride as an insulator for scaled CMOS devices based on two-dimensional materials. *Nat. Electron.* **2021**, *4*, 98–108. [CrossRef]
14. Arshad, A.; Jabbal, M.; Yan, Y.; Reay, D. A review on graphene based nanofluids: Preparation, characterization and applications. *J. Mol. Liq.* **2019**, *279*, 444–484. [CrossRef]
15. Hamze, S.; Berrada, N.; Cabaleiro, D.; Desforges, A.; Ghanbaja, J.; Gleize, J.; Bégin, D.; Michaux, F.; Maré, T.; Vigolo, B.; et al. Few-Layer Graphene-Based Nanofluids with Enhnaced Thermal Conductivity. *Nanomaterials* **2020**, *10*, 1258. [CrossRef]
16. Das, S.; Giri, A.; Samanta, S.; Kanagaraj, S. Role of graphene nanofluids on heat transfer enhancement in thermosyphon. *J. Sci. Adv. Mater. Dev.* **2019**, *4*, 163–169. [CrossRef]
17. Adnan; Abbas, W.; Bani-Fwaz, M.Z.; Asogwa, K.K. Thermal efficiency of radiated tetra-hybrid nanofluid $[(Al_2O_3\text{-}CuO\text{-}TiO_2\text{-}Ag)/water]_{tetra}$ under permeability effects over vertically aligned cylinder subject to magnetic field and combined convection. *Sci. Prog.* **2023**, *106*, 00368504221149797. [CrossRef]
18. Adnan; Alharbi, K.A.M.; Ashraf, W.; Eldin, S.M.; Yassen, M.F.; Jamshed, W. Applied heat transfer modelling in conventional hybrid $(Al_2O_3\text{-}CuO)/C_2H_6O_2$ and modified hybrid nanofluids $(Al_2O_3\text{-}CuO\text{-}Fe_3O_4)/C_2H_6O_2$ between slippery channel by using least square method (LSM). *AIMS Math.* **2022**, *8*, 4321–4341. [CrossRef]
19. Adnan; Alharbi, K.A.M.; Bani-Fwaz, M.Z.; Eldin, S.M.; Yassen, M.F. Numerical heat performance of TiO_2/Glycerin under nanoparticles aggregation and nonlinear radiative heat flux in dilating/squeezing channel. *Case Stud. Therm. Eng.* **2023**, *41*, 102568. [CrossRef]
20. Taha-Tijerina, J.; Pena-Paras, L.; Narayanan, T.N.; Garza, L.; Lapray, C.; Gonzalez, J.; Palacios, E.; Molina, D.; García, A.; Maldonado, D.; et al. Multifunctional nanofluids with 2D nanosheets for thermal and tribological management. *Wear* **2013**, *302*, 1241–1248. [CrossRef]
21. Salehirad, M.; Nikje, M.M.A. Properties of Modified Hexagonal Boron Nitride as Stable Nanofluids for Thermal Management Applications. *Russ. J. Appl. Chem.* **2019**, *92*, 78–86. [CrossRef]
22. Li, Y.; Zhou, J.; Luo, Z.; Tung, S.; Schneider, E.; Wu, J.; Li, X. Investigation on two abnormal phenomena about thermal conductivity enhancement of BN/EG nanofluids. *Nanoscale Res. Lett.* **2011**, *6*, 443. [CrossRef] [PubMed]
23. Bhunia, M.M.; Chattopadhyay, K.K.; Chattopadhyay, P. Transformer oils nanofluids by two-dimensional hexagonal boron nitride nanofillers. *Electr. Eng.* **2022**. [CrossRef]
24. Han, W.; Wang, L.; Zhang, R.; Ge, C.; Ma, Z.; Yang, Y.; Zhang, X. Water-Dispersible Boron Nitride Nanospheres with High Thermal Conductivity for Heat-Transfer Nanofluids. *Eur. J. Inorg. Chem.* **2017**, *2017*, 5466–5474. [CrossRef]
25. Zhi, C.; Xu, Y.; Bando, Y.; Golberg, D. Highly Thermo-conductive Fluid with Boron Nitride Nanofillers. *ACS Nano* **2011**, *5*, 6571–6577. [CrossRef]
26. Fang, X.; Fan, L.-W.; Ding, Q.; Yao, X.-L.; Wu, Y.-Y.; Hou, J.-F.; Wang, X.; Yu, Z.-T.; Cheng, G.-H.; Hu, Y.-C. Thermal energy storage performance of paraffin-based composite phase change materials filled with hexagonal boron nitride nanosheets. *Energy Convers. Manag.* **2014**, *80*, 103–109. [CrossRef]
27. Ilhan, B.; Kurt, M.; Erturk, H. Experimental investigation of heat transfer enhancement and viscosity change of h-BN nanofluids. *Exp. Therm. Fluid Sci.* **2016**, *77*, 272–283. [CrossRef]
28. Ilhan, B.; Ertuk, H. Experimental characterization of laminar forced convection of h-BN water nanofluid in circular pipe. *Int. J. Heat Mass Transf.* **2017**, *111*, 500–507. [CrossRef]
29. Hou, X.; Wang, M.; Fu, L.; Chen, Y.; Jiang, N.; Lin, C.-T.; Wang, Z.; Yu, J. Boron nitride nanosheet nanofluids for enhanced thermal conductivity. *Nanoscale* **2018**, *10*, 13004. [CrossRef]
30. Hussein, O.A.; Habib, K.; Muhsan, A.S.; Saidur, R.; Alawi, O.A.; Ibrahim, T.K. Thermal performance enhancement of a flat plate solar collector using hybrid nanofluid. *Sol. Energy* **2020**, *204*, 208–222. [CrossRef]
31. Zhang, Y.; Wang, M.; Li, J.; Wang, H.; Zhao, Y. Improving thermal energy storage and transfer performance in solar energy storage: Nanocomposite synthesized by dispersing nano boron nitride in solar salt. *Sol. Energy Mater. Sol. Cells* **2021**, *232*, 11378. [CrossRef]
32. Farbod, M.; Rafati, Z. Heat transfer, thermophysical and rheological behavior of highly stable few-layers of h-BN nanosheets/EG-based nanofluid. *Mater. Today Commun.* **2022**, *33*, 104921. [CrossRef]
33. Novoselov, K.S.; Geim, A.K.; Morozov, S.V.; Jiang, D.; Zhang, Y.; Dubonos, S.V.; Grigorieva, I.V.; Firsov, A.A. Electric Field Effect in Atomically Thin Carbon Films. *Science* **2004**, *306*, 666–669. [CrossRef]
34. Panjiar, H.; Gakkhar, R.P.; Daniel, B.S.S. Strain-free graphite nanoparticle synthesis by mechanical milling. *Powder Technol.* **2015**, *275*, 25–29. [CrossRef]
35. Bahiraei, M.; Heshmatian, S. Graphene family nanofluids: A critical review and future research directions. *Energy Convers. Manag.* **2019**, *196*, 1222–1256. [CrossRef]
36. Sadri, R.; Hosseini, M.; Kazi, S.N.; Bagheri, S.; Abdelrazek, A.H.; Ahmadi, G.; Zubir, N.; Ahmad, R.; Abidin, N.I.Z. A facile, bio-based, novel approach for synthesis of covalently functionalized graphene nanoplatelet nano—Coolants toward improved thermos-physical and heat transfer properties. *J. Colloid Interface Sci.* **2018**, *509*, 140–152. [CrossRef]

37. Dhar, P.; Gupta, S.S.; Chakraborty, S.; Pattamatta, A.; Das, S.K. The role of percolation and sheet dynamics during heat conduction in poly-dispersed graphene nanofluids. *Appl. Phys. Lett.* **2013**, *102*, 163114. [CrossRef]
38. Ghozatloo, A.; Shariaty-Niasar, M.; Rashidi, A.M. Preparation of nanofluids from functionalized Graphene by new alkaline method and study on the thermal conductivity and stability. *Int. Commun. Heat Mass Transf.* **2013**, *42*, 89–94. [CrossRef]
39. Park, S.D.; Lee, S.W.; Kang, S.; Bang, I.C.; Kim, J.H.; Shin, H.S.; Lee, D.W.; Lee, D.W. Effects of nanofluids containing graphene/graphene oxide nanosheets on critical heat flux. *Appl. Phys. Lett.* **2010**, *97*, 023103. [CrossRef]
40. Safaei, M.R.; Ahmadi, G.; Goodarzi, M.S.; Shadloo, M.S.; Goshayeshi, H.R.; Dahari, M. Heat Transfer and Pressure Drop in Fully Developed Turbulent Flows of Graphene Nanoplatelets-Silver/Water Nanofluids. *Fluids* **2016**, *1*, 20. [CrossRef]
41. Yarmand, H.; Gharehkhani, S.; Shirazi, S.F.S.; Goodarzi, M.; Amiri, A.; Sarsam, W.S.; Alehashem, M.S.; Dahari, M.; Kazi, S.N. Study of synthesis, stability and thermophysical properties of graphene nanoplatelet/platinum hybrid nanofluid. *Int. Commun. Heat Mass Transf.* **2016**, *77*, 15–21. [CrossRef]
42. Vincely, D.A.; Natarajan, E. Experimental investigation of the solar FPC performance using graphene oxide nanofluid under forced circulation. *Energy Convers. Manag.* **2016**, *117*, 15. [CrossRef]
43. Yu, W.; Xie, H.; Bao, D. Enhanced thermal Conductivities of nanofluids containing graphene oxide nanosheets. *Nanotechnology* **2010**, *21*, 055705. [CrossRef] [PubMed]
44. Lin, P.; Yan, Q.; Chen, Y.; Li, X.; Cheng, Z. Dispersion and assembly of reduced graphene oxide in chiral nematic liquid crystals by charged two-dimensional nanosurfactants. *Chem. Eng. J.* **2018**, *334*, 1023–1033. [CrossRef]
45. Zubir, M.N.M.; Badarudin, A.; Kazi, S.N.; Ming, H.N.; Misran, M.; Sadeghinezdah, E.; Mehrali, M.; Syuhada, N.I.; Gharehkhani, S. Experimental investigation on the use of reduced graphene oxide and its hybrid complexes in improving closed conduit turbulent forced convective heat transfer. *Exp. Therm. Fluid Sci.* **2015**, *66*, 290–303. [CrossRef]
46. Schlierf, A.; Yang, H.; Gebremedhn, E.; Treossi, E.; Ortolani, L.; Chen, L.; Minoia, A.; Morandi, V.; Samori, P.; Casiraghi, C.; et al. Nanoscale insight into the exfoliation mechanism of graphene with organic dyes: Effect of charge, dipole and molecular structure. *Nanoscale* **2013**, *5*, 4205. [CrossRef]
47. Fan, D.; Li, Q.; Chen, W.; Zeng, J. Graphene nanofluids containing core-shell nanoparticles with plasmon resonance effect enhanced solar energy absorption. *Sol. Energy* **2017**, *158*, 31. [CrossRef]
48. Lee, S.W.; Kim, K.M.; Bang, I.C. Study on flow boiling critical heat flux enhancement of graphene oxide/water nanofluid. *Int. J. Heat Mass Transf.* **2013**, *65*, 348–356. [CrossRef]
49. Yu, W.; Xie, H.; Wang, X.; Wang, X. Significant thermal conductivity enhancement for nanofluids containing graphene nanosheets. *Phys. Lett.* **2011**, *375*, 1323–1328. [CrossRef]
50. Lee, G.-J.; Rhee, C.K. Enhanced thermal conductivity of nanofluids containing graphene nanoplatelets prepared by ultrasound irradiation. *J. Mater. Sci.* **2014**, *49*, 1506–1511. [CrossRef]
51. Hamilton, R.L.; Crosser, O.K. Thermal Conductivity of Heterogeneous Two-Components Systems. *Ind. Eng. Chem. Fundamen.* **1962**, *1*, 3. [CrossRef]
52. Akhavan-Zanjani, H.; Saffar-Avval, M.; Mansourkiaei, M.; Ahadi, M.; Sharif, F. Turbulent Convective Heat Transfer and Pressure Drop of Graphene-Water nanofluid Flowing Inside a Horizontal Circular Tube. *J. Dispers. Sci. Technol.* **2014**, *35*, 1230–1240. [CrossRef]
53. Liu, J.; Wang, F.; Zhang, L.; Fang, X.; Zhang, Z. Thermodynamic properties and thermal stability of ionic liquid-based nanofluids containing graphene as advanced heat transfer fluids for medium-to-high-temperature applications. *Renew. Energy* **2014**, *63*, 519–523. [CrossRef]
54. Park, S.S.; Kim, N.J. Influence of the oxidation treatment and the average particle diameter of graphene for thermal conductivity enhancement. *J. Ind. Eng. Chem.* **2014**, *20*, 1911–1915. [CrossRef]
55. Tesfai, W.; Singh, P.; Shatilla, Y.; Iqbal, M.Z. Rheology and microstructure of dilute graphene oxide suspension. *J. Nanoparticle Res.* **2013**, *15*, 1989. [CrossRef]
56. Ijam, A.; Saidur, R.; Ganesan, P.; Golsheikh, A.M. Stability, thermo-physical properties, and electrical conductivity of graphene oxide-deionized water/ethylene glycol based nanofluid. *Int. J. Heat Mass Transf.* **2015**, *87*, 92–103. [CrossRef]
57. Sun, Z.; Poller, S.; Huang, X.; Guschin, D.; Taetz, C.; Ebbinghaus, P.; Masa, J.; Erbe, A.; Kilzer, A.; Schuhmann, W.; et al. High-yield exfoliation of graphite in acrylate polymers: A stable few-layer graphene nanofluid with enhanced thermal conductivity. *Carbon* **2013**, *64*, 288–294. [CrossRef]
58. Naghash, A.; Sattari, S.; Rashidi, A. Experimental assessment of convective heat transfer coefficient enhancement of nanofluids prepared from high surface are nanoporous graphene. *Int. Commun. Heat Mass Transf.* **2016**, *78*, 127–134. [CrossRef]
59. Bahiraei, M.; Salmi, H.K.; Safaei, M.R. Effect of employing a new biological nanofluid containing functionalized graphene nanoplatelets on thermal and hydraulic characteristics of a spiral heat exchanger. *Energy Convers. Manag.* **2019**, *180*, 72–82. [CrossRef]
60. Hu, Y.; Li, H.; He, Y.; Wang, L. Role of nanoparticles on boiling heat transfer performance of ethylene glycol aqueous solution based graphene nanosheets nanofluid. *Int. J. Heat Mass Transf.* **2016**, *96*, 565–572. [CrossRef]
61. Zhang, H.; Wang, S.; Lin, Y.; Feng, M.; Wu, Q. Stability, thermal conductivity, and rheological properties of controlled reduced graphene oxide dispersed nanofluids. *Appl. Therm. Eng.* **2017**, *119*, 132–139. [CrossRef]
62. Ahammed, N.; Asirvatham, L.G.; Wongwises, S. Effect of volume concentration and temperature on viscosity and surface tension of graphene-water nanofluid for heat transfer applications. *J. Therm. Anal. Calorim.* **2016**, *123*, 1399–1409. [CrossRef]

63. Dong, F.; Wan, J.; Feng, Y.; Wang, Z.; Ni, J. Experimental Study on Thermophysical Properties of propylene Glycol-Based Graphene Nanofluids. *Int J. Thermophys.* **2021**, *42*, 46. [CrossRef]
64. Borode, A.O.; Ahmed, N.A.; Olubambi, P.A.; Sharifpur, M.; Meyer, J.P. Effect of Various Surfactants on the Viscosity, Thermal and Electrical Conductivity of Graphene Nanoplatelets Nanofluids. *Int. J. Thermophys.* **2021**, *42*, 158. [CrossRef]
65. Kanti, P.; Sharma, K.V.; Khedkar, R.S.; Rehman, T. Synthesis, characterization, stability, and thermal properties of graphene oxide based hybrid nanofluids for thermal applications: Experimental approach. *Diam. Relat. Mater.* **2022**, *128*, 109265. [CrossRef]
66. Kanti, P.; Minea, A.A.; Sharma, K.V.; Revanasiddappa, M. Improved thermophysical properties of Graphene Ionanofluid as heat transfer fluids for thermal applications. *J. Ion. Liq.* **2022**, *2*, 100038. [CrossRef]
67. Huminic, G.; Vardaru, A.; Humicic, A.; Fleaca, C.; Dumitrache, F.; Morjan, I. Water-Based Graphene Oxide-Silicon Hybrid nanofluids—Experimental and Theoretical Approach. *Int. J. Mol. Sci.* **2022**, *23*, 3056. [CrossRef]
68. Ali, N. Graphene-Based Nanofluids: Production Parameter Effects on Thermophysical Properties and Dispersion Stability. *Nanomaterials* **2022**, *12*, 357. [CrossRef]
69. Rahman, U.Z.A.; Teng, K.H.; Yeap, S.P.; Kazi, S.N. Synthesis and characterization of green-functionalized graphene nanofluids as an enhanced working fluid in heat transfer applications. *IOP Conf. Ser. Earth Environ. Sci.* **2022**, *1074*, 012026. [CrossRef]
70. Liu, M.S.; Lin, M.C.C.; Wang, C.C. Enhancements of thermal conductivities with Cu, CuO, and carbon nanotube nanofluids and application of MWNT/water nanofluid on a water chiller system. *Nanoscale Res. Lett.* **2011**, *6*, 297. [CrossRef]
71. Sadri, R.; Ahmadi, G.; Togun, H.; Dahari, M.; Kazi, S.N.; Sadeghinezhad, E.; Zubir, N. An experimental study on thermal conductivity and viscosity of nanofluids containing carbon nanotubes. *Nanoscale Res. Lett.* **2014**, *9*, 151. [CrossRef]
72. Kumar, P.C.M.; Chandrasekar, M. CFD analysis on heat and flow characteristics of double helically coiled tube heat exchanger handling MWCNT/water nanofluids. *Heliyon* **2019**, *5*, e02030. [CrossRef]
73. Qu, J.; Zhang, R.; Wang, Z.; Wang, Q. Photo-thermal conversion properties of hybrid CuO-MWCNT/H_2O nanofluids for direct solar thermal energy harvest. *Appl. Therm. Eng.* **2019**, *147*, 390–398. [CrossRef]
74. Hjerrild, N.E.; Mesgari, S.; Crisostomo, F.; Scott, J.A.; Amal, R.; Taylor, R.A. Hybrid PV/T enhancement using selectively absorbing Ag-SiO_2/carbon nanofluids. *Sol. Energy Mater. Sol. Cells* **2016**, *147*, 281–287. [CrossRef]
75. Gorji, T.B.; Ranjbar, A.A.; Mirzababaei, S.N. Optical properties of carboxyl functionalized carbon nanotube aqueous nanofluids as direct solar thermal energy absorbers. *Solar Energy* **2015**, *119*, 332–342. [CrossRef]
76. Jabbari, F.; Saedodin, S.; Rajabpour, A. Experimental Investigation and Molecular Dynamics Simulations of CNT-Water Nanofluid at Different Temperatures and Volume Fractions of Nanoparticles. *J. Chem. Eng. Data* **2019**, *64*, 262–272. [CrossRef]
77. Sabiha, M.A.; Mostafizur, R.M.; Saidur, R.; Mekhilef, S. Experimental investigation on thermo physical properties of single walled carbon nanotube nanofluids. *Int. J. Heat Mass Transf.* **2016**, *93*, 862–871. [CrossRef]
78. Yu, L.; Bian, Y.; Liu, Y.; Xu, X. Experimental investigation on rheological properties of water based nanofluids with low MWCNT concentrations. *Int. J. Heat Mass Transf.* **2019**, *135*, 175–185. [CrossRef]
79. Hosseini, M.; Sadri, R.; Kazi, S.N.; Bagheri, S.; Zubir, N.; Teng, C.B.; Zaharinie, T. Experimental Study on Heat Transfer and Thermo-Physical Properties of Covalently Functionalized Carbon Nanotubes Nanofluids in an Annular Heat Exchanger: A Green and Novel Synthesis. *Energy Fuels* **2017**, *31*, 5635–5644. [CrossRef]
80. Halelfadl, S.; Estellé, P.; Aladag, B.; Doner, N.; Maré, T. Viscosity of carbon nanotubes water based nanofluids: Influence of concentration and temperature. *Int. J. Therm. Sci.* **2013**, *71*, 111–117. [CrossRef]
81. Tsentalovich, D.E.; Ma, A.W.K.; Lee, J.A.; Behabtu, N.; Bengio, E.A.; Choi, A.; Hao, J.; Luo, Y.; Headrick, R.J.; Green, M.J.; et al. Relationship of Extensional Viscosity and Liquid Crystalline Transition to Length Distribution in Carbon Nanotube Solutions. *Macromolecules* **2016**, *49*, 681–689. [CrossRef]
82. Ansón-Casaos, A.; Ciria, J.C.; Sanahuja-Parejo, O.; Victor-Román, S.; González-Dominguez, J.M.; Garcia-Bordejé, E.; Benito, A.M.; Maser, W.K. The viscosity of dilute carbon nanotube (1D) and graphene oxide (2D) nanofluids. *Phys. Chem. Chem. Phys.* **2020**, *22*, 11474. [CrossRef] [PubMed]
83. Maron, S.H.; Pierce, P.E. Application of ree-eyring generalized flow theory to suspensions of spherical particles. *J. Colloid Sci.* **1956**, *11*, 80–95. [CrossRef]
84. Kumaresan, V.; Velraj, R. Experimental investigation of the thermo-physical properties of water-ethylene glycol mixture base CNT nanofluids. *Therm. Acta* **2012**, *545*, 180–186. [CrossRef]
85. Glory, J.; Bonetti, M.; Helezen, M.; Mayne-L'Hermite, M.; Reynaud, C. Thermal and electrical conductivities of water-based nanofluids prepared with long multiwalled carbon nanotubes. *J. Appl. Phys.* **2008**, *103*, 094309. [CrossRef]
86. Fadhillahanafi, N.M.; Leong, K.Y.; Risby, M.S. Stability and Thermal Conductivity Characteristics of Carbon Nanotube Based nanofluid. *Int. J. Automot. Mech. Eng.* **2013**, *8*, 1376–1384. [CrossRef]
87. Tong, Y.; Kim, J.; Cho, H. Effects of thermal performance of enclosed-type evacuated U-tube solar collector with multi-walled carbon nanotube/water nanofluid. *Renew. Energy* **2015**, *83*, 463–473. [CrossRef]
88. Delfani, S.; Karami, M.; Akhavan-Behabadi, M.A. Performance characteristics of a residential-type direct absorption solar collector using MWCNT nanofluid. *Renew. Energy* **2016**, *87*, 754–764. [CrossRef]
89. Esfe, M.H.; Behbahani, P.M.; Arani, A.A.A.; Sarlak, M.R. Thermal conductivity enhancement of SiO_2-MWCNT (85:15%)—EG hybrid nanofluids. *J. Therm. Anal. Calorim.* **2017**, *128*, 249–258. [CrossRef]
90. Mahbubul, I.M.; Khan, M.M.A.; Ibrahim, N.I.; Ali, H.M.; Al-Sulaiman, F.A.; Saidur, R. Carbon nanotube nanofluid in enhancing the efficiency of evacuated tube solar collector. *Renew. Energy* **2018**, *121*, 36–44. [CrossRef]

91. Hameed, A.; Mukthar, A.; Shafiq, U.; Qizibash, M.; Khan, M.S.; Rashid, T.; Bavoh, C.B.; Rehman, W.; Guardo, A. Experimental investigation on synthesis, characterization, stability, thermos-physical properties and rheological behavior of MWCNTs-kapok seed oil based nanofluid. *J. Mol. Liq.* **2019**, *277*, 812–824. [CrossRef]
92. Martínez-Merino, P.; Estellé, P.; Alcántara, R.; Carrilo-Berdugo, I.; Navas, J. Thermal performance of nanofluids based on tungsten disulphide nanosheets as heat transfer fluids in parabolic trough solar collectors. *Sol. Energy Mater. Sol. Cells* **2022**, *247*, 111937. [CrossRef]
93. Shah, S.N.A.; Shahabuddin, S.; Sabri, M.F.M.; Salleh, M.F.M.; Said, S.M.; Khedher, K.M.; Sridewi, N. Two-Dimensional Tungsten Disulfide-based Ethylene Glycol Nanofluids: Stability, Thermal Conductivity, and Rheological Properties. *Nanomaterials* **2020**, *10*, 1340. [CrossRef]
94. Aldana, P.U. Tungsten Disulfide Nanoparticles as Lubricant Additives for the Automotive Industry. Ph.D. Thesis, Lyon University, Lyon, France, 2016.
95. Su, Y.; Gong, L.; Li, B.; Chen, D. An experimental investigation on thermal properties of molybdenum disulfide nanofluids. In Proceedings of the International Conference on Materials, Environmental and Biological Engineering (MEBE), Guilin, China, 28–30 March 2015.
96. Nagarajan, T.; Khalid, M.; Sridewi, N.; Jagadish, P.; Shahabuddin, S.; Muthoosamy, K.; Walvekar, R. Tribological, oxidation and thermal conductivity studies of microwave synthesized molybdenum disulfide (MoS_2) nanoparticles as nano-additives in diesel based engine oil. *Sci. Rep.* **2022**, *12*, 14108. [CrossRef]
97. Zeng, Y.-X.; Zhong, X.-W.; Liu, Z.-Q.; Chen, S.; Li, N. Preparation and Enhancement of Thermal Conductivity of Heat Transfer Oil-Based MoS2 Nanofluids. *J. Nanomater.* **2013**, *2013*, 270490. [CrossRef]
98. Shah, S.N.A.; Shahabuddin, S.; Khalid, M.; Sabri, M.F.M.; Salleh, M.F.M.; Sarih, N.M.; Rahman, S. Rheological and Thermal Conductivity Study of Two-Dimensional Molybdenum Disulfide-Based Ethylene Glycol Nanofluids for Heat Transfer Applications. *Nanomaterials* **2022**, *12*, 1021. [CrossRef]
99. Arani, A.A.A.; Sadripour, S. Molybdenum disulfide/water nanofluid morphology effects on the solar collector: First and second thermodynamic law analysis. *J. Braz. Soc. Mech. Sci. Eng.* **2021**, *43*, 87. [CrossRef]
100. Martínez-Merino, P.; Alcántara, R.; Aguilar, T.; Gallardo, J.J.; Carrillo-Berdugo, I.; Gómez-Villarejo, R.; Rodríguez-Fernández, M.; Navas, J. Stability and Thermal Properties Study of Metal Chalcogenide-Based Nanofluids for Concentrating Solar Power. *Energies* **2019**, *12*, 4632. [CrossRef]
101. Naguib, M.; Kurtoglu, M.; Presser, V.; Lu, J.; Niu, J.; Heon, M.; Hultman, L.; Gogotsi, Y.; Barsoum, M.W. Two-Dimensional Nanocrystals Produced by Exfoliation of Ti_3AlC_2. *Adv. Mater.* **2011**, *23*, 4248–4253. [CrossRef]
102. Rafieerad, M.; Rafieerad, A.R.; Mehmandoust, B.; Dhingra, S.; Shanbedi, M. New water-based fluorescent nanofluid containing 2D titanium carbide MXene sheets: A comparative study of its thermophysical, electrical and optical properties with amine and carboxyl covalently functionalized graphene nanoplatelets. *J. Therm. Anal. Calorim.* **2021**, *146*, 1491–1504. [CrossRef]
103. Rubbi, F.; Habib, K.; Saidur, R.; Aslfattahi, N.; Yahya, S.M.; Das, L. Performance optimization of a hybrid PV/T solar system using Soybean oil/MXene nanofluids as A new class of heat transfer fluids. *Sol. Energy* **2020**, *208*, 124–138. [CrossRef]
104. Aslfattahi, N.; Samylingam, L.; Abdelrazek, A.S.; Arifutzzaman, A.; Saidur, R. MXene base new class of silicone oil nanofluids for the performance improvement of concentrated photovoltaic thermal collector. *Sol. Energy Mater. Sol. Cells* **2020**, *211*, 110526. [CrossRef]
105. Wang, F.; Guo, J.; Li, S.; Wang, Y.; Cai, Y.; Li, Z.; Shen, Y.; Li, C. Self-assembly of MXene-decorated stearic acid/ionic liquid phase change material emulsion for effective photo-thermal conversion and storage. *Ceram. Int.* **2023**, *49*, 480–488. [CrossRef]
106. Bakthavatchalam, B.; Habib, K.; Saidur, R.; Aslfattahi, N.; Yahya, S.M.; Rashedi, A.; Khanam, T. Optimization of Thermophysical and Rheological Properties of MXene Ionanofluids for Hybrid Solar Photovoltaic/Thermal Systems. *Nanomaterials* **2021**, *11*, 320. [CrossRef] [PubMed]
107. Das, L.; Habib, K.; Irshad, K.; Saidur, R.; Algarni, S.; Alqahtani, T. Thermo-Optical Characterization of Therminol55 Based MXene-Al_2O_3 Hybridized Nanofluid and New Correlations for Thermal Properties. *Nanomaterials* **2022**, *12*, 1862. [CrossRef]
108. Said, Z.; Ghodbane, M.; Boumeddane, B.; Tiwari, A.K.; Sundar, L.S.; Li, C.; Aslfattahi, N.; Bellos, E. Energy, exergy, economic and environmental (4E) analysis of a parabolic through collector using MXene based silicone oil nanofluids. *Sol. Energy Mater. Sol. Cells* **2022**, *239*, 111633. [CrossRef]
109. Arifutzzaman, A.; Saidur, R.; Aslfattahi, N. MXene and functionalized graphene hybridized nanoflakes based silicone-oil nanofluids as new class of media for micro-cooling application. *Ceram. Int.* **2023**, *49*, 5922–5935. [CrossRef]
110. Sundar, L.S.; Shaik, F.; Said, Z. Experimental determination of thermophysical properties and figures-of-merit analysis of 80:20% water and ionic liquid mixture based MXene nanofluid. *Proc. Inst. Mech. Eng. Part C J. Mech. Eng. Sci.* **2023**, 09544062221148587. [CrossRef]
111. Qu, J.; Zhou, G.; Zhang, M.; Shang, L.; Yu, W. Effect of reverse irradiation angle on the photo-thermal conversion performance of MXene nanofluid-based direct absorption solar collector. *Sol. Energy Mater. Sol. Cells* **2023**, *251*, 112164. [CrossRef]
112. Askari, S.; Koolivand, H.; Pourkhalil, M.; Lotfi, R.; Rashidi, A. Investigation of Fe_3O_4/Graphene nanohybrid heat transfer properties: Experimental approach. *Int. Commun. Heat Mass Transf.* **2017**, *87*, 30–39. [CrossRef]
113. Barai, D.P.; Bhanvase, B.A.; Saharan, V.K. Reduced Graphene Oxide-Fe_3O_4 Nanocomposite Based Nanofluids: Study on Ultrasonic Assisted Synthesis, Thermal Conductivity, Rheology, and Convective Heat Transfer. *Ind. Eng. Chem. Res.* **2019**, *58*, 8349–8369. [CrossRef]

114. Mbambo, M.C.; Madito, M.J.; Khamliche, T.; Mtshali, C.B.; Khumalo, Z.M.; Madiba, I.G.; Mothudi, B.M.; Maaza, M. Thermal conductivity enhancement in gold decorated graphene nanosheets in ethylene glycol based nanofluid. *Sci. Rep.* **2020**, *10*, 14730. [CrossRef]
115. Wong, K.V.; De Leon, O. *Applications of Nanofluids: Current and Future*, 1st ed.; Jenny Stanford Publishing: Singapore, 2017; ISBN 9781315163574.
116. Rodrigues-Laguna, M.R.; Castro-Alvarez, A.; Sledzinska, M.; Maire, J.; Constanzo, F.; Ensing, B.; Pruneda, M.; Ordejón, P.; Torres, C.M.S.; Gómez-Romero, P.; et al. Mechanisms behind the enhancement of thermal properties of graphene nanofluids. *Nanoscale* **2018**, *10*, 15402–15409. [CrossRef]
117. Taha-Tijerina, J.; Ribeiro, H.; Avina, K.; Martinez, J.M.; Godoy, A.P.; Cremonezzi, J.M.O.; Luciano, M.A.; Benega, M.A.G.; Andrade, R.J.E.; Fechine, G.J.M.; et al. Thermal Conductivity Performance of 2D h-BN/MoS2/-Hybrid Nanostructures Used on Natural and Synthetic Esters. *Nanomaterials* **2020**, *10*, 1160. [CrossRef]
118. Yarmand, H.; Gharehkhani, S.; Shirazi, S.F.S.; Amiri, A.; Montazer, E.; Arzani, H.K.; Sadri, R.; Dahari, M.; Kazi, S.N. Nanofluid based on activated hybrid of biomass carbon/graphene oxide: Synthesis, thermo-physical and electrical properties. *Int. Commun. Heat Mass Transf.* **2016**, *72*, 10–15. [CrossRef]
119. Sundar, L.S.; Singh, M.K.; Ferro, M.C.; Sousa, A.C.M. Experimental investigation of the thermal transport properties of graphene oxide/Co_3O_4 hybrid nanofluids. *Int. Commun. Heat Mass Transf.* **2017**, *84*, 1–10. [CrossRef]
120. Ahammed, N.; Asirvatham, L.G.; Wongwises, S. Entropy generation analysis of graphene-alumina hybrid nanofluid in multiport minichannel heat exchanger coupled with thermoelectric cooler. *Int. J. Heat Mass Transf.* **2016**, *103*, 1084–1097. [CrossRef]
121. Verma, S.K.; Tiwari, A.K.; Tiwari, S.; Chauchan, D.S. Performance analysis of hybrid nanofluids in flat plate solar collector as an advanced working fluid. *Sol. Energy* **2018**, *167*, 231–241. [CrossRef]
122. Omri, M.; Aich, W.; Rmili, H.; Kolsi, L. Experimental Analysis of the Thermal Performance Enhancement of a Vertical Helical Coil Heat Exchanger Using Copper Oxide-Graphene (80–20%) Hybrid Nanofluid. *Appl. Sci.* **2022**, *12*, 11614. [CrossRef]
123. Mahamude, A.S.F.; Harun, W.S.S.; Kadirgama, K.; Ramasamy, D.; Farhana, K.; Salih, K.; Yusaf, T. Experimental Study on the Efficiency Improvement of Flat Plate Solar Collectors Using Hybrid Nanofluids Graphene/Waste Cotton. *Energies* **2022**, *15*, 2309. [CrossRef]
124. Jin, W.; Jiang, L.; Han, L.; Huang, H.; Zhang, J.; Guo, M.; Gu, Y.; Zhi, F.; Chen, Z.; Yang, G. Investigation of thermal conductivity enhancement of water-based graphene/MXene nanofluids. *J. Mol. Liq.* **2022**, *367*, 120455. [CrossRef]
125. Arzani, H.K.; Amiri, A.; Kazi, S.N.; Chew, B.T.; Badarudin, A. Experimental investigation of thermophysical properties and heat transfer rate of covalently functionalized MWCNT in an annular heat exchanger. *Int. Commun. Heat Mass Transf.* **2016**, *75*, 67–77. [CrossRef]
126. Ghozatloo, A.; Rashidi, A.; Shariaty-Niassar, M. Convective heat transfer enhancement of graphene nanofluids in shell and tube heat exchanger. *Exp. Therm. Fluid Sci.* **2014**, *53*, 136–141. [CrossRef]
127. Baby, T.T.; Ramaprabhu, S. Enhanced convective heat transfer using graphene dispersed nanofluids. *Nanoscale Res. Lett.* **2011**, *6*, 289. [CrossRef] [PubMed]
128. Esfahani, M.R.; Languri, E.M. Exergy analysis of a shell-and-tube heat exchanger using graphene oxide nanofluids. *Exp. Therm. Fluid Sci.* **2017**, *83*, 100–106. [CrossRef]
129. Poongavanam, G.K.; Panchabikesan, K.; Murugesan, R.; Duraisamy, S.; Ramalingam, V. Experimental investigation on heat transfer and pressure drop of MWCNT-Solar glycol based nanofluids in shot peened double pipe heat exchanger. *Powder Technol.* **2019**, *345*, 815–824. [CrossRef]
130. Fares, M.; Al-Mayyahi, M.; Al-Saad, M. Heat transfer analysis of a shell and tube heat exchanger operated with graphene nanofluids. *Case Stud. Therm. Eng.* **2020**, *18*, 100485. [CrossRef]
131. Sen, Y.; Variyenli, H.I. Experimental investigation of the performance of CuO-graphene nanoplatelet/water hybrid nanofluid in concentric tube heat exchanger. *Int. J. Energy Stud.* **2021**, *6*, 37–52.
132. Abdallah, M.; Salem, M.; Eissa, M.S.; Aissa, W.A. An Experimental Study of Laminar Flow for Graphene Nanofluid in Double Micro Heat Exchanger. *Int. J. Appl. Energy Syst.* **2021**, *3*, 25–34.
133. Balaji, T.; Selvam, C.; Lal, D.M.; Harish, S. Enhanced heat transfer behavior of micro channel heat sink with graphene based nanofluids. *Int. Commun. Heat Mass Transf.* **2020**, *117*, 104716. [CrossRef]
134. Aravind, S.S.J.; Ramaprabhu, S. Graphene wrapped multiwalled carbon nanotubes dispersed nanofluids for heat transfer applications. *J. Appl. Phys.* **2012**, *112*, 124304. [CrossRef]
135. Yarmand, H.; Gharehkhani, S.; Ahmadi, G.; Shirazi, S.F.S.; Baradaran, S.; Montazer, E.; Zubir, M.N.M.; Alehashem, M.S.; Kazi, S.N.; Dahari, M. Graphene nanoplatelets-silver hybrid nanofluids for enhanced heat transfer. *Energy Convers. Manag.* **2015**, *100*, 419–428. [CrossRef]
136. Zubir, M.N.M.; Badarudin, A.; Kazi, S.N.; Huang, N.M.; Misran, M.; Sadeghinezdah, E.; Mehrali, M.; Yusoff, N. Highly dispersed reduced graphene oxide and its hybrid complexes as effective additives for improving thermophysical property of heat transfer fluid. *Int. J. Heat Mass Transf.* **2015**, *87*, 284–294. [CrossRef]
137. Wahab, A.; Khan, M.A.Z.; Hassan, A. Impact of graphene nanofluid and phase change material on hybrid photovoltaic thermal system: Exergy analysis. *J. Clean. Prod.* **2020**, *277*, 123370. [CrossRef]

138. Hassan, A.; Wahab, A.; Qasim, M.A.; Janjua, M.M.; Ali, M.A.; Ali, H.M.; Jadoon, T.R.; Ali, E.; Raza, A.; Javaid, N. Thermal management and uniform temperature regulation of photovoltaic modules using hybrid phase change materials-nanofluids system. *Renew. Energy* **2020**, *145*, 282–293. [CrossRef]
139. Abdelrazik, A.S.; Tan, K.H.; Aslfattahi, N.; Saidur, R.; Al-Sulaiman, F.A. Optical properties and stability of water-based nanofluids mixed with reduced graphene oxide decorated with silver and energy performance investigation in hybrid photovoltaic/thermal solar systems. *Int. J. Energy Res.* **2020**, *44*, 11487–11508. [CrossRef]
140. Venkatesh, T.; Manikandan, S.; Selvam, C.; Harish, S. Performance enhancement of hybrid solar PV/T system with graphene based nanofluids. *Int. Commun. Heat Mass Transf.* **2022**, *130*, 105794. [CrossRef]
141. Sreekumar, S.; Shah, N.; Mondol, J.; Hewwit, N.; Chakrabarti, S. Numerical Investigation and Feasibility Study on MXene/Water Based Photovoltaic/thermal System. *Clean. Energy Syst.* **2022**, *2*, 100010. [CrossRef]
142. Kaseian, A.; Daneshazarian, R.; Rezaei, R.; Pourfayaz, F.; Kaseeian, G. Experimental investigation on the thermal behavior of nanofluid direct absorption in a trough collector. *J. Clean. Prod.* **2017**, *158*, 276–284. [CrossRef]
143. Aguilar, T.; Sani, E.; Mercatelli, L.; Carrilo-Berdugo, I.; Torres, E.; Navas, J. Exfoliated graphene oxide-base nanofluids with enhanced thermal and optical properties for solar collectors in concentrating solar power. *J. Mol. Liq.* **2020**, *306*, 112862. [CrossRef]
144. Yan, C.; Liang, J.; Zhong, X.; Li, C.; Chen, D.; Wang, Z.; Li, S.; Xu, J.; Wang, H.; Li, Y.; et al. BN white graphene well-dispersed solar salt nanofluids with significant improved thermal properties for concentrated solar power plants. *Sol. Energy Mater. Sol. Cells* **2022**, *245*, 111875. [CrossRef]
145. Hordy, N.; Rabilloud, D.; Meunier, J.-L.; Coulombe, S. High temperature and long-term stability of carbon nanotube nanofluids for direct absorption solar thermal collectors. *Sol. Energy* **2014**, *105*, 82–90. [CrossRef]
146. Hosseinghorbany, A.; Mozaffarian, M.; Pazuki, G. Application of graphene oxide IoNanofluid as a superior heat transfer fluid in concentrated solar power plants. *Int. Commun. Heat Mass Transf.* **2020**, *111*, 104450. [CrossRef]
147. Kumar, S.; Tiwari, A.K. Performance evaluation of evacuated tube solar collector using boron nitride nanofluid. *Sustain. Energy Technol. Assess.* **2022**, *53*, 102466. [CrossRef]
148. Zhu, J.; Li, X.; Yang, R.; Wen, J.; Li, X. Photothermal conversion characteristics and exergy analysis of TiN@h-BN composite nanofluids. *J. Mater. Sci.* **2022**, *57*, 19799–19816. [CrossRef]
149. Beheshti, A.; Shanbedi, M.; Heris, S.Z. Heat transfer and rheological properties of transformer oil-oxidized MWCNT nanofluid. *J. Therm. Anal. Calorim.* **2014**, *118*, 1451–1460. [CrossRef]
150. Maharana, M.; Baruah, N.; Nayak, S.K.; Sahoo, N.; Wu, K.; Goswami, L. Electrohydrodynamics Analysis of Dielectric 2D Nanofluids. *Nanomaterials* **2022**, *12*, 1489. [CrossRef]
151. Almeida, C.; Paul, S.; Asirvatham, L.G.; Manova, S.; Nimmagadda, R.; Bose, J.R.; Wongwises, S. Experimental Studies on Thermophysical and Electrical Properties of Graphene-Transformer Oil Nanofluid. *Fluids* **2020**, *5*, 172. [CrossRef]
152. Amiri, A.; Kazi, S.N.; Shanbedi, M.; Zubir, M.N.M.; Yarmand, H.; Chew, B.T. Transformer oil based multi-walled carbon nanotube-hexylamine coolant with optimized electrical, thermal and rheological enhancements. *RSC Adv.* **2015**, *5*, 107222. [CrossRef]
153. Amiri, A.; Shanbedi, M.; Ahmadi, G.; Rozali, S. Transformer oils-based graphene quantum dots nanofluid as a new generation of highly conductive and stable coolant. *Int. Commun. Heat Mass Transf.* **2017**, *83*, 40–47. [CrossRef]
154. Suhaimi, N.S.; Din, M.F.M.; Ishak, M.T.; Rahman, A.R.A.; Ariffin, M.M.; Hashim, N.I.; Wang, J. Systematic study of multi-walled carbon nanotube nanofluids based disposed transformer oil. *Sci. Rep.* **2020**, *10*, 20984. [CrossRef]
155. Alizadeh, H.; Pourpasha, H.; Heris, S.Z.; Estellé, P. Experimental investigation on thermal performance of covalently functionalized hydroxylated and non-covalently functionalized multi-wall carbon nanotubes/transformer oil nanofluid. *Case Stud. Therm. Eng.* **2022**, *31*, 101713. [CrossRef]
156. Suhaimi, N.S.; Din, M.F.M.; Ishak, M.T.; Rahman, A.R.A.; Wang, J.; Hassan, M.Z. performance and limitation of mineral-oil based carbon nanotubes nanofluid in transformer application. *Alex. Eng. J.* **2022**, *61*, 9623–9635. [CrossRef]
157. Zhang, J.; Fu, B.; Song, C.; Shang, W.; Tao, P.; Deng, T. Ethylene glycol nanofluids dispersed with monolayer graphene oxide nanosheet for high-performance subzero cold thermal energy storage. *RSC Adv.* **2021**, *11*, 30495. [CrossRef] [PubMed]
158. Faizal, M.; Bouazza, A.; Singh, R.M. Heat transfer enhancement of geothermal energy piles. *Renew. Sustain. Energy Rev.* **2016**, *57*, 16–33. [CrossRef]
159. Tarodiya, R.; Verma, V.; Thangavel, S. A study on utilization of ground source energy for space heating using a nanofluid as a heat carrier. *Heat Transf.* **2021**, *50*, 3842–3860. [CrossRef]
160. Sundar, L.S.; Ramana, E.V.; Said, Z.; Punnaiah, V.; Mouili, C.; Sousa, A.C.M. Properties, heat transfer, energy efficiency and environmental emissions analysis of flat plate collector using nanodiamond nanofluids. *Diam. Relat. Mater.* **2020**, *110*, 108115. [CrossRef]
161. Trompeta, A.-F.; Koklioti, M.A.; Perivoliotis, D.K.; Lynch, I.; Charitidis, C.A. Towards a holistic environmental impact assessment of carbon nanotube growth through chemical vapor deposition. *J. Clean. Prod.* **2016**, *129*, 384–394. [CrossRef]
162. Singh, A.; Lou, H.H.; Pike, R.W.; Agboola, A.; Li, X. Environmental Impact Assessment for Potential Continuous Processes for the Production of Carbon Nanotubes. *Am. J. Environ. Sci.* **2008**, *4*, 522–534. [CrossRef]
163. Arvidsson, R.; Molander, S.; Sandén, B.A. Review of Potential Environmental and Health Risks of the Nanomaterial Graphene. *Hum. Ecol. Risk Assess. Int. J.* **2013**, *19*, 873–887. [CrossRef]

164. Ali, A.; Suhail, M.; Mathew, S.; Shah, M.A.; Harakeh, S.M.; Ahmad, S.; Kazmi, Z.; Alhamdan, A.R.; Chaudhary, A.; Damanhouri, G.A.; et al. Nanomaterial Induced Immune Responses and Cytotoxicity. *J. Nanosci. Nanotechnol.* **2016**, *16*, 40–57. [CrossRef]
165. Fojtu, M.; Teo, W.Z.; Pumera, M. Environmental impact and potential health risks of 2D nanomaterials. *Environ. Sci. Nano* **2017**, *4*, 1617–1633. [CrossRef]
166. Malakar, A.; Kanel, S.R.; Ray, C.; Snow, D.D.; Nadagouda, M.N. Nanomaterials in the environment, human exposure pathway, and health effects: A review. *Sci. Total Environ.* **2021**, *759*, 143470. [CrossRef]
167. Arvidsson, R. Review of environmental life cycle assessment studies of graphene production. *Adv. Mater. Lett.* **2017**, *8*, 187–195. [CrossRef]
168. Arvidsson, R.; Kushnir, D.; Molander, S.; Sandén, B.A. Energy and resource use assessment of graphene as a substitute for indium tin oxide in transparent electrodes. *J. Clean. Prod.* **2016**, *136*, 289–297. [CrossRef]
169. Cossuta, M.; McKechnie, J.; Pickering, S.J. A comparative LCA study of different graphene production routes. *Green Chem.* **2017**, *19*, 5874–5884. [CrossRef]
170. Beloin-Saint-Pierre, D.; Hischier, R. Towards a more environmentally sustainable production of graphene-based materials. *Int. J. Life Cycle Assess.* **2021**, *26*, 327–343. [CrossRef]
171. Cossuta, M.; Vretenar, V.; Centeno, T.A.; Kotrusz, P.; McKechnie, J.; Pickering, S.J. A comparative life cycle assessment of graphene and activated carbon in a supercapacitor application. *J. Clean. Prod.* **2020**, *242*, 118468. [CrossRef]
172. Arvidssen, R.; Molander, S. Prospective Life Cycle Assessment of Epitaxial Graphene Production at Different Manufacturing Scales and Maturity. *J. Ind. Ecol.* **2017**, *21*, 1153–1164. [CrossRef]
173. Fadeel, B.; Bussy, C.; Merino, S.; Vázquez, E.; Flahaut, E.; Mouchet, F.; Evariste, L.; Gauthier, L.; Koivisto, A.J.; Vogel, U.; et al. Safety Assessment of Graphene-Based Materials: Focus on Human Health and the Environment. *ACS Nano* **2018**, *12*, 10582–10620. [CrossRef]
174. Deng, Y.; Li, J.; Qiu, M.; Yang, F.; Zhang, J.; Yuan, C. Deriving characterization factors on freshwater ecotoxicity of graphene oxide nanomaterial for life cycle impact assessment. *Int. J. Life Cycle Assess.* **2017**, *22*, 222–236. [CrossRef]
175. Wu, F.; Zhou, Z.; Temizel-Sekeryan, S.; Ghamkar, R.; Hicks, A.L. Assessing the environmental impact and payback of carbon nanotube supported CO_2 capature technologies using LCA methodology. *J. Clean. Prod.* **2020**, *270*, 122465. [CrossRef]
176. Sathre, R.; Chester, M.; Cain, J.; Masanet, E. A framework for environmental assessment of CO_2 capture and storage systems. *Energy* **2012**, *37*, 540–548. [CrossRef]
177. Bobba, S.; Deorsola, F.A.; Blengini, G.A.; Fino, D. LCA of tungsten dissulphide (WS_2) nano-particles synthesis: State of art and from-cradle-to-gate LCA. *J. Clean. Prod.* **2016**, *139*, 1478–1484. [CrossRef]
178. Hachhach, M.; Akram, H.; El Kasmi, A.; Hanafi, M.; Achak, O.; Chafik, T. Life cycle assessment of large-scale production of MoS_2 nanomaterials through the solvothermal method. *J. Nanopart. Res.* **2022**, *24*, 181. [CrossRef]
179. European Commission, Joint Research Center, Institute for Environment and Sustainability. ILCD Handbook: Analysis of Existing Environmental Impact Assessment Methodologies for Use in Life Cycle Assessment. 2012. Available online: https://eplca.jrc.ec.europa.eu/uploads/ILCD-Handbook-LCIA-Background-analysis-online-12March2010.pdf (accessed on 1 January 2023).
180. Ochoa-Hueso, R.; Delgado-Baquerizo, M.; King, P.T.A.; Benham, M.; Arca, V.; Power, S.A. Ecosystem type and resource quality are more important than global change drivers in regulating early stages of litter decompostion. *Soil Biol. Biochem.* **2019**, *129*, 144–152. [CrossRef]
181. Frascoli, F.; Hudson-Edwards, K.A. Geochemistry, Mineralogy and Microbiology of Molybdenum in Mining-Affected Environments. *Minerals* **2018**, *8*, 42. [CrossRef]